

Impurity Spin Dynamics and Quantum Coherence in Mesoscopic Rings

Peter Schwab

Angaben zur Veröffentlichung / Publication details:

Schwab, Peter. 1996. *Impurity Spin Dynamics and Quantum Coherence in Mesoscopic Rings*. Augsburg: Universität Augsburg.

Nutzungsbedingungen / Terms of use:

licgercopyright

Dieses Dokument wird unter folgenden Bedingungen zur Verfügung gestellt: / This document is made available under these conditions:

Deutsches Urheberrecht

Weitere Informationen finden Sie unter: / For more information see:

<https://www.uni-augsburg.de/de/organisation/bibliothek/publizieren-zitieren-archivieren/publiz/>



Impurity Spin Dynamics and Quantum Coherence in Mesoscopic Rings

Zur Erlangung des akademischen Grades eines
Doktors der Naturwissenschaften
der Mathematisch-Naturwissenschaftlichen Fakultät
der Universität Augsburg

vorgelegte
Dissertation

von
Dipl.-Phys. Peter Schwab
aus Oberkirch

Augsburg
1996

Erster Berichterstatter: Prof. Dr. U. Eckern
Zweiter Berichterstatter: Priv. Doz. Dr. K.-H. Höck
Tag der mündlichen Prüfung: 8. März 1996

Theoretische Physik II

Impurity Spin Dynamics and Quantum Coherence in Mesoscopic Rings

P. Schwab

Dissertation, Universität Augsburg 1996

In the presence of a magnetic field, a normal-metal ring carries an equilibrium current, usually called persistent current. In rings where the electron motion is diffusive, several mechanisms which produce a persistent current have been found: A persistent current exists, if the electrons can diffuse around the ring without losing their phase coherence. However, none of the mechanisms known can explain the amplitude of the currents measured in the experiments.

We study the effect of paramagnetic impurities on the persistent current. Magnetic impurities tend to destroy quantum coherence. In weak magnetic fields the persistent current is strongly reduced due to the impurity spin dynamics. Instead there are temporal current fluctuations following the actual spin configuration. By freezing out the spin dynamics in a magnetic field, the amplitude of the typical current, i.e. the current fluctuations, is of the same order as without magnetic impurities. However the mechanism of restoring the persistent current works rather badly, and the maximum value for the current is only reached for magnetic fields with a Zeeman energy larger than the spin-flip scattering rate.

We discuss the mean current in a model of non-interacting and for weakly interacting electrons, as well as the stochastic current fluctuations. We find qualitatively different behavior of the current as a function of the Zeeman energy in all these cases. For example, the interaction contribution to the mean current is strongly reduced in the presence of magnetic impurities, regardless of whether the impurity spins are polarized or not.

If the Thouless energy E_c and the temperature are below the Kondo temperature, the impurity spins are effectively screened, the magnetic impurities scatter like nonmagnetic impurities.

None of these mechanisms ever lead to a persistent current which is larger than in the clean limit, i.e. without magnetic impurities.

Although we cannot explain the large currents observed experimentally, our results for the current as a function of parameters like the impurity concentration, magnetic field and so on, may serve as a test for the applicability of the theoretical concepts (in comparison with future, systematic experiments).

In addition we consider quantum corrections to the free energy of the magnetic impurities; due to these corrections we find a contribution to the persistent current which is -- for $1/\tau_s \sim E_c$ and $T \ll E_c$ -- larger than in a theory without magnetic impurities. The current as a function of temperature is of the order $I \sim (E_c^2 / \phi_0 T) \cdot \exp(-T/3E_c)$. The current depends crucially on spin-orbit scattering: Without spin-orbit scattering, we find diamagnetic currents, and for strong spin-orbit scattering, we find paramagnetic currents.

Contents

1	Introduction	3
2	Persistent currents	7
2.1	Non-interacting electrons	8
2.1.1	Mean current, non-diagrammatic approach	8
2.1.2	Persistent current, using Green's functions	12
2.1.3	Current fluctuations	14
2.2	Interacting electrons	18
3	Perturbation theories for magnetic impurities	21
3.1	Perturbation theory for the Kondo model	21
3.1.1	Abrikosov's pseudo fermion method	23
3.2	Renormalized perturbation theory for the Anderson model	25
4	The effects of magnetic impurities on the persistent current	29
4.1	Spin polarization in magnetic fields	30
4.1.1	Non-interacting electrons	32
4.1.2	Interacting electrons (mean current)	36
4.2	Spin glasses	38
4.3	Kondo effect	39
4.4	Discussion of the results	42
5	Persistent currents induced by impurity spins	43
5.1	Phase sensitivity of the Knight shift	43
5.2	Spin-orbit scattering	46
5.3	Higher order corrections	47
6	Temporal current fluctuations	51
6.1	Static and dynamic linear response	52
6.2	Time dependent Green's functions	54
6.3	The effective electron-electron interaction	54
6.4	Diffuson and cooperon	56

6.5	Temporal fluctuations (zero magnetic field)	57
6.6	Temporal fluctuations in the presence of weak magnetic fields	60
7	Summary	62
A	From real time to imaginary time representation: Some useful relations	64
B	The electron self energy	66
C	Diffuson and cooperon in the presence of magnetic impurities	68
C.1	Zero magnetic field	68
C.2	Magnetic field effects	70
C.3	Mixed potential and spin-flip scattering	71
D	Persistent currents: Summary of results for single channel systems	72
E	Static and dynamic response in the canonical and grand canonical ensemble	74

Chapter 1

Introduction

Magnetic properties of metallic clusters, metallic rings and of ring molecules have been investigated for many years [1–5]. For low temperatures, the discreteness of the electron level structure has important consequences. This leads for example to odd-even effects in the magnetic susceptibility, i.e. the susceptibility is qualitatively different for a cluster with an odd or even number of electrons.

In a free electron model for the conduction electrons, the mean spacing between energy levels near the Fermi level is $\Delta \sim \epsilon_F/N$, where N is the number of electrons. Given a fixed density of electrons, it follows that the level spacing is proportional to the inverse of the volume of a cluster. For typical metals a level spacing of about 1K is found for particles of about 100Å in size.

However, there are also quantum corrections to the transport and equilibrium properties of metallic particles for temperatures, where $k_B T$ is far above the level spacing: In the classical theory of transport in disordered conductors, the Boltzmann theory, it is assumed that conduction electrons move along classical paths between collisions. For sufficiently low temperatures, elastic scattering is the dominant scattering mechanism. In systems with restricted geometry, it is possible to observe quantum mechanical corrections to this classical theory of transport. Famous examples are the weak localization corrections to the conductivity [6–10] and the universal conductance fluctuations [11–13]. Related to these are Aharonov Bohm oscillations of the conductance in metallic rings and cylinders, i.e. oscillations which are periodic in the magnetic field [14–18].

So far, most of the experimental studies of these mesoscopic metallic systems were devoted to transport (non-equilibrium) properties.

Recent experiments on metallic [19–21] and semiconducting [22, 23] rings have shown the existence of persistent currents in normalconducting mesoscopic rings, i.e. the existence of a contribution to the magnetic moment which is periodic in the magnetic flux. Note that the persistent current is an equilibrium phenomenon. In the first experiment, the persistent current in an ensemble of 10^7 Copper rings [19]

was measured. The current was found periodic in the flux ϕ with the periodicity of half a flux quantum $\phi_0/2 = h/2e$. The amplitude of the current was of the order $I \sim ev_F l/L^2$, where v_F is the Fermi velocity, l is the mean free path and L the circumference of the ring. In the second experiment the current in single gold rings was measured [21]. The periodicity was one flux quantum, the amplitude was $I \sim ev_F/L$.

For illustration, let us describe the phenomenon of persistent currents within a simple model: We consider non-interacting electrons in one dimension, without impurities. We have to solve the Schrödinger equation

$$\frac{\hat{p}^2}{2m}\Psi(x) = \epsilon\Psi(x). \quad (1.1)$$

Imposing periodic boundary conditions, $\Psi(x+L) = \Psi(x)$, this model describes electrons on a thin ring with circumference L . The solutions of Eq. (1.1) are plane waves with the wave vectors $k_n = p_n/\hbar = 2\pi n/L$ and energies $\epsilon_n = (\hbar k_n)^2/2m$. Applying a magnetic field B , which is perpendicular to the ring, we can choose a gauge where the vector potential is constant around the ring, and thus leads to the replacement $\hat{p} \rightarrow \hat{p} + eA$ with $A = BL/4\pi$. The ring is penetrated by a magnetic flux $\phi = BL^2/4\pi$, so we find $k_n = 2\pi(n + \phi/\phi_0)/L$. The energy levels $\epsilon_n = (\hbar k_n)^2/2m$ are functions of the magnetic flux, and the spectrum $\{\epsilon_n\}$ is periodic in ϕ with periodicity ϕ_0 . Each level carries a current $I_n = -\partial_\phi \epsilon_n$. At zero temperature, the total current in a system with N electrons is

$$I = \sum_n I_n, \quad (1.2)$$

where the sum is over the N levels which are lowest in energy; for simplicity, we ignore the spin of the electrons. The single level currents can be positive or negative, so many contributions to this sum cancel. The final result is of the same order of magnitude as a single level current! For example, for even N and small flux ($\phi \rightarrow +0$), the current is determined by the electron of highest energy: $I = ev_F/L$. For odd N and the flux in the interval $-\phi_0/2 < \phi < \phi_0/2$, the current is given by $I = -(ev_F/L)2\phi/\phi_0$. For arbitrary magnetic flux, this result is to be continued periodically. The result for even N is just shifted by half a flux quantum.

The persistent current is given by the derivative of the ground state energy with respect to the flux ϕ . The magnetic moment is given by the derivative of the ground state energy with respect to the magnetic field. Thus the persistent current is proportional to the magnetic moment of the ring.

In more realistic descriptions of the experiments, one takes into account the finite cross section of the rings, and also includes disorder with a mean free path l . This leads to nontrivial complications of the theory.

Qualitatively the experimental findings can be explained assuming strong fluctuations of the current from one sample to the other. If these fluctuations allow for different signs of the current in the different samples, it follows that the typical current measured in a single ring is much larger than the mean current in an ensemble of rings. We can also explain the different periodicities: In each ring the current can be expanded in

$$I(\phi) = I_1 \sin(2\pi\phi/\phi_0) + I_2 \sin(4\pi\phi/\phi_0) + \dots \quad (1.3)$$

plus higher harmonics. The experimental observations are consistent with the theoretical result, that the average of I_1 vanishes.

The amplitude, however, of both the mean current and the current found in the single ring experiment are larger by about two orders in the experiment than theory predicts. Many efforts have been devoted to understanding this discrepancy. Early calculations for non-interacting electrons predicted an exponentially small current in a grand canonical ensemble. An important step was to realize that a much larger current is found in a canonical calculation, i.e. if the particle number is kept fixed instead of the chemical potential [24–26]. Unfortunately the resulting current is still two orders too small. It is established that the Coulomb interaction gives an important contribution to the mean current, namely $I \sim \lambda_c ev_F l / L^2$, where λ_c is a dimensionless constant characterizing the strength of the interaction. Parametrically this is of the same order as the observed current, but the estimated value of λ_c is by far too small to explain the experiment. It is remarkable that the temperature dependence of the current is described accurately by this theory [27].

The situation is even less clear for the single ring experiment. Analytical calculations for non-interacting electrons determined the root mean square current to be $\langle I^2 \rangle^{1/2} \sim ev_F l / L^2$. This is much too small when compared with the experiment, since $l/L \sim 10^{-2}$. The role of the Coulomb interaction for the persistent current is still unclear: Analytic calculations which predicted an enhancement of the current fluctuations were not convincing [28–30]. Numerical investigations are restricted to small systems. In weakly disordered, strictly one-dimensional systems it was found that the Coulomb interaction suppresses the current [31, 32]. In systems with many transverse channels an enhancement of the current has been reported [33], however it is still too small when compared with the experiment.

In the present work we investigate the effects of magnetic scattering on quantum coherence in mesoscopic rings. In Ch. 2 we review some aspects of the theory of persistent currents in metallic rings, without magnetic scattering. Using the methods of perturbation theory, we consider both interacting and non-interacting electrons.

In Ch. 3 we introduce the methods we will use later to calculate the persistent current in the presence of magnetic impurities.

In Ch. 4 we extend the calculations of Ch. 2 to include magnetic scattering, i.e. spin-flip scattering, spin-orbit scattering and Zeeman effects. We first discuss paramagnetic impurities above the Kondo temperature, we then apply the results to the spin-glass case. At the end of the chapter we discuss the Kondo effect. We would like to make it clear from the beginning, that we are not able to explain the large persistent currents observed experimentally, as we never find a scenario where the persistent current in the presence of magnetic impurities is enhanced over the value in the “clean” limit, i.e. without magnetic impurities.

In Ch. 5 we show that due to a new mechanism, there is a range of impurity concentrations and temperatures, where the mean current in systems with magnetic impurities is larger than in systems without magnetic impurities.

In Ch. 6 we study the dynamical properties of the impurity spin induced persistent current found in Ch. 5.

Our results are summarized in Ch. 7.

In App. A we show how to convert integrations over Fermi functions into summations over Matsubara frequencies. In App. B we present details of the calculation of the electron self energy in the presence of magnetic impurities. In App. C we have collected some useful relations for the diffuson and cooperon in the presence of magnetic impurities. For completeness and for further references, we list in App. D some results for the persistent current in single channel rings. In the last appendix, we briefly discuss some subtleties of linear response in the canonical and grand canonical ensemble.

Chapter 2

Persistent currents

In the idealized situation, where the effects of magnetic field penetration can be neglected, the persistent current in a ring penetrated by a magnetic flux ϕ is given by the derivative of the thermodynamic potential,

$$I(\phi) = -\frac{\partial}{\partial \phi} K(\phi). \quad (2.1)$$

This persistent current induces a magnetic moment

$$M = \pi(L/2\pi)^2 I(\phi), \quad (2.2)$$

where L is the perimeter of the ring. In a system with fixed particle number $K(\phi) = F(N, \phi)$, where F is the canonical free energy, while for a system coupled to a particle reservoir, $K(\phi) = \Omega(\mu, \phi)$, where Ω is the grand canonical potential. $K(\phi)$ is periodic in the flux, ϕ , with the period given by the flux quantum, $\phi_0 = h/e$. The thermodynamic potentials and the current can be represented as a Fourier series,

$$K(\phi) = K_0 + \sum_{m=1}^{\infty} \left[K_m \cos(2\pi m \phi / \phi_0) + \tilde{K}_m \sin(2\pi m \phi / \phi_0) \right] \quad (2.3)$$

and

$$I(\phi) = \sum_{m=1}^{\infty} \left[I_m \sin(2\pi m \phi / \phi_0) + \tilde{I}_m \cos(2\pi m \phi / \phi_0) \right]. \quad (2.4)$$

In the case of time reversal symmetry, $K(\phi)$ is an even function in ϕ , and $I(\phi)$ is odd, i.e. $\tilde{K}_m = \tilde{I}_m = 0$ for all m . In a disordered system the impurity averaged quantities $\langle K \rangle$, $\mathcal{M}_K = \langle K K \rangle_c = \langle K K \rangle - \langle K \rangle \langle K \rangle$, and the higher correlation functions are the central objects to study. In the metallic regime (diffusive electron motion) the following results are generally accepted:

$$\langle I_{2m+1} \rangle = 0 \quad (2.5)$$

$$\langle I_m I_{m'} \rangle_c = 0 \quad \text{if } m \neq m'. \quad (2.6)$$

Higher connected correlation functions are small, provided the number of electrons is large [28–30].

We consider a weakly disordered metal in the diffusive regime. In a typical sample, we may assume the following inequalities between relevant length scales: $\lambda_F \ll l \ll L \ll \xi \sim Ml$. Here λ_F is the Fermi wavelength, l the elastic mean free path, L is the perimeter of the ring, and ξ is the localization length: the latter is in quasi one-dimensional systems proportional to the number of transverse channels $M = k_F^2 \mathcal{A}/4\pi$, where \mathcal{A} is the cross section of the ring. Alternatively, we may consider the relevant energy scales, which are in descending order: ϵ_F , the Fermi energy, $\hbar/\tau = \hbar v_F/l$, the elastic scattering rate, $\hbar v_F/L$, the energy to localize a particle in one half of the ring, $E_c = \hbar D/L^2$, the Thouless energy ($D = v_F l/3$ is the diffusion constant), $\Delta = 1/2\mathcal{N}_0\mathcal{V}$, the mean level spacing at the Fermi level (\mathcal{N}_0 is the density of states, \mathcal{V} the volume).

Unfortunately, experimental data is only available from two experiments at present. In the first experiment, the current of an ensemble of $\sim 10^7$ copper rings [19, 20] was measured, which gives information on the mean current, $\langle I \rangle$. The odd harmonics, $\langle I_{2m+1} \rangle$, seem to be absent. For the first nonvanishing harmonic and for other parameters it has been reported: $\langle I_2 \rangle \sim 0.6eE_c/\hbar$, $L \sim 2 \cdot 10^{-4}\text{cm}$, $l/L \sim 1/70$, $\Delta \sim 0.2\text{mK}$, $E_c \sim 25\text{mK}$, $\hbar v_F/L \sim 5\text{K}$. For convenience, energies are given in Kelvin. The current has been measured in the temperature range of about 7mK - 200mK. The temperature dependence can be fitted by an exponential law $\propto \exp(-T/80\text{mK})$.

In the second experiment [21], the persistent current of three single gold rings was measured. It was found that $I_1 \sim (0.3 - 2.0)e v_F/L$. The perimeter of the rings was $L \sim 8 \cdot 10^{-4}\text{cm}$, the linewidth of the rings was $L_\perp \sim 90\text{nm}$ and thickness of the gold films $\sim 60\text{nm}$. Other relevant parameters are $l/L \sim 1/110$, $\epsilon_F \sim 10^5\text{K}$, $\hbar/\tau \sim 10^2\text{K}$, $\hbar v_F/L \sim 1\text{K}$, $E_c \sim 4\text{mK}$, and $\Delta \sim 0.02\text{mK}$.

2.1 Non-interacting electrons

We start the theoretical discussion of the persistent currents within a model of non-interacting electrons. *A priori*, there is no reason to discard interaction effects, and we will see later, that interaction effects are important.

2.1.1 Mean current, non-diagrammatic approach

Since we consider free fermions, we can write the grand potential as

$$\Omega(\mu, \phi) = -2k_B T \mathcal{V} \int d\epsilon \mathcal{N}(\epsilon) \ln(1 + e^{-(\epsilon - \mu)/k_B T}), \quad (2.7)$$

where $\mathcal{N}(\epsilon)$ is the single particle density of states per volume and spin. In a disordered metal, the impurity averaged density of states is insensitive to a magnetic flux, it follows that the mean persistent current in a grand canonical ensemble is practically zero¹ [34].

In computer simulations [35, 36], the mean persistent current was determined to be of the order $I \sim \sqrt{E_c \Delta} / \phi_0$, which seems to contradict the theoretical result that the current is zero. In these computer simulations, however, the current was calculated for fixed particle number. The result from the analytical calculation [34] is correct for a fixed chemical potential.

Considering a system with fixed particle number, the persistent current is given by [24–26], $I(\phi) = -\partial_\phi F(N, \phi)$. The free energy F and the grand potential Ω are related via a Legendre transformation, $F(N, \phi) = \Omega(\mu(N, \phi), \phi) + \mu(N, \phi)N$. Hence we conclude that $\partial_\phi F(N, \phi) = \partial_\phi \Omega(\mu, \phi)|_{\mu=\mu(N, \phi)}$, where the chemical potential, $\mu(N, \phi) = \partial_N F(N, \phi)$, varies as a function of the flux ϕ such that the particle number is fixed. Writing $\mu(N, \phi) = \mu_0 + \delta\mu(\phi)$ and expanding the grand potential, the result is

$$I(\phi) = -\frac{\partial}{\partial \phi} \Omega(\mu, \phi)|_{\mu=\mu_0} - \delta\mu(\phi) \frac{\partial^2}{\partial \mu \partial \phi} \Omega(\mu, \phi)|_{\mu=\mu_0}. \quad (2.8)$$

At fixed chemical potential the particle number varies due to fluctuations of the density of states, i.e. $N(\mu_0) = -\partial_\mu \Omega(\mu, \phi)|_{\mu=\mu_0} = N + \delta N(\phi)$. On the other hand,

$$N = -\frac{\partial}{\partial \mu} \Omega(\mu, \phi)|_{\mu=\mu_0+\delta\mu} = -\frac{\partial}{\partial \mu} \Omega(\mu, \phi)|_{\mu=\mu_0} - \delta\mu(\phi) \frac{\partial^2}{\partial \mu^2} \Omega(\mu, \phi)|_{\mu=\mu_0} \quad (2.9)$$

from which we can relate $\delta N(\phi)$ and $\delta\mu(\phi)$: $\delta N(\phi) = \delta\mu(\phi) \frac{\partial^2 \Omega}{\partial \mu^2}|_{\mu=\mu_0}$. The mean level spacing, Δ , is given by $\Delta = -(\partial_\mu^2 \Omega|_{\mu=\mu_0})^{-1} \simeq (2\mathcal{N}_0 \mathcal{V})^{-1}$. Collecting these relations, we express the average persistent current at fixed particle number as follows:

$$\langle I \rangle = -\frac{\partial}{\partial \phi} \langle F(N, \phi) \rangle \simeq -\frac{\Delta}{2} \frac{\partial}{\partial \phi} \langle (\delta N)^2 \rangle. \quad (2.10)$$

The right hand side of this equation depends on expressions at the chemical potential $\mu = \mu_0$ only. The fluctuations of the particle number, $\langle (\delta N)^2 \rangle$, are related to the fluctuations of the density of states,

$$\langle (\delta N)^2 \rangle = 4\mathcal{V}^2 \int d\epsilon d\epsilon_1 n_F(\epsilon) n_F(\epsilon_1) \langle \mathcal{N}(\epsilon) \mathcal{N}(\epsilon_1) \rangle_c, \quad (2.11)$$

or equivalently to the fluctuations of the grand potential:

$$\langle (\delta N)^2 \rangle = \frac{\partial^2}{\partial \mu \partial \mu'} \langle \Omega(\mu, \phi) \Omega(\mu', \phi) \rangle_c |_{\mu=\mu'}. \quad (2.12)$$

¹To be more precise, the mean current was determined [34] to be proportional to $\exp(-L/2l)$, i.e. exponentially small.

The expression for $\mathcal{M}_\Omega = \langle \Omega(\mu, \phi) \Omega(\mu', \phi') \rangle_c$ will be given in the section 2.1.3.

Fluctuations of the density of states in a disordered conductor have been calculated, e.g. by Altshuler and Shklovskii [37]. Near the Fermi level, the (flux dependent part of) the density of states correlations have been determined as

$$\langle \mathcal{N}(\epsilon) \mathcal{N}(\epsilon_1) \rangle_c = \frac{1}{2\pi^2 \mathcal{V}^2} \sum_q \text{Re} \left[\frac{1}{-i(\epsilon - \epsilon_1) + \hbar D q^2 + \gamma} \right]^2. \quad (2.13)$$

The summation is over momenta $q = 2\pi(n + 2\phi/\phi_0)/L$. There are several mechanisms contributing to γ , e.g. magnetic field penetration [10, 38] contributes the rate $\gamma = D(eHL_\perp/\hbar)^2/3$. Other mechanisms are spin-flip and spin-orbit scattering which will be discussed later. For simplicity, we consider $\gamma \rightarrow 0$ here. The flux dependent part of the free energy is

$$\begin{aligned} \langle \delta F \rangle &= \frac{\Delta}{2} \langle (\delta N)^2 \rangle = \\ &= \frac{\Delta}{\pi^2} \int d\epsilon d\epsilon_1 n_F(\epsilon) n_F(\epsilon_1) \sum_q \text{Re} \left(-i(\epsilon - \epsilon_1) + \hbar D q^2 \right)^{-2}. \end{aligned} \quad (2.14)$$

The energy integrations can be converted into two summations over fermion frequencies, and then into one summation over a Boson frequency $\omega_n = 2\pi n k_B T$. The result is:

$$\langle \delta F \rangle = \frac{2\Delta}{\pi} T \sum_{\omega_n > 0} \sum_q \frac{\omega_n}{(\omega_n + \hbar D q^2)^2}. \quad (2.15)$$

Details can be found in App. A. In the next step we determine the Fourier coefficients, compare Eqs. (2.3) and (2.4). Writing the summation over q in the form

$$\langle \delta F \rangle = \sum_{n=-\infty}^{n=+\infty} G \left(4\pi^2 E_c (n+x)^2 \right) \quad (2.16)$$

with $x = 2\phi/\phi_0$ and a suitable function G , we obtain

$$\langle \delta F \rangle = \sum_{m=-\infty}^{m=+\infty} e^{2\pi i m x} G_m \quad (2.17)$$

where

$$G_m = \int_{-1/2}^{1/2} dx e^{-2\pi i m x} \sum_{n=-\infty}^{n=+\infty} G \left(4\pi^2 E_c (n+x)^2 \right) = \int_{-\infty}^{+\infty} \frac{dx}{2\pi} e^{-i m x} G(E_c x^2). \quad (2.18)$$

Since $G_m = G_{-m}$ only terms $\propto \cos(2\pi m x)$ survive in Eq. (2.17). The coefficients G_m are given by ($m > 0$):

$$G_m = \frac{\Delta}{2\pi} \sum_{\omega_n > 0} \frac{e^{-\sqrt{\omega_n/T_m}}}{m} \frac{T}{T_m} \left(1 + \sqrt{\frac{T_m}{\omega_n}} \right), \quad (2.19)$$

with $T_m = E_c/m^2$. The persistent current is

$$\langle I(\phi) \rangle = \sum_{m=1}^{\infty} \frac{4me}{\hbar} G_m \sin(4\pi m\phi/\phi_0), \quad (2.20)$$

i.e. the current has only even Fourier components, $\langle I_{2m} \rangle$. For low temperatures, the summation over Matsubara frequencies can be approximated by an integral,

$$\langle I_{2m} \rangle = \frac{e\Delta}{\hbar\pi^2} \int_0^{\infty} \frac{d\omega}{T_m} e^{-\sqrt{\omega/T_m}} \left(1 + \sqrt{T_m/\omega}\right), \quad (2.21)$$

and the Fourier components do not depend on m : $\langle I_{2m} \rangle = 4e\Delta/\pi^2\hbar$. Performing the m -summation, we find²

$$\langle I(\phi) \rangle = \frac{e\Delta}{\pi^2\hbar} \cot \frac{2\pi\phi}{\phi_0}, \quad (2.22)$$

which diverges as $\phi \rightarrow 0$. The origin of this divergence is the (unphysical) divergence of the density of state correlator $\sim (\epsilon - \epsilon_1)^{-2}$. The correlations of the density of states in Eq. (2.13) are found within a cooperon expansion, using the leading terms only. Weak localization corrections are not included. For $\phi \rightarrow 0$ all orders of the quantum corrections have to be taken into account. As an illustration we consider the weak localization corrections to the diffusion constant [8, 10, 39],

$$D \rightarrow D \left(1 - \frac{2}{\pi} \Delta \sum_q \frac{1}{-i\hbar\omega + \hbar D q^2}\right), \quad (2.23)$$

with $q = 2\pi(n + 2\phi/\phi_0)/L$ again. Since we assume that $E_c \gg \Delta$, the momenta q with $|q| > 2\pi/L$ give only a small correction to the diffusion constant. For small ϕ and ω , however, the zero mode becomes large. For $\phi \sim (\Delta/E_c)^{1/2}\phi_0$ the weak localization corrections are of order one. For small fluxes, the density of states correlations have to be determined using non-perturbative methods, e.g. the supersymmetry method [40–43].

At least qualitatively the same results as with the supersymmetry method can be found by a regularization of Eq. (2.14): We introduce a phase braking rate γ in the denominator of Eq. (2.14), $-i(\epsilon - \epsilon_1) \rightarrow -i(\epsilon - \epsilon_1) + \gamma$ with $\gamma \sim \Delta$. As a result, for $\phi \sim (\Delta/E_c)^{1/2}\phi_0$ there is a crossover to a linear flux dependence of the persistent current $I(\phi) \sim (eE_c/\hbar)\phi/\phi_0$ for very small flux. The current reaches a maximum of about $I \sim \sqrt{E_c\Delta}/\phi_0$, which agrees with the computer simulations. Since $\gamma \sim \Delta$, these results only apply for temperatures $k_B T < \Delta$.

For high temperatures, the leading term in Eq. (2.19) is given by the lowest Matsubara frequency, so that we have the high temperature expansion

$$\langle I_{2m} \rangle = \frac{2e\Delta}{\hbar\pi} e^{-\sqrt{2\pi T/T_m}} \left(\frac{T}{T_m} + \sqrt{\frac{T}{2\pi T_m}} \right). \quad (2.24)$$

²We introduce a finite cutoff γ which leads to $\langle I_{2m} \rangle \propto \exp(-m\sqrt{\gamma/E_c})$, then we sum over m and let $\gamma \rightarrow 0$ in the result.

For temperatures $k_B T \sim E_c$, the higher harmonics of the current are strongly suppressed, so that $I(\phi) \approx I_2 \sin(4\pi\phi/\phi_0)$ with $I_2 \approx 4e\Delta/\pi^2\hbar$. The temperature dependence of the current will also be discussed in Fig. 2.6. There it will be compared with the temperature dependence of the interaction contribution of the current.

Some rewriting of the density of states correlations also leads to an interesting result. Defining

$$P(q, \omega) = \frac{1}{-i\omega + Dq^2}, \quad (2.25)$$

i.e. $P(q, \omega)$ is the retarded propagator of the diffusion equation, we find

$$\begin{aligned} \langle \mathcal{N}(\epsilon) \mathcal{N}(\epsilon + \hbar\omega) \rangle_c &= \frac{1}{2\pi^2 \hbar^2 \mathcal{V}^2} \sum_q \operatorname{Re} \left[-i \frac{\partial}{\partial \omega} P(q, \omega) \right] \\ &= \frac{1}{2\pi^2 \hbar^2 \mathcal{V}^2} \operatorname{Re} \int_0^\infty dt e^{i\omega t} \left[P(x=0, t) + 2 \sum_{m=1}^\infty P(x=mL, t) \cos(4\pi m\phi/\phi_0) \right] \end{aligned} \quad (2.26)$$

with

$$P(q, \omega) = \int_{-\infty}^\infty dx \int_0^\infty dt e^{i\omega t - iqx} P(x, t). \quad (2.27)$$

The interpretation of Eq. (2.26) is, that the $(2m)^{\text{th}}$ Fourier component of the density of states correlations is due to processes where a particle, that is an electron, diffuses m -times around the ring and is still able to interfere with itself. A finite γ leads to $P(x, t) \rightarrow e^{-t\gamma/\hbar} P(x, t)$, i.e. the electrons loose coherence after $t > \hbar/\gamma$.

2.1.2 Persistent current, using Green's functions

Alternatively, we can directly calculate the expectation value of the current operator. Using the standard Green's functions, the (thermal average of the) current is

$$\begin{aligned} I(\phi) &= \int \frac{d\epsilon}{2\pi i} \sum_{\mathbf{k}\sigma} I_x n_F(\epsilon) \left[G_{\mathbf{k}\sigma, \mathbf{k}\sigma}^A(\epsilon) - G_{\mathbf{k}\sigma, \mathbf{k}\sigma}^R(\epsilon) \right] \\ &= \int \frac{d\epsilon}{2\pi i} \sum_{\mathbf{k}\sigma} I_x e^{i\epsilon 0^+} \left\{ n_F(\epsilon) G_{\mathbf{k}\sigma, \mathbf{k}\sigma}^A(\epsilon) + [1 - n_F(\epsilon)] G_{\mathbf{k}\sigma, \mathbf{k}\sigma}^R(\epsilon) \right\}. \end{aligned} \quad (2.28)$$

$n_F(\epsilon)$ is the Fermi function, and the current vertex is given by $I_x = (-e)\hbar k_x/mL$. In the ring geometry under consideration k_x assumes the values $k_x = 2\pi(n + \phi/\phi_0)/L$. Furthermore, $G^R(G^A)$ is the retarded (advanced) Green's function, $G_{\mathbf{k}\sigma, \mathbf{k}'\sigma'}^{R(A)}(\epsilon)$ denotes the exact Green's function, before impurity averaging. In a clean system, the retarded Green's function is

$$G_{\mathbf{k}\sigma, \mathbf{k}'\sigma'}^R(\epsilon) = \frac{1}{\epsilon - \epsilon_{\mathbf{k}} + \mu + i0} \delta_{\mathbf{k}\mathbf{k}'} \delta_{\sigma\sigma'}. \quad (2.29)$$

We describe non-magnetic impurities by the Hamiltonian

$$H_{imp} = -\frac{W}{V} \sum_{\mathbf{R}} \sum_{\mathbf{k}, \mathbf{k}', \sigma} \exp[-i(\mathbf{k} - \mathbf{k}') \cdot \mathbf{R}] c_{\mathbf{k}\sigma}^+ c_{\mathbf{k}'\sigma}, \quad (2.30)$$

where \mathbf{R} are the impurity sites. In the presence of this perturbation, the Green's functions are no longer diagonal in momentum space, since there is no translation symmetry. If we average over impurity configurations,

$$\int \frac{d^3 R}{V} (\dots), \quad (2.31)$$

the averaged Green's function, for which we use the notation $G^R(\epsilon, \mathbf{k})$, is diagonal in momentum space. The averaged Green's function is given by

$$G^R(\epsilon, \mathbf{k}) = \frac{1}{\epsilon - \epsilon_{\mathbf{k}} + \mu + i\hbar/2\tau}, \quad (2.32)$$

where (in Born approximation³)

$$-i\hbar/2\tau = nW^2 \int \frac{d^2 k}{(2\pi)^3} G^R(\epsilon, \mathbf{k}). \quad (2.33)$$

and $n = N/V$ denotes the density of impurities. If the system is only weakly disordered, $\hbar/\tau \ll \epsilon_F$, the relaxation rate is determined as $\hbar/\tau = 2n\pi\mathcal{N}_0 W^2$.

To determine the mean current at fixed particle number within the Green's function approach, we follow the procedure described in section 2.1.1: The chemical potential is set equal to $\mu = \mu_0 + \delta\mu$, and we expand Eq. (2.28) to first order in $\delta\mu$:

$$\langle I(\phi) \rangle = \int \frac{d\epsilon}{2\pi} \sum_{\mathbf{k}, \sigma} I_x n_F(\epsilon) (-2) \text{Im} \left\{ G^R(\epsilon, \mathbf{k})|_{\mu=\mu_0} - \delta\mu \left[G^R(\epsilon, \mathbf{k})|_{\mu=\mu_0} \right]^2 \right\}. \quad (2.34)$$

The first term gives the mean current at a fixed chemical potential μ_0 and can be neglected. We rewrite the second term using $I_x [G^R(\epsilon, \mathbf{k})]^2|_{\mu=\mu_0} = -\partial_\phi G^R(\epsilon, \mathbf{k})$ and find the expression

$$\langle I(\phi) \rangle = -\delta\mu(\phi) \frac{\partial}{\partial \phi} \sum_{\mathbf{k}\sigma} \int \frac{d\epsilon}{2\pi} n_F(\epsilon) 2\text{Im} G^R(\epsilon, \mathbf{k})|_{\mu=\mu_0} \quad (2.35)$$

$$= +\delta\mu(\phi) \frac{\partial}{\partial \phi} N(\mu_0, \phi) \quad (2.36)$$

which agrees with Eq. (2.8).

³Impurity scattering beyond Born approximation, and for more general scattering potentials is discussed in the book of Mahan [44].

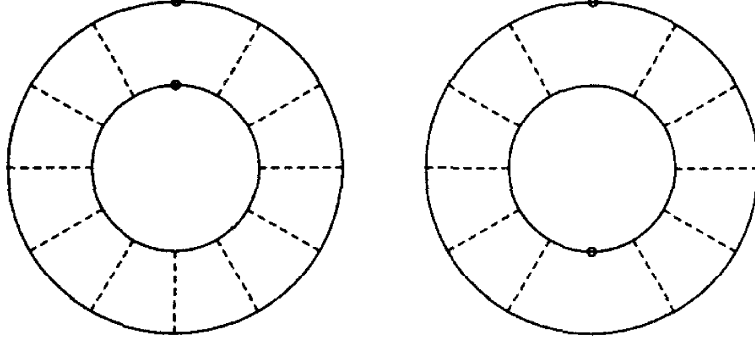


Figure 2.1: Diagrams used for the calculation of the current correlator.

2.1.3 Current fluctuations

The current fluctuations, $\langle I(\phi)I(\phi') \rangle_c$, which were first estimated in [34], can be found from the fluctuations of the thermodynamic potential, $\langle I(\phi)I(\phi') \rangle_c = \partial_\phi \partial_{\phi'} \langle K(\phi)K(\phi') \rangle_c$. For this quantity, the condition of fixed particle number does not seem to be significant. Within the Green's function formulation, our starting equation is Eq. (2.28).

The calculation of the current correlator involves averages of products of retarded and advanced Green's functions. The average of two retarded or two advanced Green's functions factorises, $\langle G_{\mathbf{k}\mathbf{k}}^R G_{\mathbf{k}'\mathbf{k}'}^R \rangle \approx \langle G_{\mathbf{k}\mathbf{k}}^R \rangle \langle G_{\mathbf{k}'\mathbf{k}'}^R \rangle$, while products of a retarded and an advanced Green's function give a connected, flux sensitive contribution: $\langle G_{\mathbf{k}\mathbf{k}}^R G_{\mathbf{k}'\mathbf{k}'}^A \rangle = \langle G_{\mathbf{k}\mathbf{k}}^R G_{\mathbf{k}'\mathbf{k}'}^A \rangle_c + \langle G_{\mathbf{k}\mathbf{k}}^R \rangle \langle G_{\mathbf{k}'\mathbf{k}'}^A \rangle$. Using Eq. (2.28) we find

$$\langle I(\phi)I(\phi') \rangle_c = -\frac{2}{\pi^2} \int d\epsilon_- d\epsilon_+ n_F(\epsilon_-) [1 - n_F(\epsilon_+)] \times \sum_{\mathbf{k}, \mathbf{k}'} I_x I'_x \text{Re} \langle G_{\mathbf{k}'\mathbf{k}'}^A(\epsilon_-) G_{\mathbf{k}\mathbf{k}}^R(\epsilon_+) \rangle_c, \quad (2.37)$$

where a spin factor of four has been included.

We consider now explicitly the expression for $\langle I(\phi)I(\phi') \rangle_c$ and relate it to the expression for \mathcal{M}_Ω , within the usual perturbative treatment for the average $\langle G_{\mathbf{k}'\mathbf{k}'}^A(\epsilon_-) G_{\mathbf{k}\mathbf{k}}^R(\epsilon_+) \rangle_c$. Note that this approach has some limitations [41, 42]. The leading diagrams are shown in Fig. 2.1. The full lines represent Green's functions, averaged over impurity configurations. The broken lines are impurity lines, and current vertices are represented by small circles. The leading diagrams are those which do not have crossed impurity lines [45]. We did not explicitly assign arrows to the Green's functions, since there are always two possibilities (parallel or antiparallel) which have to be added. The diagrams are built up by the following elements, compare Fig. 2.2:

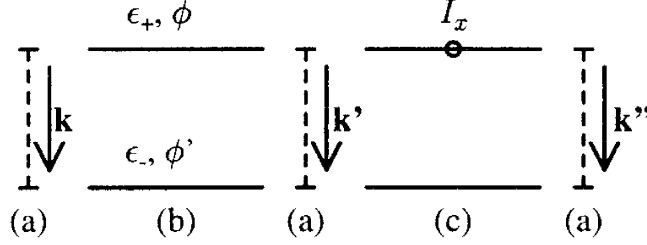


Figure 2.2: The elements building up the diagrams in Fig. 2.1. The broken lines are impurity lines, the full lines represent Green's functions. The small circle is a current vertex.

- (a) Impurity lines, associated with a factor $X^0 = \hbar/2\pi\mathcal{N}_0\tau$. These lines carry a momentum \mathbf{k} but no energy.
- (b) Products of an advanced and a retarded Green's function, integrated over the momentum:

$$\Pi^{C,D}(\mathbf{q}, \epsilon_+ - \epsilon_-) = \int \frac{d^3k}{(2\pi)^3} G^R(\epsilon_+, \mathbf{k}) G^A(\epsilon_-, \mp \mathbf{k} \pm \mathbf{q}). \quad (2.38)$$

C and D denote the cooperon and the diffuson. If we include the arrows in Fig. 2.1, the diagrams with the parallel arrows correspond to cooperon contributions, and \mathbf{q} is the sum of the momenta of the two Green's functions. For antiparallel arrows we have a diffuson contribution, and \mathbf{q} is the difference of the momenta.

- (c) Blocks build up of three or four Green's function plus one or two current vertices. Since $I_x[G^{R,A}(\epsilon, \mathbf{k})]^2 = -\partial_\phi G^{R,A}(\epsilon, \mathbf{k})$, these blocks can be related to derivatives of $\Pi^{C,D}$.

In three dimensions and for $q \ll k_F$; $\epsilon_+, \epsilon_- \ll \epsilon_F$, we find

$$\Pi^{C,D}(q, \epsilon_+ - \epsilon_-) = \frac{\pi\mathcal{N}_0\tau}{\hbar} \frac{i}{ql} \ln \frac{ql + (\epsilon_+ - \epsilon_-)\tau/\hbar + i}{-ql + (\epsilon_+ - \epsilon_-)\tau/\hbar + i}, \quad (2.39)$$

where $l = v_F\tau$ is the elastic mean free path. In the limit $ql \ll 1$; $(\epsilon_+ - \epsilon_-)\tau/\hbar \ll 1$,

$$\Pi^{C,D}(q, \epsilon_+ - \epsilon_-) \simeq [1 + i(\epsilon_+ - \epsilon_-)\tau/\hbar - D\tau q^2] 2\pi\mathcal{N}_0\tau/\hbar, \quad (2.40)$$

with $D = v_F l/3$ the diffusion constant. Note that it is essential to integrate in Eq. (2.38) over the product of an advanced and a retarded Green's function. Within the same accuracy as Eq. (2.39), the integral over two advanced or two retarded Green's functions is

$$\begin{aligned} & \int \frac{d^3k}{(2\pi)^3} G^R(\epsilon_+, \mathbf{k}) G^R(\epsilon_-, \mathbf{k} - \mathbf{q}) \\ & \approx \frac{\mathcal{N}_0}{2} \int d\xi \int_{-1}^1 dx \frac{1}{\epsilon_+ - \xi + i\hbar/2\tau} \frac{1}{\epsilon_- - \xi + qv_Fx - (\hbar q)^2/2m + i\hbar/2\tau} \end{aligned} \quad (2.41)$$

$$\approx 0 \quad (2.42)$$

since the poles of the Green's functions are on the same side in the complex plane.

Summing up an impurity ladder leads to the following result:

$$X(q, \epsilon_+ - \epsilon_-) = X^0 \sum_{M=0}^{\infty} (\Pi^{C,D} X^0)^M \quad (2.43)$$

$$= X^0 \frac{1}{1 - \Pi^{C,D} X^0} = \frac{\hbar^2}{2\pi \mathcal{N}_0 \tau^2} \frac{1}{-i(\epsilon_+ - \epsilon_-) + \hbar D q_{\pm}^2} \quad (2.44)$$

where $X = C, D$ is usually called cooperon or diffuson. The notation q_{\pm} indicates that q is the sum or difference of two momenta.

Now we can translate the diagrams in Fig. 2.1 into an analytic expression. The contribution to the current fluctuation from the left diagram of Fig. 2.1, for example, is

$$\begin{aligned} \langle I(\phi) I(\phi') \rangle_c = & -\frac{2}{\pi^2} \int d\epsilon_- d\epsilon_+ n_F(\epsilon_-) [1 - n_F(\epsilon_+)] \\ & \times \text{Re} \left[\sum_q \left(\partial_{\phi} \partial_{\phi'} \Pi^{C,D} \right) \frac{X^0}{1 - \Pi^{C,D} X^0} \right]_{C+D}. \end{aligned} \quad (2.45)$$

While in general, \mathbf{q} is a three-dimensional vector, for the ring geometry q can be considered one-dimensional. The subscript $C + D$ indicates that we have to sum over both (cooperon and diffuson) contributions.

After a change of variables to $y = \epsilon_+ - \epsilon_-$ we can integrate over ϵ_- :

$$\int d\epsilon_- n_F(\epsilon_-) [1 - n_F(y + \epsilon_-)] = \frac{y e^{y/2k_B T}}{e^{y/2k_B T} - e^{-y/2k_B T}}. \quad (2.46)$$

The combined contribution of both diagrams in Fig. 2.1 is of the form

$$\begin{aligned} \left(\partial_{\phi} \partial_{\phi'} \Pi^{C,D} \right) \frac{X^0}{1 - \Pi^{C,D} X^0} + \left(\partial_{\phi} \Pi^{C,D} \right) \left(\partial_{\phi'} \Pi^{C,D} \right) \left(\frac{X^0}{1 - \Pi^{C,D} X^0} \right)^2 \\ = -\partial_{\phi} \partial_{\phi'} \ln(1 - \Pi^{C,D} X^0). \end{aligned} \quad (2.47)$$

Note that only $\Pi^{C,D}$ depends on the fluxes. Here we realize that it is more convenient to consider the correlations of the thermodynamic potential,

$$\langle \Omega(\phi) \Omega(\phi') \rangle_c = \frac{2}{\pi^2} \int_0^{\infty} dy y \coth \frac{y}{2k_B T} \text{Re} \left[\sum_q \ln(-iy + \hbar D q_{\pm}^2) \right]_{C+D}. \quad (2.48)$$

The diagrammatic representation of this expression is shown in Fig. 2.3: Graphically one only has to remove the current vertices from the diagrams for the current fluctuations. The remaining diagrams are vacuum diagrams, as is normal for the thermodynamic potential. The summation is over momenta $q_{\pm} = 2\pi[n + (\phi \pm \phi')/\phi_0]/L$, with integer n and plus or minus for the cooperon or diffuson contributions. Problems of convergence can be overcome by subtracting, in Eq. (2.48), a flux independent

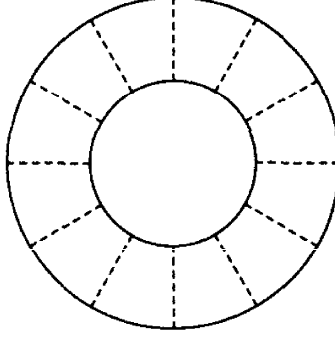


Figure 2.3: Diagram used for the calculation of the fluctuations of the grand potential \mathcal{M}_Ω .

constant. Note that for the vacuum diagram with M impurity lines, there is a symmetry factor $1/M$. Thus the impurity ladder does not sum up to $(1 - \Pi^{C,D} X^0)^{-1}$, but to

$$\sum_{M=1}^{\infty} \frac{1}{M} (\Pi^{C,D} X^0)^M = -\ln(1 - \Pi^{C,D} X^0). \quad (2.49)$$

Now we determine the Fourier coefficients, as before for the mean current. We write the summation over q in the form

$$\mathcal{M}_\Omega = \sum_{n=-\infty}^{n=+\infty} \left[G(4\pi^2 E_c (n+x)^2) \right]_{C+D}, \quad (2.50)$$

here $x = (\phi \pm \phi')/\phi_0$ since we have both cooperon and diffuson contributions. We obtain

$$\mathcal{M}_\Omega = \sum_{m=-\infty}^{m=+\infty} \left[e^{2\pi i m x} G_m \right]_{C+D} \quad (2.51)$$

with

$$G_m = \int_{-1/2}^{1/2} dx e^{-2\pi i m x} \sum_{n=-\infty}^{n=+\infty} G(4\pi^2 E_c (n+x)^2) = \int_{-\infty}^{+\infty} \frac{dx}{2\pi} e^{-i m x} G(E_c x^2). \quad (2.52)$$

Again, $G_m = G_{-m}$ which means that only terms $\propto \cos(2\pi m x)$ survive in Eq. (2.51). In the present example, Eq. (2.48), the integration over x is easily achieved after integrating by parts:

$$\begin{aligned} \int_{-\infty}^{\infty} \frac{dx}{2\pi} e^{-i m x} \text{Re} \ln(-iy + E_c x^2) &= \int_{-\infty}^{\infty} \frac{dx}{2\pi i m} e^{-i m x} \left(\frac{E_c x}{-iy + E_c x^2} + \frac{E_c x}{iy + E_c x^2} \right) \\ &= -\frac{1}{m} e^{-\sqrt{y m^2 / 2 E_c}} \cos \sqrt{y m^2 / 2 E_c}. \end{aligned} \quad (2.53)$$

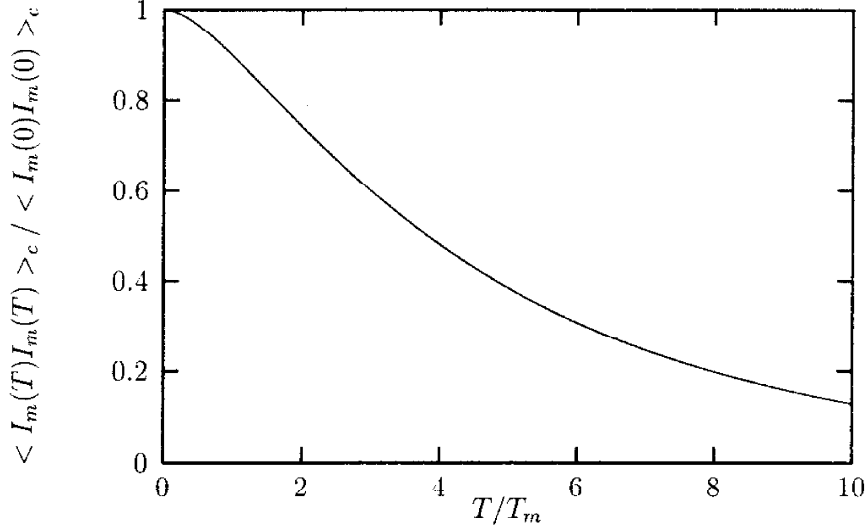


Figure 2.4: Temperature dependence of the m^{th} harmonic of the current fluctuations.

The combination of cooperon and diffuson terms is of the form

$$2 \sum_{m=1}^{\infty} G_m \left[\cos \left(\frac{\phi + \phi'}{\phi_0} 2\pi m \right) + \cos \left(\frac{\phi - \phi'}{\phi_0} 2\pi m \right) \right] = 4 \sum_{m=1}^{\infty} G_m \cos \left(\frac{2\pi m \phi}{\phi_0} \right) \cos \left(\frac{2\pi m \phi'}{\phi_0} \right). \quad (2.54)$$

The explicit result at zero temperature is the following:

$$\mathcal{M}_{\Omega} = \frac{96 E_c^2}{\pi^2} \sum_{m=1}^{\infty} \frac{1}{m^5} \cos \frac{2\pi m \phi}{\phi_0} \cos \frac{2\pi m \phi'}{\phi_0}, \quad (2.55)$$

from which we find $\langle I_m I_{m'} \rangle_c = \delta_{mm'} (e E_c)^2 96 / (\hbar^2 \pi^2 m^3)$.

Here the summation over all Fourier components does not lead to a singular behavior for the current for $\phi, \phi' \rightarrow 0$, as is the case for the mean current. The current fluctuations are of the order $\langle I^2 \rangle_c \sim (E_c / \phi_0)^2$ for all temperatures $k_B T < E_c$. Figure 2.4 shows the temperature dependence of the m^{th} harmonic. For $T > T_m = E_c / m^2$ it is strongly reduced. The temperature dependence will also be discussed in Ch. 4.

2.2 Interacting electrons

As pointed out in [24], the flux dependent contribution to the canonical potential given in Eq. (2.10) can be explained by the absence of global charge fluctuations. This becomes apparent by considering a grand canonical ensemble, and adding a capacitive energy [46, 47], i.e.

$$H_C = \frac{e^2}{2C} (\delta N)^2. \quad (2.56)$$

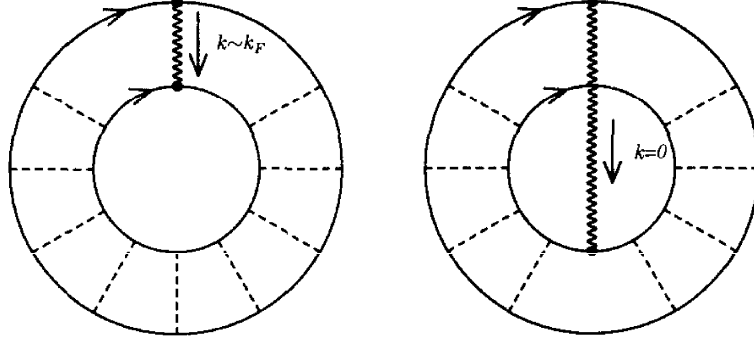


Figure 2.5: Diagrams representing the flux sensitive part of the grand potential Ω (Hartree contribution). The wavy line represents the Coulomb interaction. In the diagram on the left, the Coulomb interaction couples to local charge fluctuations, i.e. the interaction line carries a momentum of typically $k \sim k_F$. In the diagram on the right, the Coulomb interaction couples to global charge fluctuations, i.e. the interaction line carries zero momentum. The latter corresponds to the capacitance model.

If we take this expression – which is similar to (2.10) except that the charging energy $e^2/2C$ replaces the level spacing – directly, we find a persistent current which is comparable in size to the result for one-dimensional non-interacting electrons on a perfect ring (since $C \sim L$, and $e^2 \sim \hbar v_F$ for metallic densities, implying $e^2/2C \sim \hbar v_F/L$). However standard RPA approximation leads to the replacement

$$\frac{e^2}{C} \rightarrow \frac{e^2/C}{1 + \Delta^{-1}e^2/C} \simeq \Delta \quad (2.57)$$

since $\Delta \ll e^2/C$, and we are back to (2.10), i.e.

$$\langle \delta\Omega^C \rangle = \frac{1}{2} \Delta \langle (\delta N)^2 \rangle. \quad (2.58)$$

From this argument, it appears reasonable that an interaction, which suppresses the charge fluctuations locally and hence is a stronger constraint, leads to a larger persistent current. For example, consider the Hartree contribution to the grand potential,

$$\langle \delta\Omega^{EEI} \rangle = \frac{1}{2} \int d^3r d^3r' \tilde{v}(\mathbf{r} - \mathbf{r}') \langle \delta n(\mathbf{r}) \delta n(\mathbf{r}') \rangle \quad (2.59)$$

where \tilde{v} denotes the screened Coulomb interaction. The superscripts C and EEI denote capacitance and electron-electron interaction. Both parts of $\langle \delta\Omega \rangle$ are represented graphically in Fig. 2.5. By definition, the momentum transfer of an interaction line in $\langle \delta\Omega^C \rangle$ is $\mathbf{k} = 0$. The leading diagram consists of two cooperons. The momentum transfer of the local interaction line in $\langle \delta\Omega^{EEI} \rangle$ is of the order $k \sim k_F$, i.e. the leading diagram consists of only one cooperon. The latter calculation is

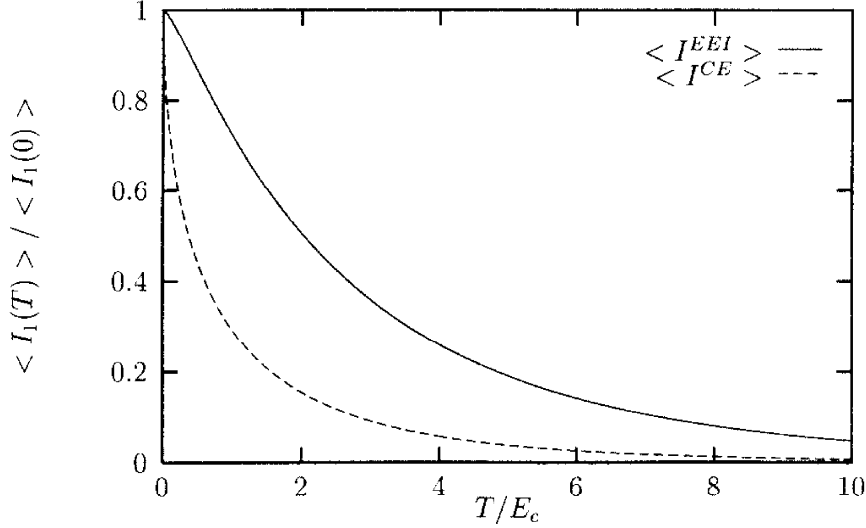


Figure 2.6: Temperature dependence of the first harmonic of the mean current. The solid line shows the normalized amplitude of the interaction contribution. Over the whole range plotted, this curve can be approximated by an exponential law, $\exp(-T/3E_c)$, which is in agreement with the experimental findings. The free electron contribution (dashed line) drops much more rapidly

more involved since Hartree and exchange (Fock) contributions are of the same order, and also higher orders in the interaction \tilde{v} have to be considered. Approximating \tilde{v} by a local interaction, $\tilde{v}(\mathbf{x}) \approx \tilde{v}\delta(\mathbf{x})$, we introduce the dimensionless coupling constant, $\lambda_0 = \tilde{v}\mathcal{N}_0$. Higher order corrections [38, 48, 49] can be absorbed in a renormalization of the coupling constant, $\lambda_0 \rightarrow \lambda_c \ll \lambda_0$. While the bare coupling constant can be reliably determined (copper: $\lambda_0 \sim 0.3$), the estimate $\lambda_c \sim \lambda_0/10$ is unfortunately very rough. Including Hartree and Fock contribution [27], the electron-electron interaction contribution to the grand potential is the following:

$$\langle \delta\Omega^{EEI} \rangle = -2\lambda_c \sum_q \int_0^\infty \frac{dy}{2\pi} y \coth \frac{y}{2k_B T} \text{Re} \frac{1}{-iy + \hbar D q^2}, \quad (2.60)$$

where at present $q = 2\pi(n + 2\phi/\phi_0)/L$. The final result for the Fourier coefficients of the persistent current at $T = 0$ is $\langle I_{2m}^{EEI} \rangle = eE_c \lambda_c 8 / \hbar \pi m^2 \sim \lambda_c (ev_F l / L^2) m^{-2}$.

In Fig. 2.6 we compare the temperature dependence of the first harmonic of the mean current, $\langle I^{CE} \rangle$ and $\langle I^{EEI} \rangle$. Both curves are scaled to their zero temperature values. Although the temperature scale for the suppression of the current is $T \sim E_c$ in both cases, it is apparent that $\langle I^{CE} \rangle$ (dashed line) is reduced stronger for finite temperatures than $\langle I^{EEI} \rangle$.

Chapter 3

Perturbation theories for magnetic impurities

As a preparation for the next chapter, where we study the effects of magnetic scattering on the persistent current, we introduce here two different perturbation schemes for magnetic impurities. The first method, a perturbation theory for the Kondo model, works well only for high temperatures, i.e. temperatures which are high compared to the Kondo temperature $T_K \sim \epsilon_F \exp(-1/2|J|\mathcal{N}_0)$.

In order to calculate the persistent current in systems with magnetic impurities for temperatures below the Kondo temperature we need another method. In the second part of the chapter we describe a local magnetic moment in the framework of the single impurity Anderson model. For this model, there exists a rather convenient perturbation theory which is valid for low temperatures, i.e. $T < T_K$.

From now on we use units, where $\hbar = k_B = 1$.

3.1 Perturbation theory for the Kondo model

For simplicity, we consider a system with a single paramagnetic impurity at the origin, $\mathbf{R} = 0$. The Hamiltonian in the presence of a magnetic field is

$$H = H_0 + H_{sd} \quad (3.1)$$

$$H_0 = \sum_{\mathbf{k}\sigma} \left(\epsilon_{\mathbf{k}} - \sigma \frac{\omega_s}{2} - \mu \right) c_{\mathbf{k}\sigma}^+ c_{\mathbf{k}\sigma} - \omega_s S^z \quad (3.2)$$

$$H_{sd} = -\frac{J}{\mathcal{V}} \sum_{\mathbf{k}\sigma\mathbf{k}'\sigma'} c_{\mathbf{k}\sigma}^+ c_{\mathbf{k}'\sigma'} \vec{\sigma}_{\sigma\sigma'} \cdot \vec{S}, \quad (3.3)$$

with $\omega_s = -2\mu_B H$ and $\sigma = \pm 1$. $c_{\mathbf{k}\sigma}^+$ and $c_{\mathbf{k}\sigma}$ are Fermi operators, $\vec{\sigma}$ are the Pauli matrices, and \vec{S} are the spin operators for a impurity with spin S . Here we only discuss spin $S = 1/2$ impurities. Electron Green's functions are defined as usual:

$$G_{\mathbf{k}\sigma\mathbf{k}'\sigma'}(\tau) = -\langle T_\tau c_{\mathbf{k}\sigma}^{(H)}(\tau) c_{\mathbf{k}'\sigma'}^{(H)+}(0) \rangle, \quad (3.4)$$

where $\langle \dots \rangle$ is the thermal average over the exact statistical operator, and $c_{\mathbf{k}\sigma}^{(H)}(\tau)$ is a Heisenberg operator. Following the procedure, described e.g. in [44], this can be written as

$$G_{\mathbf{k}\sigma\mathbf{k}'\sigma'}(\tau) = \frac{-\langle T_\tau S(\beta) c_{\mathbf{k}\sigma}(\tau) c_{\mathbf{k}'\sigma'}^\dagger(0) \rangle_0}{\langle S(\beta) \rangle_0}. \quad (3.5)$$

Here, $\langle \dots \rangle_0$ is the thermal average over the unperturbed statistical operator, $c_{\mathbf{k}\sigma}(\tau)$ is an operator in interaction representation, and $S(\beta)$ is defined by

$$S(\beta) = T_\tau \exp \left[- \int_0^\beta d\tau' H_{sd}(\tau') \right]. \quad (3.6)$$

A perturbation expansion leads to averages over spin operators, like $-\langle S^a(\tau) \rangle_0$, $-\langle T_\tau S^a(\tau_1) S^b(\tau_2) \rangle_0$, and so on ($a, b, c = x, y, z$). Unfortunately, the spin operators obey neither Fermi nor Bose commutation rules, and Wick's theorem does not exist.

We expand the S -matrix in the nominator and the denominator of Eq. (3.5). For example an expansion up to second order in H_{sd} is graphically represented as

$$G = \frac{\text{Nominator diagrams}}{1 + \text{Denominator diagrams}}$$

The solid lines represent electron Green's functions, the small circles are the interactions. The dashed lines which are connecting two such circles indicate that the thermal average of two (or more) spin-operators, like e.g. $\langle T_\tau S^z(\tau) S^z(0) \rangle$ has to be calculated.

Usually, the denominator just cancels the unconnected diagrams of the nominator. Here we do not have a linked cluster theorem, and the Green's function in second order in H_{sd} is

$$G = \text{solid line} + \text{solid line with dot} + \text{solid line with two dots connected by dashed line} + \text{solid line with dot and self-energy loop} - \text{solid line with dot and self-energy loop}$$

All effects of magnetic scattering on the electron Green's function can be absorbed into the T -matrix, which is defined by

$$G_{\mathbf{k}\sigma\mathbf{k}'\sigma'} = G_{\mathbf{k}\sigma}^0 \delta_{\mathbf{k}\sigma\mathbf{k}'\sigma'} + G_{\mathbf{k}\sigma}^0 T_{\mathbf{k}\sigma\mathbf{k}'\sigma'} G_{\mathbf{k}'\sigma'}^0. \quad (3.7)$$

with $G_{\mathbf{k}\sigma}^0 = (i\omega_n - \epsilon_{\mathbf{k}} + \mu + \sigma\omega_s/2)^{-1}$.

3.1.1 Abrikosov's pseudo fermion method

Abrikosov described a method to evaluate thermal averages over spin operators within a diagrammatic approach. This method is frequently used and also explained in the literature, see e.g. [50, 51]. The spin operators are represented using an expression which is quadratic in Fermi operators,

$$\vec{S} = \sum_{mm'} \vec{S}_{mm'} a_m^+ a_{m'}, \quad (3.8)$$

where a_m^+ and a_m are the Fermi operators. $\vec{S}_{mm'}$ are matrices, for spin 1/2 they are proportional to the Pauli matrices, $\vec{S}_{mm'} = \vec{\sigma}_{mm'}/2$. For the full equivalence of spin states and pseudo fermion states, the number of fermions has to be one, i.e. the constraint $\sum_m a_m^+ a_m = 1$ has to be fulfilled. In an average

$$\text{Tr} \{ e^{-\beta H_0} O \}, \quad (3.9)$$

where the operator O is the product of an arbitrary number of spin operators, the contribution of states with more than one pseudo fermion will vanish, if we add to the Hamiltonian a term $\lambda(\sum_m a_m^+ a_m - 1)$ and let $\lambda \rightarrow \infty$, i.e.

$$\text{Tr} \{ e^{-\beta H_0} O \} = \lim_{\lambda \rightarrow \infty} e^{\beta \lambda} \text{Tr} \{ e^{-\beta(H_0 + H_\lambda)} O \}. \quad (3.10)$$

where $H_\lambda = \lambda \sum_m a_m^+ a_m$. The partition sum is represented in a similar way,

$$\text{Tr} \{ e^{-\beta H_0} \} = \lim_{\lambda \rightarrow \infty} e^{\beta \lambda} \text{Tr} \left\{ e^{-\beta(H_0 + H_\lambda)} \sum_m a_m^+ a_m \right\}. \quad (3.11)$$

For the thermal average of an operator we find:

$$\frac{\text{Tr} \{ e^{-\beta H_0} O \}}{\text{Tr} \{ e^{-\beta H_0} \}} = \lim_{\lambda \rightarrow \infty} \frac{\text{Tr} \{ e^{-\beta(H_0 + H_\lambda)} O \}}{\text{Tr} \{ e^{-\beta(H_0 + H_\lambda)} \}} \frac{\text{Tr} \{ e^{-\beta(H_0 + H_\lambda)} \}}{\text{Tr} \{ e^{-\beta(H_0 + H_\lambda)} a_m^+ a_m \}} \quad (3.12)$$

The first of these factors can be evaluated using Wick's theorem, i.e. standard diagrammatic rules, for the pseudo fermions. The second factor is given by

$$\frac{\text{Tr} \{ e^{-\beta(H_0 + H_\lambda)} \}}{\text{Tr} \{ e^{-\beta(H_0 + H_\lambda)} a_m^+ a_m \}} = \frac{e^{\beta \lambda}}{\sum_m e^{m \omega_s / T}}, \quad (3.13)$$



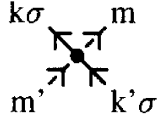
where we used that $\lambda \rightarrow \infty$. The free pseudo fermion Green's function is

$$g_{mm'}^0(\tau) = - \frac{\text{Tr} \{ e^{-\beta(H_0 + H_\lambda)} T_\tau c_m(\tau) c_{m'}^+(0) \}}{\text{Tr} \{ e^{-\beta(H_0 + H_\lambda)} \}}, \quad (3.14)$$

which gives in frequency representation

$$g_{mm'}^0(i\omega_n) = \delta_{mm'} \frac{1}{i\omega_n - \lambda + m\omega_s}. \quad (3.15)$$

The elements of the diagrammatic expansion are:

- The electron Green's function, $G^0(i\omega_n, \mathbf{k}\sigma)$: 
- The pseudo fermion Green's function, $g_{mm'}^0(i\omega_n)$: 
- The vertex, $-(J/\mathcal{V})\vec{\sigma}_{\sigma\sigma'} \cdot \vec{S}_{mm'}$: 

As an example, we consider the diagram

$$T_{\mathbf{k}\sigma\mathbf{k}'\sigma'}^{(1)} = \text{Feynman diagram: a solid line with a loop (Feynman loop) on top, connected to a vertex, which is then connected to another solid line.} \quad (3.16)$$

which is the first order contribution to the T -matrix. Without any pseudo fermions it is evaluated as $T_{\mathbf{k}\sigma\mathbf{k}'\sigma'}^{(1)} = -(J/\mathcal{V})\sigma_{\sigma\sigma'}^z \langle S^z \rangle$. Within the pseudo fermion approach, this is found from

$$\begin{aligned} T_{\mathbf{k}\sigma\mathbf{k}'\sigma'}^{(1)} &= \lim_{\lambda \rightarrow \infty} \frac{e^{\lambda/T}}{e^{\omega_s/2T} + e^{-\omega_s/2T}} (-) (-J/\mathcal{V}) (-T) \sum_{\omega_n} \sum_m \sigma_{\sigma\sigma'}^z S_{mm}^z g_{mm}^0(i\omega_n) \\ &= -\left(\frac{J}{2\mathcal{V}} \tanh \frac{\omega_s}{2T} \right) \sigma_{\sigma\sigma'}^z. \end{aligned} \quad (3.17)$$

The extra minus sign in the first line of the equation is due to the Fermi loop. As a general rule, each pseudo Fermi loop produces a factor $e^{-\beta\lambda}$, i.e. diagrams with more than one closed loop can be discarded.

The pseudo fermion self energy, first order in J is:

$$\Sigma_{mm}^{(1)}(i\omega_n) = \frac{J}{\mathcal{V}} (-T) \sum_{\omega_n} \sum_{\mathbf{k}\sigma} \sigma_{\sigma\sigma}^z S_{mm}^z G(i\omega_n, \mathbf{k}\sigma) \quad (3.18)$$

$$= -S_{mm}^z J \mathcal{N}_0 \omega_s, \quad (3.19)$$

i.e. there is a correction to the Zeeman energy, which is called Knight shift: $\omega_s \rightarrow \omega_s(1 + J\mathcal{N}_0)$. In the previous section, we found three diagrams for the second order correction to the Green's function, i.e. to $T_{\mathbf{k}\sigma\mathbf{k}'\sigma'}^{(2)}$. Two of these, and especially the unlinked diagram, appear due to the Knight shift.

In the second order in J , there appear the typical logarithmic singularities. The T -matrix, second order in J is calculated in App. B. For the second order self energy, we refer to the literature, e.g. [50–52]. For $\omega_s = 0$, the result is ($T = 0$, $i\omega_n - \lambda \rightarrow \omega + i0$):

$$\text{Re}\Sigma_{mm}^{(2)}(\omega) = -(J\mathcal{N}_0)^2 2S(S+1)\omega \ln \frac{\epsilon_F}{\omega}. \quad (3.20)$$

The imaginary part of the retarded self energy is ($\omega \ll T$):

$$\text{Im}\Sigma_{mm}^{(2)}(\omega) = -2S(S+1)(J\mathcal{N}_0)^2 \pi T. \quad (3.21)$$

The imaginary part of this self energy is of the same order of magnitude as the Korringa relaxation rate $1/\tau_K = 4(J\mathcal{N}_0)^2\pi T$, which appears in the spin-spin correlation function [52, 53].

3.2 Renormalized perturbation theory for the Anderson model

The perturbation theory introduced in the previous section breaks down if the temperature approaches the Kondo temperature T_K . For low temperature, analytic calculations can be performed within the framework of a phenomenological Fermi liquid theory [54], or within a Fermi liquid approach based on perturbation theory for the Anderson model. Here we choose the second method. It has been developed by Yosida and Yamada [55–57], later formulated by Hewson [58, 59] as a renormalized perturbation expansion. The Hamiltonian for the Anderson model is

$$H = \sum_{\mathbf{k}, \sigma} \left(\epsilon_{\mathbf{k}} - \sigma \frac{\omega_s}{2} - \mu \right) c_{\mathbf{k}\sigma}^\dagger c_{\mathbf{k}\sigma} + \sum_{\sigma} \left(\epsilon_d - \sigma \frac{\omega_s}{2} - \mu \right) d_{\sigma}^\dagger d_{\sigma} + U n_{d\uparrow} n_{d\downarrow} + \frac{V}{\sqrt{\mathcal{V}}} \sum_{\mathbf{k}\sigma} (d_{\sigma}^\dagger c_{\sigma} + c_{\sigma}^\dagger d_{\sigma}), \quad (3.22)$$

with d_{σ}^\dagger and d_{σ} the creator and annihilator of a d -electron, U the on-site repulsion, V the hybridization with the conduction band. For $U = 0$, the model can be solved without problems, the Green's function for the d -electrons is

$$G_{d\sigma}(i\omega_n) = \frac{1}{i\omega_n - \epsilon_d + \sigma\omega_s/2 + \mu + i\delta(i\omega_n)} \quad (3.23)$$

with

$$-i\delta(i\omega_n) = V^2 \int \frac{d^3k}{(2\pi)^3} G(i\omega_n, \mathbf{k}). \quad (3.24)$$

For a flat and wide conduction band, this results in $\delta = \pi\mathcal{N}_0 V^2 \text{sgn}(\omega_n)$. However, we are interested in the case, where the Anderson model and the Kondo model describe the same physics, which is true in the limit where the interaction U is strong. To be more precise, the conditions $\epsilon_d \ll \epsilon_F$, $\epsilon_d + U \gg \epsilon_F$ with $|\epsilon_d + U - \epsilon_F|$, $|\epsilon_F - \epsilon_d| \gg \delta$ have to be valid (see for example [59]).

The (retarded) Green's function for the interacting model is

$$G_{d\sigma}(\omega) = \frac{1}{\omega - \epsilon_d + \mu + i\delta - \Sigma_{\sigma}^R(\omega)}. \quad (3.25)$$

and the Green's function for the conduction band electrons

$$G_{\mathbf{k}\sigma\mathbf{k}'\sigma}(\omega) = G_{\mathbf{k}\sigma}^0 \delta_{\mathbf{k}\mathbf{k}'} + G_{\mathbf{k}\sigma}^0 T_{\mathbf{k}\sigma\mathbf{k}'\sigma} G_{\mathbf{k}'\sigma}^0 \quad (3.26)$$

$$= G_{\mathbf{k}\sigma}^0 \delta_{\mathbf{k}\mathbf{k}'} + G_{\mathbf{k}\sigma}^0 \frac{V}{\sqrt{\mathcal{V}}} G_{d\sigma}(\omega) \frac{V}{\sqrt{\mathcal{V}}} G_{\mathbf{k}'\sigma}^0. \quad (3.27)$$

A perturbation theory in U works well for small U , but since we are interested in the large U limit, a finite order perturbation theory does not work. What helps is a renormalized perturbation theory, as described by Hewson [58, 59].

We assume that the Green's function can be written as

$$G_{d\sigma}(\omega) = \frac{z}{\omega - \tilde{\epsilon}_d + i\tilde{\delta} - \tilde{\Sigma}_\sigma^R(\omega)} \quad (3.28)$$

with the conditions

$$\tilde{\Sigma}_\sigma(0, 0) = 0; \quad \frac{\partial}{\partial \omega} \tilde{\Sigma}_\sigma(0, 0) = 0. \quad (3.29)$$

The self energy as a function of two arguments indicates that it has to be taken not only at $\omega = 0$, but also $T = \omega_s = 0$. It is possible to write down the self energy in the form given above, if the derivative of the self-energy for $\omega = 0$ and $T = 0$ exists,

$$\Sigma_\sigma(\omega) = \Sigma_\sigma(0) + \omega \frac{\partial}{\partial \omega} \Sigma_\sigma(0) + \Sigma_\sigma^{Rem}(\omega). \quad (3.30)$$

This equation defines $\Sigma^{Rem}(\omega)$. The so called wave function renormalization factor, z , is defined as $z = [1 - \partial_\omega \Sigma_\sigma(0, 0)]^{-1}$. Using this quantity, the renormalized parameters can be expressed as

$$\tilde{\epsilon}_d = z[\epsilon_d - \mu + \Sigma_\sigma(0, 0)] \quad (3.31)$$

$$\tilde{\delta} = z\delta \quad (3.32)$$

$$\tilde{\Sigma}(\omega) = z\Sigma^{Rem}(\omega) \quad (3.33)$$

The renormalized four point vertex function is defined as $\tilde{\Gamma}_{\sigma\sigma'} = z^2\Gamma_{\sigma\sigma'}$, and especially the renormalized interaction constant is

$$\tilde{U} = \tilde{\Gamma}_{\uparrow\downarrow}(0, 0). \quad (3.34)$$

After defining rescaled operators for the d -electrons, $\tilde{d}_\sigma = d_\sigma/\sqrt{z}$, $\tilde{d}_\sigma^\dagger = d_\sigma^\dagger/\sqrt{z}$ and a rescaled hybridization $\tilde{V} = \sqrt{z}V$ we rewrite the Hamiltonian $H = H_{qp} - H_c$, where H_{qp} is the quasi-particle Hamiltonian

$$H_{qp} = \sum_{\mathbf{k}, \sigma} (\epsilon_{\mathbf{k}} - \mu) c_{\mathbf{k}\sigma}^\dagger c_{\mathbf{k}\sigma} + \sum_{\sigma} \tilde{\epsilon}_d \tilde{d}_\sigma^\dagger \tilde{d}_\sigma + \tilde{U} \tilde{n}_{d\uparrow} \tilde{n}_{d\downarrow} + \frac{\tilde{V}}{\sqrt{V}} \sum_{\mathbf{k}\sigma} (\tilde{d}_\sigma^\dagger c_\sigma + c_\sigma^\dagger \tilde{d}_\sigma). \quad (3.35)$$

The counter terms ensure, that H is not changed by our rewriting:

$$H_c = \lambda_1 \sum_{\sigma} \tilde{d}_\sigma^\dagger \tilde{d}_\sigma + \lambda_2 \tilde{n}_{d\uparrow} \tilde{n}_{d\downarrow}, \quad (3.36)$$

with $\lambda_1 = z\Sigma(0, 0)$ and $\lambda_2 = z^2[\Gamma_{\uparrow\downarrow}(0, 0) - U]$. Instead of a perturbation theory for the strongly interacting bare electrons, a perturbation theory for the weakly interacting quasi particles is now possible. We take the renormalized parameters $\tilde{\epsilon}_d$,

$\tilde{\delta}$, and \tilde{U} as given. They can be determined by comparing results from this renormalized perturbation expansion with results found from the Bethe Ansatz solution¹: For the Kondo model, the scattering resonance is at the Fermi level, $\tilde{\epsilon}_d = 0$, the width is of the order of the Kondo temperature, $\tilde{\delta} = 4T_K/\pi w$ where $w \approx 0.41$. The strength of the quasi particle interaction is $\tilde{U} = \pi\tilde{\delta} = 4T_K/w$.

λ_1 , λ_2 , and z are expressed as power series in \tilde{U} , $\lambda_1 = \sum_{n=0}^{\infty} \lambda_1^{(n)} \tilde{U}^n$, ... and the coefficients are adjusted in the way that the renormalization conditions, Eqs. (3.29) and (3.34) are fulfilled in each order in the expansion.

The effects of the quasi particle interaction go to zero for $T \rightarrow 0$ and $\omega \rightarrow 0$. In this limit, the quasi particle Green's function and the T -matrix are given by

$$\tilde{G}_{d\sigma}(\omega) = \frac{1}{\omega + i\tilde{\delta}} = \frac{1}{\omega + i4T_K/\pi w} \quad (3.37)$$

$$T_{\mathbf{k}\sigma\mathbf{k}'\sigma'}(\omega) = \frac{\tilde{V}^2}{\mathcal{V}} \frac{1}{\omega + i\tilde{\delta}} = \frac{1}{\pi\mathcal{N}_0\mathcal{V}} \frac{4T_K}{\pi w} \frac{1}{\omega + i4T_K/\pi w} \quad (3.38)$$

In first order in the quasi-particle interaction, we have

$$\Sigma_{\sigma}^{(1)}(\omega) = \text{[Diagram: a circle with a wavy line below it]} = \tilde{U}n_{d-\sigma} \quad \text{and} \quad \Gamma_{\sigma\sigma'} = \text{[Diagram: a wavy line with arrows labeled } \sigma \text{ and } \sigma'] = \tilde{U}(1 - \delta_{\sigma\sigma'})$$

from which we find for the three renormalization constants: $z^{(1)} = 1$, $\lambda_1^{(1)} = \tilde{U}n_{d-\sigma}$, and $\lambda_2^{(1)} = 0$. A small change in the chemical potential, $\mu \rightarrow \mu + \delta\mu$, does not change the occupancy of the d -level, i.e. the charge susceptibility is zero. In first order in the quasi particle interaction, this can be seen from the relation

$$\frac{\partial}{\partial \mu} \tilde{\Sigma}_{\sigma}|_{\omega=0, T=0} = -\tilde{U} \int \frac{d\omega}{2\pi} \left(\frac{1}{i\omega + i\tilde{\delta}\text{sgn}(\omega)} \right)^2 \quad (3.39)$$

$$= \frac{\tilde{U}}{\pi\tilde{\delta}} = 1, \quad (3.40)$$

such that the Green's function,

$$\tilde{G}_{d\sigma}(\omega) = \frac{1}{\omega + \delta\mu + i\tilde{\delta} - \delta\mu\partial_{\mu}\tilde{\Sigma}} = \frac{1}{\omega + i\tilde{\delta}} \quad (3.41)$$

does not depend on $\delta\mu$. On the other hand, the quasi particle interaction enhances the effect of a magnetic field by a factor two, $\partial_{\omega_s} \tilde{\Sigma}_{\sigma}|_{\omega=0, T=0} = -\sigma/2$ and $\tilde{G}_{d\sigma}(\omega) = (\omega + i\tilde{\delta} + \sigma\omega_s)^{-1}$.

The self energy in second order in \tilde{U} is found from the diagram

$$\Sigma_{\sigma}^{(2)}(\omega) = \text{[Diagram: a circle with two wavy lines below it, one on each side]} =$$

¹Exact results for the Kondo and Anderson model are reviewed in [60].

We only give the result for the self energy to order ω^2 and T^2 ,

$$-\text{Im}\tilde{\Sigma}_\sigma(\omega) = \left(\frac{\tilde{U}}{\pi\delta}\right)^2 \frac{1}{2\delta}(\omega^2 + \pi^2 T^2). \quad (3.42)$$

It has been shown [59], that this result is exact in all orders in \tilde{U} . With the self energy as given above, it is possible to determine many physical properties (specific heat, spin- and charge susceptibility, conductivity) exactly for low temperature.

Chapter 4

The effects of magnetic impurities on the persistent current

The sensitivity of quantum coherence with respect to magnetic scattering is well known. It has been discussed in detail for weak localization [8, 10, 61–63] and conductance fluctuations [17, 64–67]. Persistent currents in the presence of magnetic impurities have been discussed in [49, 68, 69], including effects of spin-flip scattering, spin-orbit scattering and Zeeman splitting. In these papers the spin configuration was considered static, leaving the role of impurity spin dynamics an open problem.

In order to include impurity spin dynamics we start from the Hamiltonian where the local magnetic moments are coupled to the conduction band electrons by a local exchange coupling

$$H = H_0 + H_{imp} + H_{sd} \quad (4.1)$$

$$H_0 = \sum_{\mathbf{k}, \sigma} \left(\epsilon_{\mathbf{k}} - \mu - \sigma \frac{\omega_s}{2} \right) c_{\mathbf{k}\sigma}^+ c_{\mathbf{k}\sigma} - \omega_s \sum_{\mathbf{R}_s} S_{\mathbf{R}_s}^z \quad (4.2)$$

$$H_{imp} = -\frac{W}{\mathcal{V}} \sum_{\mathbf{R}_i} \sum_{\mathbf{k}\mathbf{k}'\sigma} \exp[-i(\mathbf{k} - \mathbf{k}') \cdot \mathbf{R}_i] c_{\mathbf{k}\sigma}^+ c_{\mathbf{k}'\sigma} \quad (4.3)$$

$$(4.4)$$

$$H_{sd} = -\frac{J}{\mathcal{V}} \sum_{\mathbf{R}_s} \sum_{\mathbf{k}\mathbf{k}'\sigma\sigma'} \exp[-i(\mathbf{k} - \mathbf{k}') \cdot \mathbf{R}_s] c_{\mathbf{k}\sigma}^+ c_{\mathbf{k}'\sigma'} \vec{\sigma}_{\sigma\sigma'} \cdot \vec{S}_{\mathbf{R}_s}. \quad (4.5)$$

W and J are the coupling constants for the non-magnetic and the magnetic impurities, \mathbf{R}_i and \mathbf{R}_s are the sites of non-magnetic and magnetic impurities, $c_{\mathbf{k}\sigma}^+$ and $c_{\mathbf{k}\sigma}$ the Fermi operators, $\vec{\sigma}$ are the Pauli matrices and $\vec{S}_{\mathbf{R}_s}$ denotes the spin-operator for a spin $S = 1/2$ impurity at site \mathbf{R}_s .

This model contains a number of energy scales that determine the behavior of the system [70]: The spin-flip scattering rate $1/\tau_s = n_s S(S+1) J^2 2\pi \mathcal{N}_0$ ($n_s = N_s/\mathcal{V}$ is the density of magnetic impurities), the Korringa time which determines spin relaxation,

$1/\tau_K \sim T(J\mathcal{N}_0)^2$, the Kondo temperature given by $T_K \sim \epsilon_F \exp(-1/2|J|\mathcal{N}_0)$, and finally the spin glass temperature which is of the order of $T_{SG} \sim n_s J^2 \mathcal{N}_0$.

The plan of this chapter is as follows. We calculate the persistent current under different assumptions: In Ch. 4.1 we assume that the spin-flip scattering rate $1/\tau_s$ is comparable in size with the Thouless energy, but the concentration of impurities is low enough to exclude spin glass ordering. We also assume that the Kondo temperature is far below the Thouless energy. Due to these conditions, we neglect the RKKY interaction between the magnetic impurities and we take into account the coupling of the impurity spins with the conduction band only to second order in the coupling J .

In Ch. 4.2 we discuss the persistent current in spin glasses. This is relevant for systems with a high concentration of magnetic impurities.

In Ch. 4.3 we will neglect the RKKY interaction, i.e. the results are relevant for systems with a low concentration of magnetic impurities. Here we extend the calculations of Ch. 4.1 to the case where the Kondo temperature is comparable to the Thouless energy.

In the entire chapter, we assume that the non-magnetic scattering rate is large compared to the magnetic scattering rate.

4.1 Spin polarization in magnetic fields

Here we discuss magnetic scattering perturbatively in J , i.e. we exclude the Kondo effect. The concentration of magnetic impurities is assumed to be low, so that interactions between magnetic impurities can be neglected. We include both the Zeeman splitting of the conduction band and the effect of Zeeman splitting on exchange scattering. In a magnetic field, the impurity spins are polarized, $\langle \vec{S} \rangle \neq 0$. Assuming that the magnetic field is in z -direction, we have¹ $\langle S^x \rangle = \langle S^y \rangle = 0$, and $\langle S^z \rangle = \tanh(\omega_s/2T)/2$. $\langle \dots \rangle$ denotes the thermal average. The corresponding first order contribution to the electron self energy is

$$\Sigma_{\alpha\beta}^{(1)} = -n_s J \vec{\sigma}_{\alpha\beta} \langle \vec{S} \rangle = -n_s J \sigma_{\alpha\beta}^z \frac{1}{2} \tanh \frac{\omega_s}{2T}. \quad (4.6)$$

In second order in J , there is an effective electron-electron interaction due to the coupling of conduction band electrons and magnetic impurities. In imaginary time representation it is given by

$$V_{\alpha\beta\gamma\delta}(i\omega_n) = -\left(\frac{J}{\mathcal{V}}\right)^2 \int_0^\beta d\tau e^{i\omega_n \tau} \sum_{a,b=x,y,z} \sigma_{\alpha\gamma}^a \sigma_{\beta\delta}^b \langle T_\tau S^a(\tau) S^b(0) \rangle. \quad (4.7)$$

¹We neglect the Knight shift.

T_τ is the time ordering. The result is

$$V_{\alpha\beta\gamma\delta}(i\omega_n) = -\left(\frac{J}{V}\right)^2 \frac{1}{T} \frac{1}{4} \delta_{0\omega_n} \sigma_{\alpha\gamma}^z \sigma_{\beta\delta}^z - \left(\frac{J}{V}\right)^2 \tanh \frac{\omega_s}{2T} \frac{1}{i\omega_n + \omega_s} \sigma_{\alpha\gamma}^+ \sigma_{\beta\delta}^- + \left(\frac{J}{V}\right)^2 \tanh \frac{\omega_s}{2T} \frac{1}{i\omega_n - \omega_s} \sigma_{\alpha\gamma}^- \sigma_{\beta\delta}^+ \quad (4.8)$$

where $\omega_n = 2\pi nT$ is a bosonic Matsubara frequency. There is no energy transfer if no spins are flipped, i.e. in the $\sigma_{\alpha\gamma}^z \sigma_{\beta\delta}^z$ term. For weak magnetic fields, $\omega_s/T \rightarrow 0$, all contributions to $V_{\alpha\beta\gamma\delta}$ become static,

$$V_{\alpha\beta\gamma\delta}(i\omega_n) = -\frac{1}{T} \frac{1}{4} \left(\frac{J}{V}\right)^2 \bar{\sigma}_{\alpha\gamma} \bar{\sigma}_{\beta\delta} \delta_{0\omega_n}. \quad (4.9)$$

The electron self energy in second order in J is

$$\Sigma_\gamma^{(2)}(i\epsilon_n) = N_s(-T) \sum_{\omega_l} \sum_{\mathbf{k}\alpha} V_{\gamma\alpha\alpha\gamma}(i\omega_l) G(i\epsilon_n - i\omega_l, \mathbf{k}). \quad (4.10)$$

Since $\Sigma^{(2)}$ (and $\Sigma^{(1)}$) is diagonal in the spin, here and below we use a simplified notation, $\Sigma_{++} \rightarrow \Sigma_+$, $\Sigma_{--} \rightarrow \Sigma_-$. Details of the calculation of the self energy are given in App. B. After analytical continuation, $i\epsilon_n \rightarrow \epsilon + i0$, the retarded self energy in second order is found as

$$\text{Re}\Sigma_\gamma^{R(2)}(\epsilon, \omega_s) = n_s J^2 \mathcal{N}_0 \tanh \frac{\gamma\omega_s}{2T} \left[\ln \frac{\epsilon_F}{2\pi T} - \text{Re}\Psi \left(\frac{1}{2} - i \frac{\epsilon + \gamma\omega_s}{2\pi T} \right) \right] \quad (4.11)$$

$$\begin{aligned} \text{Im}\Sigma_\gamma^{R(2)}(\epsilon, \omega_s) &= -n_s \pi \mathcal{N}_0 J^2 \tanh \frac{\gamma\omega_s}{2T} [n_B(\gamma\omega_s) + n_F(\gamma\omega_s + \epsilon)] \\ &\quad - \frac{1}{4} \pi \mathcal{N}_0 n_s J^2. \end{aligned} \quad (4.12)$$

n_s is the density of the magnetic impurities, n_B and n_F the Bose and Fermi functions, $\gamma = \pm 1$, and Ψ the digamma function. The term first order in J , Eq. (4.6), renormalizes the electron Zeeman energy,

$$\omega_s \rightarrow \omega_s + n_s J \tanh(\omega_s/2T), \quad (4.13)$$

compare Eq. (4.14) below. Above the Kondo temperature, the second order correction to the real part of Σ is small compared to the first order, nevertheless it has to be included since it is of the same order as $1/\tau_s$.

For $\omega_s = 0$, only the second order contribution to the self energy survives, which is purely imaginary, $-\text{Im}\Sigma_\gamma^R(\epsilon) = n_s 3\pi \mathcal{N}_0 J^2/4 = 1/2\tau_s$. In the presence of magnetic fields, $\text{Im}\Sigma_\gamma^R(\epsilon)$ is energy and spin dependent. The first of the two terms on the right hand side of Eq. (4.12) describes spin-flip processes; for $|\omega_s| \gg T$ and $|\epsilon| < \omega_s$, spin-flip is forbidden and this term is negligible.

The impurity averaged retarded Green's function is given by

$$G_\gamma^R(\epsilon_+, \mathbf{k}) = \frac{1}{\epsilon_+ - \mathbf{k}^2/2m + \mu + \gamma\omega_s/2 + i/2\tau + i/2\tau_{so} - \Sigma_\gamma^R(\epsilon_+)}, \quad (4.14)$$

where $1/\tau$ and $1/\tau_{so}$ are the non-magnetic and the spin-orbit scattering rates, and $\Sigma_\gamma^R(\epsilon_+)$ is the spin and energy dependent contribution of the paramagnetic impurities to the self energy as calculated above in Eqs. (4.6,4.11,4.12). Spin-orbit scattering is briefly discussed in App. C.1.

4.1.1 Non-interacting electrons

For non-interacting electrons the main task is to determine the potential correlator $\langle \Omega(\phi)\Omega(\phi') \rangle_c$, from which both the mean current and the current fluctuations can be found. $\Pi_{\gamma\delta}^{C,D}$, defined now by (compare Eq. (2.38))

$$\Pi_{\gamma\delta}^{C,D} = \int \frac{d^3k}{(2\pi)^3} G_\gamma^R(\epsilon_+, \mathbf{k}) G_\delta^A(\epsilon_-, \mp \mathbf{k} \pm \mathbf{q}) \quad (4.15)$$

is given by

$$\Pi_{\gamma\delta}^{C,D}/2\pi\mathcal{N}_0\tau = 1 - \tau \left[-i(\epsilon_+ - \epsilon_-) + Dq_\pm^2 - i\frac{\gamma\omega_s - \delta\omega'_s}{2} + \gamma_{\gamma\delta} + \frac{1}{\tau_{so}} \right] \quad (4.16)$$

where $\gamma_{\gamma\delta} = i(\Sigma_\gamma^R - \Sigma_\delta^A)$. We omitted the dependence of $\Pi_{\gamma\delta}^{C,D}$ on the difference of chemical potentials. The spin-flip scattering rate, the spin-orbit scattering rate, and the Zeeman energy are assumed to be small compared to the non-magnetic elastic scattering rate, $1/\tau$.

Considering correlations between two different systems, the bare impurity vertices $X_{\alpha\beta\gamma\delta}^0$ are given by

$$2\pi\mathcal{N}_0 D_{\alpha\beta\gamma\delta}^0 = \frac{1}{\tau} \delta_{\alpha\gamma} \delta_{\delta\beta} + \frac{1}{3\tau_{so}} \vec{\sigma}_{\alpha\gamma} \vec{\sigma}_{\delta\beta} + \gamma_z \sigma_{\alpha\gamma}^z \sigma_{\delta\beta}^z \quad (4.17)$$

and

$$2\pi\mathcal{N}_0 C_{\alpha\beta\gamma\delta}^0 = \frac{1}{\tau} \delta_{\alpha\gamma} \delta_{\beta\delta} - \frac{1}{3\tau_{so}} \vec{\sigma}_{\alpha\gamma} \vec{\sigma}_{\beta\delta} + \gamma_z \sigma_{\alpha\gamma}^z \sigma_{\beta\delta}^z \quad (4.18)$$

where

$$\gamma_z = 2\pi\mathcal{N}_0 n_s J^2 \langle S^z \rangle \langle S^z \rangle' = n_s \frac{1}{2} \pi \mathcal{N}_0 J^2 \tanh\left(\frac{\omega_s}{2T}\right) \tanh\left(\frac{\omega'_s}{2T}\right). \quad (4.19)$$

In order to determine the potential correlator \mathcal{M}_Ω , we have to compute the eigenvalues λ_j^X of $X_{\alpha\beta\gamma\delta}^0 \Pi_{\gamma\delta}^X$, which can be considered as a 4×4 matrix:

$$\begin{aligned} \langle \Omega(\phi)\Omega(\phi') \rangle_c &= \sum_{X=C,D} \sum_{m=1}^{\infty} \frac{1}{m} \text{Tr}(X^0 \Pi^X)^m \\ &= \sum_{X=C,D} \sum_{m=1}^{\infty} \sum_{j=1}^4 \frac{1}{m} (\lambda_j^X)^m = - \sum_{X=C,D} \sum_{j=1}^4 \ln(1 - \lambda_j^X). \end{aligned} \quad (4.20)$$

In principle, the summation should be from $m = 2$ instead of $m = 1$ due to charge neutrality [29]. However, $m = 1$ gives a non-flux dependent constant and after differentiation with respect to the flux it is equal if we add this term or not. We express the cooperon parts using the combinations

$$N_0 = -i(\epsilon_+ - \epsilon_-) + Dq_+^2 + \frac{\gamma_{+-} + \gamma_{-+}}{2} + \gamma_z \quad (4.21)$$

$$N_1 = -i(\epsilon_+ - \epsilon_-) + Dq_+^2 + \frac{4}{3\tau_{so}} + \frac{\gamma_{+-} + \gamma_{-+}}{2} + \gamma_z \quad (4.22)$$

$$N_2 = -i(\epsilon_+ - \epsilon_-) + Dq_+^2 + \frac{4}{3\tau_{so}} + \frac{\gamma_{+-} + \gamma_{-+}}{2} - \gamma_z, \quad (4.23)$$

and the diffuson contributions using the combinations

$$M_0 = -i(\epsilon_+ - \epsilon_-) + Dq_-^2 + \frac{\gamma_{++} + \gamma_{--}}{2} - \gamma_z \quad (4.24)$$

$$M_1 = -i(\epsilon_+ - \epsilon_-) + Dq_-^2 + \frac{4}{3\tau_{so}} + \frac{\gamma_{++} + \gamma_{--}}{2} - \gamma_z \quad (4.25)$$

$$M_2 = -i(\epsilon_+ - \epsilon_-) + Dq_-^2 + \frac{4}{3\tau_{so}} + \frac{\gamma_{++} + \gamma_{--}}{2} + \gamma_z. \quad (4.26)$$

The notation $N_0 \dots M_2$ is chosen such that N_0 and M_0 correspond to singlet contributions, N_1 , M_1 correspond to triplets with $m = 0$, and N_2 , M_2 to triplets with $m = 1$.

The explicit result for the potential correlator is

$$\begin{aligned} \langle \Omega(\phi)\Omega(\phi') \rangle_c = 2 \int \frac{d\epsilon_-}{2\pi} \frac{d\epsilon_+}{2\pi} n_F(\epsilon_-)[1 - n_F(\epsilon_+)] \text{Re} \sum_q \ln \left\{ \right. \\ \left[N_2 N_2 - \left(\frac{\gamma_{++} - \gamma_{--}}{2} - i \frac{\omega_s - \omega'_s}{2} \right)^2 \right] \left[N_0 N_1 - \left(\frac{\gamma_{+-} - \gamma_{-+}}{2} + i \frac{\omega_s + \omega'_s}{2} \right)^2 \right] \\ \left[M_2 M_2 - \left(\frac{\gamma_{+-} - \gamma_{-+}}{2} + i \frac{\omega_s + \omega'_s}{2} \right)^2 \right] \left[M_0 M_1 - \left(\frac{\gamma_{++} - \gamma_{--}}{2} - i \frac{\omega_s - \omega'_s}{2} \right)^2 \right] \left. \right\}. \end{aligned} \quad (4.27)$$

In the absence of spin effects, $N_0 = \dots = M_0 = \dots = -i(\epsilon_+ - \epsilon_-) + Dq_\pm^2$, $\gamma_{\mu\nu} = \omega_s = 0$, i.e. the terms in the logarithm depend only on the difference of energies, $y = \epsilon_+ - \epsilon_-$. One of the two energy integrations is feasible and, finally, we recover Eq. (2.48).

If we reverse the sign of the magnetic field in one of the thermodynamic potentials, $\phi, \omega_s \rightarrow -\phi, -\omega_s$, we have to replace $\gamma_z \rightarrow -\gamma_z$, $\gamma_{++} \rightarrow \gamma_{-+}$, and so on. In that way diffuson contributions transform into cooperon contributions, and vice versa. As a result, we have shown explicitly that $\mathcal{M}_\Omega(-\omega_s, -\phi, \omega'_s, \phi') = \mathcal{M}_\Omega(\omega_s, \phi, \omega'_s, \phi')$, as implied by time reversal symmetry.

For the following discussion, we consider ω_s and ϕ as independent variables. The persistent current is a periodic function in ϕ , but the Fourier components depend on the Zeeman energy ω_s :

$$I = \sum_{m=1}^{\infty} \left[I_m(\omega_s) \sin(2\pi m\phi/\phi_0) + \tilde{I}_m(\omega_s) \cos(2\pi m\phi/\phi_0) \right]. \quad (4.28)$$

Due to time reversal symmetry $I_m(\omega_s)$ and $\tilde{I}_m(\omega_s)$ are even and odd, respectively; in particular, $\tilde{I}_m(\omega_s = 0) = 0$.

In the ideal case, i.e. $T = 0$, and $1/\tau_s = 1/\tau_{so} = \omega_s = 0$, one finds for the Fourier components of the current correlator

$$\langle I_m I_{m'} \rangle_{id} = \delta_{mm'} \frac{96}{\pi^2} e^2 E_c^2 \frac{1}{m^3}. \quad (4.29)$$

In general, we define h_m through the relation $\langle I_m(\omega_s) I_m(\omega'_s) \rangle_c = h_m \langle I_m^2 \rangle_{id}$, i.e. h_m is a function of the T , $1/\tau_s$, $1/\tau_{so}$, ω_s , ω'_s . For example, the temperature suppression is given by

$$h_m(\Gamma) = -\frac{2}{3} \int_0^\infty ds s^3 \coth(s^2/\Gamma) e^{-s} \cos(s) \quad (4.30)$$

with $\Gamma = T/T_m$, $T_m = D/(\hbar m L)^2$. The asymptotic results for low and high temperatures are $h_m(0) = 1$, and $h_m(\Gamma \gg 1) \simeq (\pi^2 \Gamma^2/3) \exp(-\sqrt{2\pi\Gamma})$. The temperature scale for the decay of the m^{th} Fourier component is set by T_m , so at a given temperature T the higher components are suppressed stronger than the lower Fourier components. Considering the suppression of the current due to exchange scattering, we find at zero temperature, and for $1/\tau_{so} = \omega_s = \omega'_s = 0$:

$$h_m(\Gamma) = e^{-\sqrt{\Gamma}} \left(1 + \sqrt{\Gamma} + \frac{1}{3}\Gamma\right), \quad (4.31)$$

with $\Gamma = 1/\tau_s T_m$. If Zeeman splitting is the only mechanism destroying the coherence, i.e. $T = 0$, $1/\tau_s = 1/\tau_{so} = 0$, and for $\omega_s = \omega'_s$, we find

$$h_m(\Gamma) = \frac{1}{2} + \frac{1}{2} e^{-\sqrt{\Gamma/2}} \left[\cos\left(\sqrt{\Gamma/2}\right) \left(1 + \sqrt{\Gamma/2}\right) + \sin\left(\sqrt{\Gamma/2}\right) \left(\sqrt{\Gamma/2} + \frac{\Gamma}{3}\right) \right]; \quad (4.32)$$

here $\Gamma = \omega_s/T_m$. Equation (4.32) can be obtained from Eq. (4.31), taking into account that only two of the four diffuson/cooperon channels are suppressed, and $\Gamma \rightarrow \pm i\Gamma$ in the remaining channels. Fig. 4.1 depicts h_l as a function of the Zeeman energy in the two limiting cases, $1/\tau_s = 0$, compare Eq. (4.32), and for strong spin-flip scattering, $1/\tau_s \gg E_c$. Remarkably, h_l is a non-monotonic function in ω_s/E_c . The asymptotic value $h_l \rightarrow 1/2$ is only reached for rather high values of the magnetic field, if we have in mind the situation in the experiment: The Zeeman energy can be expressed as

$$-\omega_s = 2\mu_B H = E_c \frac{24\pi^2}{k_F l} \frac{\phi}{\phi_0}, \quad (4.33)$$

inserting realistic parameters as given in Ch. 2, $\epsilon_F \tau = k_F l/2 \sim 10^3$, we find $-\omega_s \sim 0.1 E_c \phi/\phi_0$. Note, however that the effectiveness of Zeeman splitting is enhanced² in the presence of magnetic impurities, even for $1/\tau_s \ll E_c$, compare Eq. (4.13).

²A similar effect exists for the universal conductance fluctuations, and has been observed in a recent experiment [71].

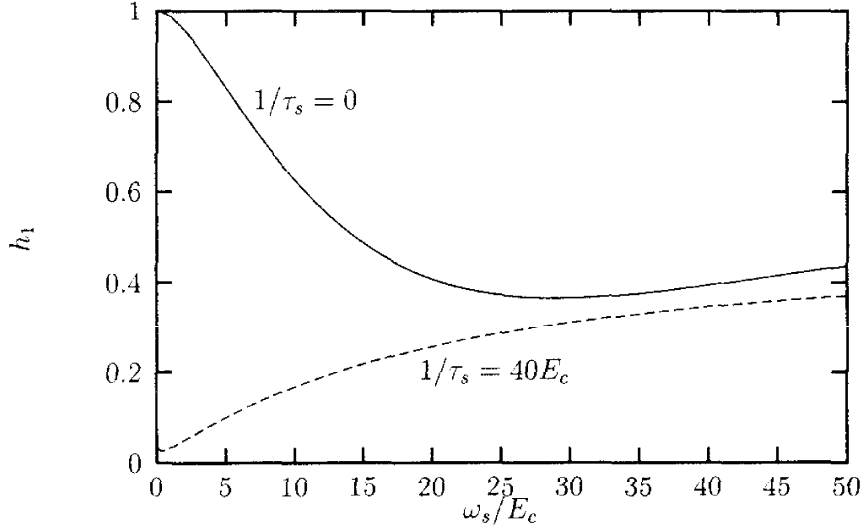


Figure 4.1: Normalized amplitude of the first harmonic of the current, $\langle I_1^2 \rangle_c = h_1 \langle I_1^2 \rangle_{id}$ as a function of ω_s/E_c . The continuous line shows the result in the absence of magnetic impurities, where the current is reduced due to Zeeman splitting. The dashed line shows the result in the presence of strong spin-flip scattering. The temperature is $T = 0.2E_c$.

The broken line in Fig. 4.1 is the curve for strong spin scattering, we have chosen $1/\tau_s = 40E_c$, and $T = 0.2E_c$. We took into account the second order self energy $\Sigma_{\pm}^{(2)}(\epsilon)$, only, since the first order term $\Sigma_{\pm}^{(1)}$ is irrelevant: For $1/\tau_s \gg E_c$ and $\omega_s = \omega'_s$, the relevant parts for the potential correlator are the N_2 contributions for the cooperon, and M_0, M_1 for the diffuson. $\Sigma_{\pm}^{(1)}$ cancels in γ_{++} and γ_{--} , i.e. the relevant parts are independent of $\Sigma_{\pm}^{(1)}$.

The limit $\omega_s \ll T$ has been discussed before (compare Eq. (4.31)) and explains the limiting value of h_1 for low ω_s . Note that the condition $\omega_s \gg T$ is not at all sufficient to find a “large” current³. For $T \ll \omega_s \ll T_m$, spin-flip processes are still allowed since, for calculating $\langle I_m^2 \rangle_c$ typical energies ϵ_{\pm} in the integrations are of the order $\epsilon_{\pm} \sim T_m$ or even larger. Further increasing the strength of the magnetic field, spin-flip processes will be forbidden for $\omega_s \gg T_m$, i.e. $\text{Im}\Sigma_{\gamma}^R = -1/6\tau_s$ in the energy range of interest. Using the relation $\partial_{\epsilon}\Sigma_{\pm}^R\Big|_{\epsilon=0} = -2/(3\pi\tau_s\omega_s)$, we find an algebraic reduction of the current:

$$h_m = \frac{1}{2} \frac{1}{(1 + 2/3\pi\tau_s\omega_s)^2}. \quad (4.34)$$

This function fits the dashed curve in Fig. 4.1 for high values of ω_s/E_c .

³This is unlike for the universal conductance fluctuations, where $\omega_s > T$ seems to be sufficient to find the universal values for the fluctuations [17].

4.1.2 Interacting electrons (mean current)

In this case the two Green's functions which determine the cooperon correspond to the same thermodynamic potential. Because of this the bare impurity vertex $C_{\alpha\beta\gamma\delta}^0$ is different to that in Eq. (4.18): Instead of inserting the term $\gamma_z \sigma_{\alpha\gamma}^z \sigma_{\beta\delta}^z$, the Green's functions are connected by the interaction $V_{\alpha\beta\gamma\delta}$ as defined in Eq. (4.8). We restrict ourselves to two cases, $\omega_s \ll T$, and $\omega_s \gg T, E_c$. For a weak magnetic field $V_{\alpha\beta\gamma\delta}$ is dominated by its static part from which we find

$$2\pi\mathcal{N}_0 C_{\alpha\beta\gamma\delta}^0 = \frac{1}{\tau} \delta_{\alpha\gamma} \delta_{\beta\delta} + \left(\frac{1}{3\tau_s} - \frac{1}{3\tau_{so}} \right) \vec{\sigma}_{\alpha\gamma} \vec{\sigma}_{\beta\delta} \quad (4.35)$$

for the bare cooperon. It is interesting that in this case the current related to global charge fluctuations, $\langle I(\phi) \rangle = -\partial_\phi \langle \delta\Omega^C \rangle$, is *not* equal to the mean current found for non-interacting electrons. Although the current is reduced in the presence of magnetic impurities in both cases, the decay of the cooperons is not identical. $\langle I^{EEI} \rangle = -\partial_\phi \langle \delta\Omega^{EEI} \rangle$ has been discussed in detail in [49], where expressions similar to Eqs. (4.30)-(4.32) have been given. The flux dependent part of the grand potential was found as

$$\langle \delta\Omega^{EEI} \rangle = -\lambda_c 2\pi\mathcal{N}_0 \tau^2 \sum_{q,\alpha,\beta} \int_0^\infty \frac{dy}{2\pi} y \coth \frac{y}{2T} \text{Re} (C_{\alpha\beta\alpha\beta} - C_{\alpha\beta\beta\alpha}). \quad (4.36)$$

We assumed λ_c , the effective interaction constant in the Cooper channel, to be the same for Hartree and exchange contributions. $C_{\alpha\beta\gamma\delta}$ is the spin dependent cooperon. It can be expressed in terms of singlet and triplet components, $\sum_{\alpha\beta} C_{\alpha\beta\alpha\beta} = 3C_1 + C_0$, and $\sum_{\alpha\beta} C_{\alpha\beta\beta\alpha} = 3C_1 - C_0$, so that only the singlet component is relevant for $\langle \delta\Omega^{EEI} \rangle$. In particular, $C_0(q, \omega) = (1/2\mathcal{N}_0\tau^2)(-i\omega + Dq^2 + 2/\tau_s)^{-1}$. Note that C_0 is independent of spin-orbit scattering.

In the opposite limit, $\omega_s \gg E_c, T$, the inelastic parts of $V_{\alpha\beta\gamma\delta}$, that is the spin-flip contributions, can be neglected. As a consequence $C_{\alpha\beta\gamma\delta}^0$ is given by

$$2\pi\mathcal{N}_0 C_{\alpha\beta\gamma\delta}^0 = \frac{1}{\tau} \delta_{\alpha\gamma} \delta_{\beta\delta} - \frac{1}{3\tau_{so}} \vec{\sigma}_{\alpha\gamma} \vec{\sigma}_{\beta\delta} + \gamma_z \sigma_{\alpha\gamma}^z \sigma_{\beta\delta}^z \quad (4.37)$$

which is identical to $C_{\alpha\beta\gamma\delta}^0$ given in Eq. (4.18). To express the thermodynamic potential we can use the previously defined N_0 and N_1 as well as the expressions for the cooperon $C_{\alpha\beta\gamma\delta}$ given in the App. B. We find

$$\langle \delta\Omega^{EEI} \rangle = -2\lambda_c \sum_q \int_0^\infty \frac{dy}{2\pi} y \coth \frac{y}{2T} \text{Re} \frac{N_1}{N_0 N_1 - [(\gamma_{-+} - \gamma_{+-})/2 + i\omega_s]^2}. \quad (4.38)$$

Note that N_0, N_1 are functions of $q = 2\pi(n + 2\phi/\phi_0)/L$ and $y = \epsilon_+ - \epsilon_-$.

Some results are collected in Table 4.1 and 4.2. We consider the zero temperature limit and the asymptotic results only. We give both the results for the current

	$1/\tau_s \ll T_m$		$1/\tau_s \gg T_m$	
	$\omega_s \ll T_m$	$\omega_s \gg T_m$	$\omega_s \ll T_m$	$\omega_s \gg T_m, 1/\tau_s$
$\langle I_m^2 \rangle_c$:	1	1/2	0	1/2
$\langle I_{2m}^{CE} \rangle$:	1	1/2	0	1/2
$\langle I_{2m}^{EEI} \rangle$:	1	0	0	0

Table 4.1: Relative magnitude of the typical current, the free electron contribution, and the collective contribution to the mean current as a function of the exchange scattering rate $1/\tau_s$ and the Zeeman energy ω_s . In the regime $T_m < \omega_s < 1/\tau_s$ the current is suppressed algebraically, compare Eq. (4.34). The spin-orbit scattering rate $1/\tau_{so}$ is set equal to zero.

	$1/\tau_s \ll T_m$		$1/\tau_s \gg T_m$	
	$\omega_s(\omega_s \tau_{so}) \ll T_m$	$\omega_s(\omega_s \tau_{so}) \gg T_m$	$\omega_s \ll T_m$	$\omega_s \gg T_m, 1/\tau_s$
$\langle I_m^2 \rangle_c$:	1/4	1/8	0	1/8
$\langle \tilde{I}_m^2 \rangle_c$:	0	1/8	0	1/8
$\langle I_{2m}^{CE} \rangle$:	1/4	0	0	0
$\langle I_{2m}^{EEI} \rangle$:	1	0	0	0

Table 4.2: Relative magnitude of the current in the presence of strong spin-orbit scattering. Treating ω_s and ϕ as independent variables, we find odd and even contributions to the current, compare Eq. (4.28).

fluctuation, $\langle I_m^2 \rangle_c$, and for the mean current, i.e. the free electron contribution in a canonical ensemble, $\langle I_{2m}^{CE} \rangle$, and the collective contribution due to electron-electron interaction, $\langle I_{2m}^{EEI} \rangle$. All the numbers in the tables are normalized to the values without spin effects (see second row in Table 4.1). Table 4.1 shows the results in the absence of spin-orbit scattering. All contributions are strongly suppressed if $1/\tau_s \gg T_m$ and for weak magnetic fields. In the presence of strong magnetic fields, $\omega_s \gg T_m$, the collective contribution remains suppressed, the free electron contributions are only suppressed algebraically (Eq. 4.34) and can reach one half of their ideal values.

In the presence of strong spin-orbit scattering, the results are somewhat different (see Table 4.2). In this case, only the singlet components, i.e. the M_0 and N_0 components, contribute to the current. If there are no exchange scatterers, the current is only weakly dependent on Zeeman splitting, in the sense that the typical energy scale is set by $\omega_s \omega_s \tau_{so} \sim T_m$, instead of $\omega_s \sim T_m$ as before. Note that the collective contribution is not reduced by spin-orbit scattering. For very high Zeeman energies only the M_0 component contributes to the current, so $\langle I_{2m}^{CE} \rangle = 0$ and $\langle I_m^2 \rangle_c$ is reduced by eight. Since the symmetry of diffuson and cooperon contributions is broken, there are also even harmonics, $\langle \tilde{I}_m^2 \rangle_c = \langle I_m^2 \rangle_c$.

4.2 Spin glasses

We now discuss the situation where the concentration of magnetic impurities is high. An interaction of the type given in Eq. (4.5) induces an effective interaction among the localized spins, which is called the RKKY interaction [70],

$$H_{eff} = - \sum_{i,j} J_{RKKY}(\mathbf{R}_i, \mathbf{R}_j) \vec{S}_i \vec{S}_j. \quad (4.39)$$

For long distances the RKKY interaction is proportional to $J_{RKKY} \propto (k_F |\mathbf{R}_i - \mathbf{R}_j|)^{-3}$ and thus becomes important if the typical spacing between the impurity spins is low, i.e. if the concentration is high. Below the spin glass temperature, T_{SG} , the spins are in an ordered phase. Within a mean field description each impurity spin can be considered in an effective magnetic field H_{SG} due to the other spins [65]. This magnetic field is of the order $\mu_B H_{SG} \sim T_{SG}$. Generally, the electron self energy $\Sigma_{\alpha\beta}(\epsilon)$ is the sum of a scalar part, Σ , and a vector part, $\vec{\Sigma}$: $\Sigma_{\alpha\beta}(\epsilon) = \Sigma(\epsilon)\delta_{\alpha\beta} + \vec{\Sigma}(\epsilon)\vec{\sigma}_{\alpha\beta}$. If the internal magnetic fields are distributed isotropically and no external magnetic field is present the vector part of the self energy is zero. The scalar part of the self energy can be found from Eqs. (4.11) and (4.12), $\Sigma = (\Sigma_+ + \Sigma_-)/2$. The result is ($\sigma = \pm$):

$$\text{Re}\Sigma^R(\epsilon) = -\frac{1}{2V}J^2\mathcal{N}_0 \sum_{\mathbf{R},\sigma} \tanh \frac{\sigma\omega_{\mathbf{R}}}{2T} \text{Re}\Psi\left(\frac{1}{2} - i\frac{\epsilon + \sigma\omega_{\mathbf{R}}}{2\pi T}\right) \quad (4.40)$$

$$\begin{aligned} \text{Im}\Sigma^R(\epsilon) &= -\frac{1}{2V}\pi\mathcal{N}_0J^2 \sum_{\mathbf{R},\sigma} \tanh \frac{\sigma\omega_{\mathbf{R}}}{2T} [n_B(\sigma\omega_{\mathbf{R}}) + n_F(\sigma\omega_{\mathbf{R}} + \epsilon)] \\ &\quad - \frac{1}{4}\pi\mathcal{N}_0n_sJ^2. \end{aligned} \quad (4.41)$$

Here $\omega_{\mathbf{R}} > 0$ is the Zeeman energy associated with the internal magnetic field H_{SG} at the impurity $S_{\mathbf{R}}$. In the fully polarized regime, $T \ll T_{SG}$, the spin-flip scattering rate is $1/\tau_s = 2\pi\mathcal{N}_0n_sJ^2S^2 = \pi\mathcal{N}_0n_sJ^2/2$, which is by a factor three smaller than the scattering rate of paramagnetic impurities. Another consequence of the random distribution of the directions of internal fields is that $\sum_{\mathbf{R}}\langle S_{\mathbf{R}}^a \rangle \langle S_{\mathbf{R}}^b \rangle = \delta_{ab} \sum_{\mathbf{R}}(\langle \vec{S}_{\mathbf{R}} \rangle)^2/3$. For $\omega_{\mathbf{R}} \gg T$ the bare impurity vertices are

$$2\pi\mathcal{N}_0D_{\alpha\beta\gamma\delta}^0 = \frac{1}{\tau}\delta_{\alpha\gamma}\delta_{\delta\beta} + \left(\frac{1}{3\tau_s} + \frac{1}{3\tau_{so}}\right)\vec{\sigma}_{\alpha\gamma}\vec{\sigma}_{\delta\beta} \quad (4.42)$$

$$2\pi\mathcal{N}_0C_{\alpha\beta\gamma\delta}^0 = \frac{1}{\tau}\delta_{\alpha\gamma}\delta_{\beta\delta} + \left(\frac{1}{3\tau_s} - \frac{1}{3\tau_{so}}\right)\vec{\sigma}_{\alpha\gamma}\vec{\sigma}_{\beta\delta} \quad (4.43)$$

A scattering of this type has been considered in [68] and [69]. In the present work we consider the full energy dependent electron self energy given in Eqs. (4.40) and (4.41), instead of $\Sigma^R = -i/2\tau_s$, which is the second term in Eq. (4.41). For $1/\tau_s > E_c$

only the diffuson singlet component contributes to the potential correlator, which is of the form

$$\langle \Omega(\phi)\Omega(\phi') \rangle_c: \quad \text{Re} \sum_q \ln \left[-i(\epsilon_+ - \epsilon_-) + Dq^2 + i(\Sigma^R(\epsilon_+) - \Sigma^A(\epsilon_-)) - 1/\tau_s \right]. \quad (4.44)$$

The internal magnetic fields break time reversal invariance and Ω is not an even function in ϕ , equivalently $I(\phi)$ has odd and even parts I_m, \tilde{I}_m . They are of the same order, $\langle I_m^2 \rangle_c = \langle \tilde{I}_m^2 \rangle_c$. Considering the amplitude of the current we can use the results from the previous section. Spin polarization has the tendency to restore the current, but as long as $\omega_{\mathbf{R}} < E_c$ the current remains small, i.e. the current is strongly reduced if $T_{SG} \ll E_c \ll 1/\tau_s$. For $T_{SG} \gg E_c$ there is no exponential suppression of the current, but there remains a suppression of the Fourier components $\langle I_m^2 \rangle_c$ given by $(1/8)(1 + 1/\pi\tau_s\mu_B H_{SG})^{-2}$, compare Eq. (4.34). The factor eight takes into account that only one diffuson channel, instead of four diffuson and four cooperon channels, contributes to the current. In the presence of an external magnetic field there is a crossover from the regime of random spin directions to the regime of aligned spins at $\omega_s \sim \mu_B H_{SG}$. The regime of aligned spins has been discussed in the previous chapter. For weak spin-orbit scattering the current increases, since more diffuson and cooperon channels contribute.

4.3 Kondo effect

Here we calculate the persistent current for the situation, where the concentration of magnetic impurities is low, so we neglect the RKKY interaction. In Ch. 4.1 we used a second order perturbation theory in J , which can be justified as long as the perturbation series converges rapidly. For temperatures lower than the Kondo temperature, $T_K \sim \epsilon_F \exp(-1/2|J|\mathcal{N}_0)$, perturbation theory in J breaks down, so the results of Ch. 4.1 do not apply in this case.

In principle we can calculate the potential correlator as before in Ch. 4.1. We express the self energies using the T -matrix,

$$\Sigma_\gamma^{R,A}(\epsilon) = N_s T_\gamma^{R,A}(\epsilon). \quad (4.45)$$

The T -matrix has to be determined within some non-perturbative method. In addition, we replace in Eqs. (4.17) and (4.18)

$$\gamma_z \sigma_{\alpha\gamma}^z \sigma_{\beta\delta}^z \rightarrow N_s 2\pi \mathcal{N}_0 \mathcal{V} T_\gamma^R(\epsilon_+) T_\delta^A(\epsilon_-) \delta_{\alpha\gamma} \delta_{\beta\delta}. \quad (4.46)$$

In the weak coupling limit $T_\gamma^R = \gamma(-J/2\mathcal{V}) \cdot \tanh(\omega_s/2T)$ and we recover the results given in Eqs. (4.11) and (4.19).

Neglecting Zeeman effects and spin-orbit scattering the potential correlator can be determined from an expression of the form

$$\langle \Omega(\phi)\Omega(\phi') \rangle: \quad \text{Re} \sum_q \ln \left[-i(\epsilon_+ - \epsilon_-) + Dq_\pm^2 + 1/\tau_\varphi \right] \quad (4.47)$$

where $1/\tau_\varphi = N_s[iT^R(\epsilon_+) - iT^A(\epsilon_-) - 2\pi\mathcal{N}_0\mathcal{V}T^R(\epsilon_+)T^A(\epsilon_-)]$. Although many exact results for the Kondo model exist, an analytic expression for the T -matrix is not known. As an approximation for the T -matrix we use (for $E_c > T_K$) the expression given by Haman [72]

$$T_{Ha}^R(\epsilon) = \frac{1}{i2\pi\mathcal{N}_0\mathcal{V}} \left[1 - x \left(x^2 + 3\pi^2/4 \right)^{-1/2} \right] \quad (4.48)$$

with $x = \ln[(\epsilon + iT)/iT_K]$. This approximation gives the correct behavior for high energy or temperature. It interpolates into the low temperature regime such that $T^R(\epsilon = 0, T = 0)$ is correct, i.e. the so called unitarity limit is reached, $T_0^R = 1/(i\pi\mathcal{N}_0\mathcal{V})$. If $T^R(\epsilon, T)$ is replaced by this constant value, there is no suppression of the persistent current since $i(T_0^R - T_0^A) - 2\pi\mathcal{N}_0\mathcal{V}T_0^RT_0^A = 0$. However Eq. (4.48) is not sufficiently accurate in the low energy regime. Exact results for low temperature can be found from Fermi liquid theory. A systematic expansion around the Fermi liquid fixed point has been formulated by Hewson [58]. For low energy the T matrix is given by [59]

$$T_{FL}^R(\epsilon) = \frac{1}{\pi\mathcal{N}_0\mathcal{V}} \frac{4T_K}{\pi w} \frac{1}{\epsilon + i4T_K/\pi w}. \quad (4.49)$$

$w \approx 0.41$ is the Wilson number. Higher corrections are of the order $(T/T_K)^2$ or $(\epsilon/T_K)^2$, see Ch. 3. Fig. 4.2 shows the normalized current as a function of E_c/T_K . Fixing E_c/T_K one parameter remains undetermined, namely the impurity concentration n_s . Here we choose $n_s = 50 \cdot 2\pi\mathcal{N}_0E_c$. This means, the electron self-energy due to magnetic impurities is at zero temperature given by $\Sigma^R = N_sT_0^R = -100iE_c$. For the continuous line we used T_{Ha}^R as an approximation for the T -matrix, and for the broken line we used T_{FL}^R . There is a maximum suppression of the current for $E_c \sim T_K$. The physical reason is that the spin-flip scattering rate has a maximum at $T \sim T_K$ (or equivalently $\epsilon \sim T_K$). For $E_c \ll T_K$, i.e. when the impurity spins are well screened, we find from Eqs. (4.47) and (4.49) for the relative magnitude of the current fluctuation

$$h_m = 1/(1 + n_s w/4\mathcal{N}_0T_K)^2. \quad (4.50)$$

Note that Eq. (4.49) for the T -matrix is exact for $\epsilon \ll T_K$, for the single impurity problem. Finite size effects or interactions in the conduction band are not taken into account. For the present situation with a finite concentration of magnetic impurities, Eq. (4.49) is thus only appropriate if the concentration of magnetic impurities is low.

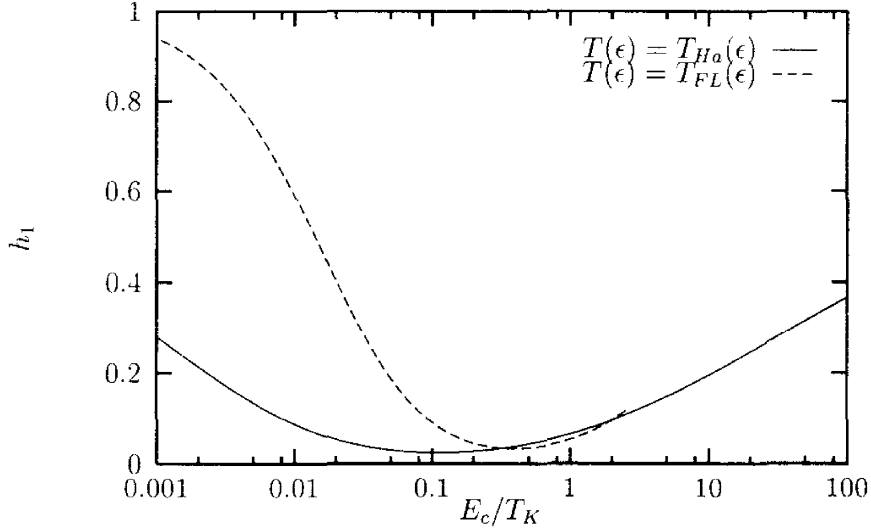


Figure 4.2: Normalized amplitude of the first harmonic of the current, $\langle I_1^2 \rangle_c = h_1 < I_1^2 >_{id}$, as a function of E_c/T_K . We use two different approximations for the T -matrix, as explained in the text. The impurity concentration is $n_s = 50 \cdot 2\pi\mathcal{N}_0 E_c$. If we estimate the ratio $E_c/\Delta = 2\mathcal{N}_0\mathcal{V}E_c \sim 10^2$, and the number of electrons in the sample to be $N_{el} \sim 10^{10}$, this concentration of magnetic impurities is $N_s/N_{el} \sim 1.5 \cdot 10^{-6}$.

A rough estimate [73] for the minimum number of electrons needed to form the Kondo ground state is given by comparing the ratio of the number of magnetic impurities, N_s , and the number of electrons, N_{el} , with the ratio of the Kondo temperature and the Fermi energy: $N_s/N_{el} \sim T_K/\epsilon_F$. Since $N_s/\mathcal{V} = n_s$ and $\epsilon_F/N_{el} \sim \Delta = 1/2\mathcal{N}_0\mathcal{V}$ we can rewrite this condition as $n_s/2\mathcal{N}_0T_K \sim 1$. As a consequence we expect that the result given in Eq. (4.50) is not applicable in systems with Kondo screening, when h_m becomes much smaller than one.

Finite size effects or interactions in the conduction band are also not taken into account. Recent experiments have shown a size dependence of the Kondo effect in systems of reduced dimensionality [74–77]: At low temperature, there is a logarithmic contribution to the resistivity, $\Delta\rho(T) = -B\ln(T)$. In thin films and wires a reduction of the factor B below the bulk value was observed. The Kondo effect in disordered systems of reduced dimensionality has been considered using high temperature perturbation theory [78–82], but no additional logarithmic contributions to the resistivity were found such that the reduction of B remained unexplained. Recently it has been proposed [83] that a spin-orbit induced magnetic anisotropy might explain the finite size dependence in the Kondo effect. We emphasize that the experimental results are still controversial since they could not be confirmed by all groups [84].

We would point out that the limits of applicability of the single impurity results are far from clear.

4.4 Discussion of the results

Let us summarize the results of Ch. 4. First of all, we can clearly state that magnetic scattering is relevant for both the mean current as well as the persistent current fluctuations.

In Ch. 4.1 we investigated the situation, where the temperature is higher than both the Kondo temperature and the spin glass temperature. In measurements of the universal conductance fluctuations it was found that magnetic impurities strongly suppress the fluctuations, but in magnetic fields of the strength $\omega_s > T$ the impurity spins are polarized and the fluctuations can be observed experimentally [17]. We predict similar results for the persistent current fluctuations. The fluctuations are suppressed in weak magnetic fields, and should be observable for high magnetic fields. However, the relevant scale for the magnetic field is *not* the temperature, but the spin-flip scattering rate, compare Eq. (4.34).

In Ch. 4.2 we calculated the persistent current fluctuations in a spin glass. The persistent current is strongly suppressed, if the transition temperature T_{SG} is below the Thouless energy. If the transition temperature is far above the Thouless energy, the spins can be considered as fixed vectors and we find the persistent current fluctuations to be suppressed by a factor $\sim 1/8$ compared to the situation without magnetic impurities. The latter result has also been found in an earlier calculation [69], but there the impurity spins were considered fixed from the beginning, so the different results for $T_{SG} \ll E_c$ and $T_{SG} \gg E_c$ were not found.

In Ch. 4.3 we discussed the role of the Kondo effect. If a sample contains magnetic impurities, but with a Kondo temperature far above the Thouless energy, the impurity spins are well screened for $T \sim E_c$, so there is no suppression of the persistent current due to these magnetic impurities. Magnetic impurities suppress the persistent current most effectively for $T_K \sim E_c$.

Chapter 5

Persistent currents induced by impurity spins

In Ch. 2 we presented three different mechanisms which induce a persistent current. In Ch. 4, we investigated the ways in which these mechanisms are affected by magnetic impurities – the current may be suppressed, but an enhancement of the persistent current due to magnetic impurities was never found.

In this chapter we will show, that due to a different mechanism, there is a range of impurity concentrations and temperatures, where the mean persistent current is larger than in systems without magnetic impurities.

In Ch. 5.1 we start by considering the free energy of a (single) impurity spin in a magnetic field. When we include the coupling to the conduction electrons, the free energy is a function of the electron spin density at the impurity site. The electron spin density depends on the magnetic flux ϕ . As a consequence, there is a flux dependent contribution to the free energy, i.e. there is a contribution to the persistent current.

In Ch. 5.2 and Ch. 5.3 we will extend the calculations including spin-orbit scattering and also higher concentrations of magnetic impurities.

5.1 Phase sensitivity of the Knight shift

The free energy of a single impurity spin, which is coupled to a conduction band, is given by

$$\Omega = -T \ln \left[2 \cosh \left(\frac{\omega_s + J s^z(\mathbf{R})}{2T} \right) \right]. \quad (5.1)$$

We assume that the temperature is much higher than the Kondo temperature, thus we neglect higher order corrections in J . $s^z(\mathbf{R})$ is the electron spin density at the

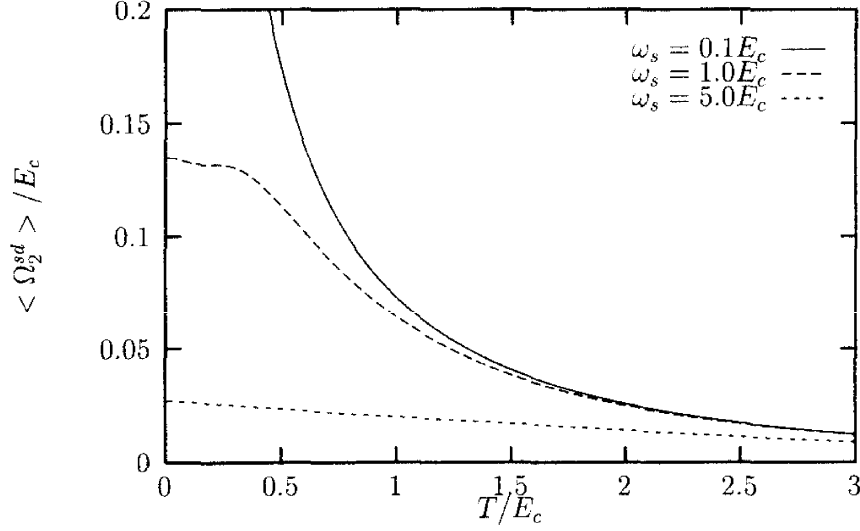


Figure 5.2: Temperature dependence of the second harmonic of the thermodynamic potential for strong spin-orbit scattering ($1/\tau_s = E_c$). The amplitude is to be compared with $\langle \Omega_2^{EEI} \rangle = 4\lambda_c E_c / \pi$ ($T = 0$), where $\lambda_c \sim 0.03$, compare Ch. 2.

5.2 Spin-orbit scattering

Taking into account spin-orbit scattering, Eq. (5.7) can be generalized to

$$\langle \delta \Omega^{sd} \rangle = \frac{1}{2} \sum_{\alpha\beta\gamma\delta} \tilde{v}_{\alpha\beta\gamma\delta} (2\pi \mathcal{N}_0 \tau)^2 T \sum_{q, \omega_n} \frac{|\omega_n|}{2\pi} C_{\gamma\delta\alpha\beta}. \quad (5.11)$$

This formula is found in a diagrammatic approach, in analogy to the diagrams which are evaluated for the Coulomb interaction contribution to the mean free energy. $C_{\gamma\delta\alpha\beta}$ is the cooperon in the presence of spin-orbit scattering. The ‘interaction’ is given by

$$\begin{aligned} \tilde{v}_{\alpha\beta\gamma\delta} &= -n_s J^2 \int_0^\beta d\tau [\langle S^z(\tau) S^z(0) \rangle - \langle S^z(\tau) \rangle \langle S^z(0) \rangle] \sigma_{\alpha\gamma}^z \sigma_{\beta\delta}^z \\ &\quad - n_s J^2 \int_0^\beta d\tau [\langle S^+(\tau) S^-(0) \rangle \sigma_{\alpha\gamma}^- \sigma_{\beta\delta}^+ + \langle S^-(\tau) S^+(0) \rangle \sigma_{\alpha\gamma}^+ \sigma_{\beta\delta}^-] \end{aligned} \quad (5.12)$$

$$\begin{aligned} &= -n_s \frac{J^2}{4T} \left(1 - \tanh^2 \frac{\omega_s}{2T} \right) \sigma_{\alpha\gamma}^z \sigma_{\beta\delta}^z \\ &\quad - n_s \frac{J^2}{\omega_s} \tanh \frac{\omega_s}{2T} (\sigma_{\alpha\gamma}^- \sigma_{\beta\delta}^+ + \sigma_{\alpha\gamma}^+ \sigma_{\beta\delta}^-). \end{aligned} \quad (5.13)$$

This ‘interaction’ is very similar in form to the expression given in Eq. (4.8). It differs in the prefactor, n_s replacing $1/\mathcal{V}^2$, and there is the additional term proportional to $\langle S^z(\tau) \rangle \langle S^z(0) \rangle$. This term appears since there is no linked cluster theorem for magnetic impurities, as we explained in Ch. 3.

The relevant components of the cooperon are (compare App. B):

$$2\pi\mathcal{N}_0\tau^2C_{++++} = 2\pi\mathcal{N}_0\tau^2C_{----} = \frac{1}{N_1} \quad (5.14)$$

$$2\pi\mathcal{N}_0\tau^2C_{+--+} = 2\pi\mathcal{N}_0\tau^2C_{-++-}^* = \frac{1}{2} \frac{N_0 + N_1 + 2i\omega_s \text{sgn}(\omega_n)}{N_0 N_1 + \omega_s^2} \quad (5.15)$$

$$2\pi\mathcal{N}_0\tau^2C_{+--+} = 2\pi\mathcal{N}_0\tau^2C_{-++-} = \frac{1}{2} \frac{N_0 - N_1}{N_0 N_1 + \omega_s^2}, \quad (5.16)$$

where N_0 and N_1 are defined in Eqs. (4.21) and (4.22), but now we use Matsubara representation. Since we consider only the first order term in $1/\tau_s$, we can set $\gamma_{\mu\nu} = 0$ in Eqs. (5.14) - (5.16). In the limit of zero spin-orbit scattering $N_0 = N_1$, so the components of the cooperon in Eq. (5.16) are zero, and the other components become identical to the expressions given in Eqs. (5.8) and (5.9). For very strong spin-orbit scattering ($1/\tau_{so} \gg E_c$ and $\omega_s^2 \ll E_c/\tau_{so}$), the expressions simplify considerably: $C_{++++} \approx 0$, $2\pi\mathcal{N}_0\tau^2C_{+--+} \approx 1/2N_0$, and $2\pi\mathcal{N}_0\tau^2C_{-++-} \approx -1/2N_0$. The flux dependent part of the thermodynamic potential is then given by:

$$\langle \delta\Omega^{sd} \rangle = \frac{1}{2} \frac{1}{\tau_s} \left[\frac{1}{3} \left(1 - \tanh^2 \frac{\omega_s}{2T} \right) + \frac{4T}{3\omega_s} \tanh \frac{\omega_s}{2T} \right] \sum_{q, \omega_n} \frac{|\omega_n|}{2\pi} \frac{1}{|\omega_n| + Dq_+^2}. \quad (5.17)$$

In Fig. 5.2 we show the amplitude of the second harmonic, $\langle \Omega_2^{sd} \rangle$, for the same values of ω_s and T as previously in Fig. 5.1. Spin-orbit scattering changes the sign of $\langle \Omega_2^{sd} \rangle$, it does not go to zero for $\omega_s \rightarrow 0$, and especially the amplitude of $\langle \Omega_2^{sd} \rangle$ is much larger than without spin-orbit scattering.

The summation over momenta q and Matsubara frequencies ω_n in Eq. (5.17) is identical to the summation necessary for calculating $\langle \Omega_{2m}^{EII} \rangle$. It follows that approximately

$$\langle \Omega_2^{sd} \rangle = \left(1 - \tanh^2 \frac{\omega_s}{2T} + \frac{4T}{\omega_s} \tanh \frac{\omega_s}{2T} \right) \frac{E_c}{\tau_s} \frac{\exp(-T/3E_c)}{3\pi^2 T} \quad (5.18)$$

for the temperature range in the figure. Especially, we find for $\omega_s \ll T \ll E_c$: $\langle \Omega_2^{sd} \rangle = E_c/(\tau_s T \pi^2)$, and for $T \ll \omega_s \ll E_c$: $\langle \Omega_2^{sd} \rangle = 4E_c/(\tau_s \omega_s 3\pi^2)$.

5.3 Higher order corrections

We pointed out an analogy of Eq. (5.3) to the Coulomb interaction contribution to $\delta\Omega$, and exploited this analogy when we explicitly calculated the Fourier components $\langle \Omega_{2m}^{sd} \rangle$. Here we consider higher order corrections in $\tilde{v}_{\alpha\beta\gamma\delta}$. These corrections are relevant, when the concentration of magnetic impurities is so high, that the spin-flip scattering rate is comparable to the Thouless energy or larger.

In the case of the Coulomb interaction, higher order corrections result in a renormalization of the coupling constant. In the present case, the results are different

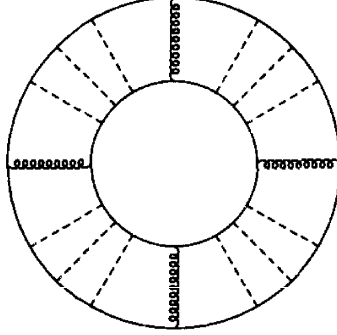


Figure 5.3: Fourth order diagram to $\langle \delta\Omega^{sd} \rangle$. The dashed lines represent scattering events at non-magnetic impurities, the curly lines represent scattering at magnetic impurities. The symmetry factor for the shown diagram is $1/(2 \cdot 4) = 1/8$.

due to the different structure in spin space of $\tilde{v}_{\alpha\beta\gamma\delta}$ and the Coulomb interaction, and due to the different energy dependencies: The Coulomb interaction acts very fast, such that it is often approximated as frequency independent up to a cut-off energy $\sim \epsilon_F$. In contrast to that, the spin dynamics is rather slow. In this section, we only consider the limit of weak magnetic field ($\omega_s = 0$). In this case, the spin dynamics is determined by spin relaxation processes, where the typical energy scale is smaller than the temperature as we will discuss in Ch. 6. Therefore, the magnetic impurities can be considered static, i.e. $\tilde{v}_{\alpha\beta\gamma\delta}(i\omega_n) = \tilde{v}_{\alpha\beta\gamma\delta}\delta_{0\omega_n}$.

A typical diagram for the higher order corrections is shown in Fig. 5.3. We consider $\omega_s = 0$ only. In this case, the singlet-triplet representation is very convenient (see App. C.1). The summation over all contributions of the type shown in Fig. 5.3 leads to the result

$$\begin{aligned} \langle \delta\Omega^{sd} \rangle = & - \sum_{q, \omega_n} \frac{|\omega_n|}{4\pi} \sum_{n=1}^{\infty} \frac{1}{n} \left(\frac{-c_0/\tau_s}{|\omega_n| + Dq_+^2 + 1/\tau_s} \right)^n \\ & - 3 \sum_{q, \omega_n} \frac{|\omega_n|}{4\pi} \sum_{n=1}^{\infty} \frac{1}{n} \left(\frac{-c_1/\tau_s}{|\omega_n| + Dq_+^2 + 1/\tau_s + 4/3\tau_{so}} \right)^n, \end{aligned} \quad (5.19)$$

where $c_0 = 1$ and $c_1 = -1/3$ for the singlets and the triplets, respectively. The factor $1/n$ is due to the symmetry of the diagrams. Performing the n -summation, we find

$$\langle \delta\Omega^{sd} \rangle = \frac{1}{2} \sum_{q, \omega_n} \frac{|\omega_n|}{2\pi} \ln \left[\frac{N_0 + c_0/\tau_s}{N_0} \frac{(N_1 + c_1/\tau_s)^3}{N_1^3} \right]. \quad (5.20)$$

This expression is very similar in form to \mathcal{M}_Q , as given in Eqs. (2.48) and (4.27).

Using results of Ch. 4 we find the expansion

$$T \sum_{q, \omega_n > 0} \frac{|\omega_n|}{2\pi} \ln(|\omega_n| + Dq_+^2 + \gamma) = -\frac{6}{\pi^2} E_c^2 \sum_{m=1}^{\infty} \frac{h_m^0(\gamma)}{m^5} \cos(4\pi m\phi/\phi_0). \quad (5.21)$$

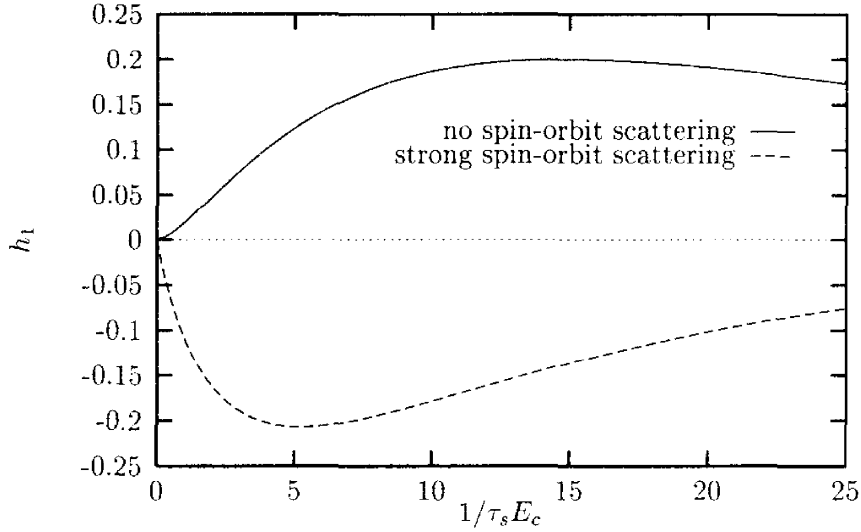


Figure 5.4: The function h_1 , defined in Eq. (5.24). For low temperatures, the amplitude of the second harmonic of the grand potential is given by $\langle \Omega_2^{sd} \rangle = -6E_c^2 h_1 / \pi^2 T$.

where at low temperature ($T \ll E_c$)

$$h_m^0(\gamma) = e^{-\sqrt{\gamma m^2/E_c}} \left(1 + \sqrt{\gamma m^2/E_c} + \frac{\gamma m^2}{3E_c} \right) \quad (5.22)$$

compare Eq. (4.31). Using these relations, we can expand Eq. (5.20) as

$$\langle \delta \Omega^{sd} \rangle = -\frac{1}{T} \frac{6}{\pi^2} E_c^2 \sum_{m=1}^{\infty} \frac{h_m}{m^5} \cos(4\pi m \phi / \phi_0), \quad (5.23)$$

with

$$h_m = h_m^0(2/\tau_s) + 3h_m^0(2/3\tau_s + 4/3\tau_{so}) - h_m^0(1/\tau_s) - 3h_m^0(1/\tau_s + 4/3\tau_{so}). \quad (5.24)$$

Note that there is a prefactor $1/T$ in Eq. (5.23), and the Fourier components can become large at low temperature. For illustration, we plot h_1 as a function of $1/\tau_s E_c$ in Fig. 5.4. The limit of weak spin-flip scattering, which we investigated in detail in sections 5.1 and 5.2, corresponds to $1/\tau_s E_c < 1$: Expanding Eq. (5.24) for small $1/\tau_s$ leads in the limit of strong spin-orbit scattering to $h_1 = -1/6\tau_s E_c$. For $1/\tau_{so} = 0$ there is no linear term $\propto 1/\tau_s$, the leading term is quadratic, $h_1 = (1/\tau_s E_c)^2/18$. For larger spin-flip scattering rates, the absolute values of h_1 with and without strong spin-orbit scattering are comparable in amplitude. For both cases the maximum is of the order $|h_1| \approx 0.2$. Note that the sign of $\langle \Omega_2^{sd} \rangle$ is negative if $1/\tau_{so} = 0$, but positive for $1/\tau_{so} \rightarrow \infty$.

In this chapter we found that the mean persistent current in systems with magnetic impurities can be much larger than in systems without magnetic impurities.

This result is very surprising, since it is contrary to the theoretical experience and experiments on weak localization and universal conductance fluctuations. Neither an enhancement of the weak localization corrections to the conductivity nor enhanced conductance fluctuations have been reported in systems containing magnetic impurities.

For low temperature ($T < E_c$), the persistent current is proportional to $1/T$. This is different from the temperature dependence ($I \propto \exp(-T/80\text{mK})$) found in the experiment by Lévy et al. We are therefore unable to explain the amplitude of the current found in the experiment.

Chapter 6

Temporal current fluctuations

We found in Ch. 5 that the leading contribution to the (mean) persistent current in systems where $1/\tau_s \sim E_c$ is induced by the coupling of impurity spins and conduction electrons.

In this chapter, we investigate the dynamic properties of this impurity spin induced current. We consider the situation, where in addition to the static flux ϕ , there is a small time dependent contribution to the magnetic flux: $\phi(\omega) = \phi + \delta\phi(\omega)$.

In Ch. 6.1 we consider the linear response of the current to this small perturbation: $\delta I(\omega) = \chi(\phi, \omega) \delta\phi(\omega)$. In the static limit, this response function is given by the derivative of the persistent current with respect to the flux:

$$\chi(\phi, \omega=0) = \frac{\partial I(\omega)}{\partial \phi} = -\frac{\partial^2 \Omega(\phi)}{\partial^2 \phi}. \quad (6.1)$$

We will see, that $\chi(\phi, \omega)$ is strongly frequency dependent even for low frequencies ($\omega < T$). Explicitly calculating the frequency dependence for $\omega < T$, however, is not straightforward. From the frequency dependence of $\chi(\phi, \omega)$ one concludes, that slow temporal current fluctuations exist. In this chapter, we calculate (the slow part of the) symmetric current-current correlation function. The imaginary part of the response function $\chi(\phi, \omega)$ can be determined using the fluctuation-dissipation theorem.

These slow fluctuations can be understood as follows: Considering the impurity spins as fixed vectors, it has been shown [68], that the persistent current fluctuations in the limit of strong spin-flip scattering are given by

$$\langle I(\phi) I(\phi) \rangle_c = \sum_{m=1}^{\infty} \frac{12e^2 E_c^2}{\pi^2 m^3}. \quad (6.2)$$

Taking into account a slow dynamics of the impurities, it is possible to calculate the persistent current for an impurity potential which changes slowly in time. As a result, one finds time dependent current correlations. If the dynamics of the impurity spins is sufficiently slow, one can expect that the current follows the spin

configuration adiabatically, i.e. when calculating time dependent current correlations, $\langle I(\phi, t)I(\phi, t') \rangle_c$, the spins can be considered static at both times t and t' .

We give arguments that the picture of the current following the spin configuration adiabatically is adequate, if we take into account spin-relaxation in a realistic way. We follow the ideas of Refs. [63, 66, 67], where the effects of spin-relaxation on conductance fluctuations and on weak localization were studied.

Our calculations are very similar in form to the determination of a dynamic non-linear response. At finite temperature, we find it convenient to use the real time Green's function formalism. In Ch. 6.2 and 6.3 we will define the most important quantities, which are used in this formalism. In Ch. 6.3 we will show the formal analogy of the (slowly) relaxing magnetic impurities to a time dependent external field. In Ch. 6.4 we determine the cooperon and the diffuson, which we need in Ch. 6.5 in order to calculate the current-current correlation function. In Ch. 6.5 we restrict ourselves to situations where $1/\tau_{so} = \omega_s = 0$. The role of spin-orbit scattering and weak magnetic fields are discussed in Ch. 6.6.

In the entire chapter, we assume low temperature and weak magnetic fields: $T \ll E_c$ and $\omega_s \ll T$.

6.1 Static and dynamic linear response

The static response of the current to a small change in the magnetic flux is given by the derivative of the persistent current with respect to the magnetic flux: $\chi(\phi) = -\partial_\phi I(\phi)$. Using the notation of Ch. 6, this response function is given by

$$\chi(\phi) = \sum_{m=1}^{\infty} \langle \Omega_{2m}^{sd} \rangle \left(\frac{4\pi m}{\phi_0} \right)^2 \cos \left(\frac{4\pi m \phi}{\phi_0} \right). \quad (6.3)$$

In order to generalize this result to finite frequencies, we consider the diagrams needed to calculate $\langle \delta \Omega^{sd} \rangle$ and $\chi(\phi)$. A typical diagram for $\langle \delta \Omega^{sd} \rangle$ is shown in Fig. 5.3: There are two electronic loops, which are connected by magnetic and non-magnetic impurity lines. $\chi(\phi)$ is proportional to the second derivative of $\langle \delta \Omega^{sd} \rangle$. It is useful to distinguish two types of contributions: All contributions to $\chi(\phi)$, where the second derivative of one of the electron loops has been taken are denoted by $\chi_1(\phi)$. All contributions to $\chi(\phi)$, where both electron loops are derived once are denoted by $\chi_2(\phi)$. The total susceptibility is the sum of these two contributions: $\chi(\phi) = \chi_1(\phi) + \chi_2(\phi)$. The diagrams for $\chi_2(\phi)$ are found from the diagrams of $\langle \delta \Omega^{sd} \rangle$ by inserting two current vertices. One vertex is on the inner electron loop, the other vertex is on the outer electron loop. In the static limit both contributions to the susceptibility are equal: $\chi_1(\phi) = \chi_2(\phi)$.

Note that for the flux dependent part of the thermodynamic potential, we need the cooperons only. The diffusons are flux independent. However, it is important to take into account the diffusons when we calculate the dynamic response. Defining a χ_1 and χ_2 for the diffuson parts of the response functions, we find in the static limit $\chi_1 = -\chi_2$ so that the sum of both contributions cancels.

The dynamic response functions are computed from diagrams which are of the same structure as the diagrams for the static response, but with an energy transfer through the current vertices. For low frequency ($\omega < T$), we do not find a frequency dependence in $\chi_1(\phi, \omega)$. The total susceptibility, however, has a strong frequency dependence: In the diagrams for $\chi_2(\phi, \omega)$, there is an energy transfer from the inner to the outer electron loop. The normal (non-magnetic) impurities do not transfer energy, so the energy transfer can only be due to the magnetic impurities, i.e. through the ‘interaction’ lines $\tilde{v}_{\alpha\beta\gamma\delta}$. When we consider the impurity spins static, i.e. $\tilde{v}_{\alpha\beta\gamma\delta}(i\omega_n) \propto \delta_{0\omega_n}$, it follows immediately that $\chi_2(\phi, \omega) = 0$ for all frequencies! A non-zero $\chi_2(\phi, \omega)$ can only be found beyond the static approximation for $\tilde{v}_{\alpha\beta\gamma\delta}(i\omega_n)$.

Since $\chi_2(\phi, \omega)$ has a structure for low frequencies but not $\chi_1(\phi, \omega)$, we will only consider $\chi_2(\phi, \omega)$ in the following (including the diffuson contributions).

For technical reasons, instead of calculating $\chi_2(\phi, \omega)$, we calculate the symmetric current-current correlation function. This correlation function is related to $\chi_2(\phi, \omega)$ by the fluctuation dissipation theorem:

$$\begin{aligned} \int dt e^{i\omega t} \left\{ \frac{1}{2} \langle \{ \hat{I}(t), \hat{I}(0) \} \rangle > - \langle \hat{I} \rangle \langle \hat{I} \rangle > \right\} \\ = \coth \left(\frac{\omega}{2T} \right) \text{Im} \chi_2(\phi, \omega) \approx \frac{2T}{\omega} \text{Im} \chi_2(\phi, \omega), \end{aligned} \quad (6.4)$$

where $\langle \dots \rangle$ denotes the thermal average, $\langle \dots \rangle$ the impurity averaging, \hat{I} the current operator and $\{, \}$ the anti-commutator. Note that for the subset of diagrams we consider here, the second term in the upper line of Eq. (6.4) is identical to the persistent current fluctuations which we calculated in Ch. 4: $\langle \langle \hat{I} \rangle \langle \hat{I} \rangle \rangle = \langle I(\phi) I(\phi) \rangle_c$.

For this subset of diagrams, also the first term in the upper line of Eq. (6.4) is similar in form to the persistent current fluctuations as we show now: The thermal average can be decomposed in two partial averaging procedures:

- thermal average over electronic states
- thermal average over (impurity) spin states

The persistent current fluctuations are found from an average of the form:

$$\text{persistent current:} \quad \langle \langle \hat{I} \rangle_{\text{el}} \rangle_{\text{spin}} \langle \langle \hat{I} \rangle_{\text{el}} \rangle_{\text{spin}} > . \quad (6.5)$$

In contrast to this we find temporal fluctuations, if the order of the averaging procedures is changed:

$$\text{temporal fluctuations:} \quad < \langle \hat{I}(t) \rangle_{\text{el}} \langle \hat{I}(0) \rangle_{\text{el}} \rangle_{\text{spin}} > . \quad (6.6)$$

In section 6.3 we will show that the impurity spin dynamics can be considered classical under realistic assumptions. As a consequence, calculation of the temporal fluctuations is equivalent to determination of the persistent current fluctuations in a time dependent external field (or a time dependent impurity potential).

In the following we will use the notation $< I(t)I(0) >$ for the temporal current fluctuations, i.e. for $< \langle \hat{I}(t), \hat{I}(0) \rangle \rangle > /2$.

6.2 Time dependent Green's functions

For the calculations in this chapter we use the real time Green's function formalism, originally formulated by Keldysh [85]. This section is not intended to give an introduction into this formalism. We only define the most important quantities. Our notation follows the review by Rammer and Smith [86]. In this formalism, Green's functions are matrices,

$$G = \begin{pmatrix} G^R & G^K \\ 0 & G^A \end{pmatrix}, \quad (6.7)$$

with

$$G_{\mathbf{k}\sigma, \mathbf{k}'\sigma'}^R(t, t') = -i\Theta(t - t') \langle \{ c_{\mathbf{k}\sigma}^{(H)}(t), c_{\mathbf{k}'\sigma'}^{(H)+}(t') \} \rangle \quad (6.8)$$

$$G_{\mathbf{k}\sigma, \mathbf{k}'\sigma'}^A(t, t') = +i\Theta(t' - t) \langle \{ c_{\mathbf{k}\sigma}^{(H)}(t), c_{\mathbf{k}'\sigma'}^{(H)+}(t') \} \rangle \quad (6.9)$$

$$G_{\mathbf{k}\sigma, \mathbf{k}'\sigma'}^K(t, t') = -i \langle [c_{\mathbf{k}\sigma}^{(H)}(t), c_{\mathbf{k}'\sigma'}^{(H)+}(t')] \rangle \quad (6.10)$$

where $c_{\mathbf{k}\sigma}^{(H)}$ and $c_{\mathbf{k}\sigma}^{(H)+}$ are Fermi operators in Heisenberg representation, $[,]$ is the commutator, and $\{, \}$ is the anti-commutator. G^R and G^A are the usual retarded and advanced Green's functions. G^K is the Keldysh component. In equilibrium the Green's functions are functions of the time differences $(t - t')$, and the Keldysh component is related to the retarded and advanced function by $G^K(\epsilon) = \tanh(\epsilon/2T)[G^R(\epsilon) - G^A(\epsilon)]$.

6.3 The effective electron-electron interaction

Interactions are also represented by matrices. The effective electron-electron interaction due to magnetic impurities, which we presented in Eq. (4.8) in Matsubara

representation, is now given by

$$V_{\alpha\beta\gamma\delta}^R(t-t') = -i\Theta(t-t') \left(\frac{J}{V}\right)^2 \sum_{a,b=x,y,z} \sigma_{\alpha\gamma}^a \sigma_{\beta\delta}^b \langle [S^a(t), S^b(t')] \rangle \quad (6.11)$$

$$V_{\alpha\beta\gamma\delta}^A(t-t') = i\Theta(t'-t) \left(\frac{J}{V}\right)^2 \sum_{a,b=x,y,z} \sigma_{\alpha\gamma}^a \sigma_{\beta\delta}^b \langle [S^a(t), S^b(t')] \rangle \quad (6.12)$$

$$V_{\alpha\beta\gamma\delta}^K(t-t') = -i \left(\frac{J}{V}\right)^2 \sum_{a,b=x,y,z} \sigma_{\alpha\gamma}^a \sigma_{\beta\delta}^b \langle \{S^a(t), S^b(t')\} \rangle. \quad (6.13)$$

Compared with the expressions for the electron Green's functions, commutators are replaced by anti-commutators and vice versa. For fixed impurities (time independent), $\langle S^a(t)S^b(0) \rangle = \delta_{ab}S(S+1)/3$, and retarded and advanced components of $V_{\alpha\beta\gamma\delta}$ are exactly zero. The impurity spin dynamics is induced by a magnetic field or due to coupling to the conduction band. The retarded and advanced components of $V_{\alpha\beta\gamma\delta}$ are related to the dynamical response functions, which have been studied in detail in the context of spin resonance experiments. Using phenomenological arguments it has been found that for small magnetic fields, $\omega_s \ll T$,

$$i \int_0^\infty dt \langle [S^z(t), S^z(0)] \rangle e^{i\omega t} \simeq \frac{i\Gamma_1}{\omega + i\Gamma_1} \chi_0 \quad (6.14)$$

$$\frac{i}{2} \int_0^\infty dt \langle [S^-(t), S^+(0)] \rangle e^{i\omega t} \simeq \frac{-\omega_R + i\Gamma_2}{\omega - \omega_R + i\Gamma_2} \chi_0, \quad (6.15)$$

where $\chi_0 = 1/4T$ is proportional to the static spin susceptibility. In a microscopic calculation (see e.g. [52,53]) these quantities can be determined under the conditions $|\omega - \omega_R| \ll T$, and $\Gamma_1, \Gamma_2 \ll T$, with the following results:

The resonance frequency ω_R is shifted by the coupling to the conduction band, $\omega_R = \omega_s(1 + JN_0 + \dots)$, and the relaxation rates are by $\Gamma_1 = \Gamma_2 = 4\pi(JN_0)^2T = 1/\tau_K$. The Keldysh component can be determined using the fluctuation dissipation theorem, $V^K(\omega) = \coth(\omega/2T)[V^R(\omega) - V^A(\omega)] \approx (2T/\omega)[V^R(\omega) - V^A(\omega)]$. For the frequencies we consider, $\omega \ll T$, the retarded and advanced components of the interaction are much smaller than the Keldysh component, $|V^{R,A}(\omega)| \ll |V^K(\omega)|$, and will therefore be neglected in the following. In the absence of magnetic fields this is equivalent to the ansatz in [63,66,67] where the impurity spin dynamics was considered to be $\langle S^a(t)S^b(0) \rangle = \delta_{ab}S(S+1)e^{-|t|/\tau_K}/3$. This expression is symmetric in S^a and S^b so that the commutators of two spin operators and therefore the retarded and advanced components of the effective interaction are neglected from the beginning.

One may criticize this approximation, since it violates the fluctuation-dissipation theorem. Note, however, that we simply expand in ω/T and Γ_1/T , keeping the leading terms only. This means that the non-equilibrium contributions, which may arise due to violation of the fluctuation dissipation theorem, are smaller than leading order in these two small parameters, ω/T and Γ_1/T , and will therefore be neglected.

In the Keldysh formalism an interaction generally has a rather complicated structure. We already mentioned that Green's functions and interactions are matrices. Vertices are tensors of third rank, and absorption γ_{ij}^k and emission vertices $\tilde{\gamma}_{ij}^k$ are distinct. An interaction, $V_{kk'}$, where k and k' are these matrix indices, is to be translated into $i \sum_{kk'} \gamma_{ii'}^k V_{kk'} \tilde{\gamma}_{jj'}^{k'}$. Within the notation used in [86], $\tilde{\gamma}_{ij}^1 = \gamma_{ij}^2 = \sigma_{ij}^x / \sqrt{2}$. If we only consider the Keldysh component ($V^K = V_{12}$) of the interaction, this structure simplifies considerably according to $i \sum_{kk'} \gamma_{ii'}^k V_{kk'} \tilde{\gamma}_{jj'}^{k'} \rightarrow i \delta_{ii'} \delta_{jj'} V^K$. Within this approximation, the structure of the interaction is identical in form to a time-dependent external field.

6.4 Diffuson and cooperon

We determine the diffuson and cooperon in the absence of magnetic fields, $\omega_s = 0$. In the absence of magnetic impurities we found the following result, see Eq. (2.43):

$$C(\epsilon_+ - \epsilon_-) = \frac{1}{2\pi \mathcal{N}_0 \tau^2} \frac{1}{-i(\epsilon_+ - \epsilon_-) + Dq_+^2}. \quad (6.16)$$

In the presence of spin effects the cooperon is an object with four spin indices, and with diagonal and off-diagonal components. However, the cooperon can be represented conveniently in the form of singlets and triplets, see App. C.1. As shown in the previous section, spin-flip scattering is formally identical to a time-dependent external field, and we can make use of the methods in [38, 87], where the cooperon in the presence of a time-dependent electromagnetic field was discussed.

The cooperon including spin-flip scattering is expressed as a function of the “unperturbed” cooperon as

$$C_j(\epsilon_+, \epsilon_-; \epsilon'_+, \epsilon'_-) = C(\epsilon_+ - \epsilon_-) \left[(2\pi)^2 \delta(\epsilon_+ - \epsilon'_+) \delta(\epsilon_- - \epsilon'_-) + \hat{\zeta}_j C_j(\epsilon_+, \epsilon_-; \epsilon'_+, \epsilon'_-) \right], \quad (6.17)$$

where C denotes the cooperon without spin effects. The δ -functions reflect that there is no energy transfer between the two Green's functions defining C . C_j is the singlet ($j = 0$) or triplet ($j = 1$) component of the full cooperon. Spin-flip scattering is incorporated using the operator

$$\hat{\zeta}_j = -2\pi \mathcal{N}_0 \tau^2 \left[\frac{1}{\tau_s} + c_j \frac{1}{\tau_s} \int \frac{d\omega}{2\pi} \frac{2\tau_K}{(\omega\tau_K)^2 + 1} e^{-\omega\partial_{\epsilon_-} + \omega\partial_{\epsilon_+}} \right]. \quad (6.18)$$

For convenience, we set $1/\tau_{so} = 0$. A graphical representation is shown in Fig. 6.1. The first term appears as a result of the two self energy diagrams, the second term corresponds to the diagram where both sides are connected by an interaction line. The interaction transfers an energy ω , so the cooperon energies are shifted by $\pm\omega$. ($c_0 = 1$ and $c_1 = -2/3$ for the singlet and triplet channel, respectively.) We multiply

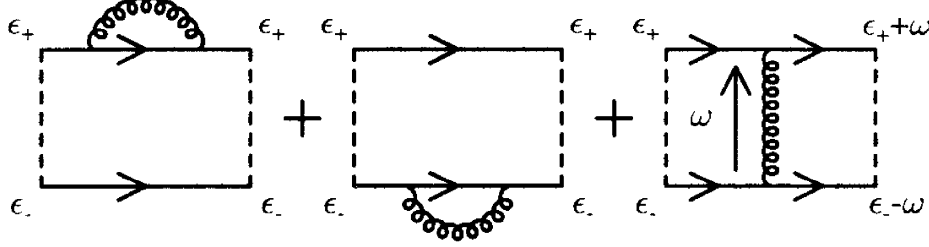


Figure 6.1: Graphical representation of the operator $\hat{\zeta}$. The curly line is the effective interaction due to spin-spin correlations.

Eq. (6.17) with $[C(\epsilon_+ - \epsilon_-)]^{-1}$ and Fourier transform into the time representation, $\epsilon_+ \rightarrow t_+$, and so on. After a change of variables, defining $t = (t_+ + t_-)/2$ and $\eta = t_+ - t_-$, we find, for the cooperon, an expression that depends on four time variables, but only two are relevant: It has been shown [38] that the cooperon can always be represented as $C(t, t', \eta, \eta') = \delta(t - t')C(t, \eta, \eta')$. In the present case $C(t, \eta, \eta')$ does not depend on t , i.e. we have to consider the function $C(\eta, \eta')$ only. It is related to the cooperon in frequency representation by

$$C_j(\epsilon_+, \epsilon_-; \epsilon'_+, \epsilon'_-) = 2\pi\delta(\epsilon'_+ + \epsilon'_- - \epsilon_+ - \epsilon_-) \times \int d\eta d\eta' C_j(\eta, \eta') \exp \left\{ i\frac{\eta}{2}(\epsilon_+ - \epsilon_-) - i\frac{\eta'}{2}(\epsilon'_+ - \epsilon'_-) \right\}. \quad (6.19)$$

The cooperon obeys the following differential equation:

$$\left[2\partial_\eta + Dq_+^2 + \frac{1}{\tau_s} \left(1 + c_j e^{-|\eta|/\tau\kappa} \right) \right] C_j(\eta, \eta') = \frac{1}{2\pi\mathcal{N}_0\tau^2} \delta(\eta - \eta'). \quad (6.20)$$

The diffuson can be determined analogously. Again we use a notation with two time variables, $D(t, t', \eta, \eta') = \delta(\eta - \eta')D(t - t', \eta)$. The Fourier transformation from time to frequency representation is

$$D_j(\epsilon_+, \epsilon_-; \epsilon'_+, \epsilon'_-) = 2\pi\delta(\epsilon_+ - \epsilon_- - \epsilon'_+ + \epsilon'_-) \times \int dt d\eta D_j(t, \eta) \exp \left\{ it(\epsilon_+ - \epsilon_-) + i\frac{\eta}{2}(\epsilon_+ + \epsilon_- - \epsilon'_+ - \epsilon'_-) \right\}. \quad (6.21)$$

The differential equation for the diffuson is

$$\left[\partial_t + Dq_-^2 + \frac{1}{\tau_s} \left(1 + d_j e^{-|\eta|/\tau\kappa} \right) \right] D_j(t, \eta) = \frac{1}{2\pi\mathcal{N}_0\tau^2} \delta(t) \quad (6.22)$$

with $d_0 = -1$ and $d_1 = 2/3$ for the singlet and triplet, respectively.

6.5 Temporal fluctuations (zero magnetic field)

Again, we use the approximation, that spin-flip scattering is in form identical to a time-dependent external field. We determine the thermal average of the current

operator over electron states form the Keldysh component of the Green's function,

$$I(t) = \langle \hat{I}(t) \rangle_{\text{el}} = -\frac{i}{2} \sum_{\mathbf{k}\sigma} I_x G_{\mathbf{k}\sigma, \mathbf{k}\sigma}^K(t, t). \quad (6.23)$$

In equilibrium, this is by definition the persistent current. The temporal current fluctuations can be determined from

$$\langle I(t)I(0) \rangle = -\frac{1}{4} \langle \left(\sum_{\mathbf{k}\sigma} I_x G_{\mathbf{k}\sigma, \mathbf{k}\sigma}^K(t, t) \sum_{\mathbf{k}'\sigma'} I_x G_{\mathbf{k}'\sigma', \mathbf{k}'\sigma'}^K(0, 0) \right)_{\text{spin}} \rangle. \quad (6.24)$$

The relevant diagrams are given in Fig. 2.1, showing that they are of the same structure as the diagrams for the persistent current fluctuations. Consider for example the one-cooperon diagram. Concentrating on the frequency dependencies, it is of the form

$$\int \frac{d\omega}{2\pi} \int \frac{d\epsilon_+}{2\pi} \frac{d\epsilon_-}{2\pi} n_F(\epsilon_+) [1 - n_F(\epsilon_-)] \text{Re} \left[e^{-i\omega t} C_j(\epsilon_+, \epsilon_- + \omega; \epsilon_+ + \omega, \epsilon_-) \right] \quad (6.25)$$

$$= \int \frac{d\epsilon_+}{2\pi} \frac{d\epsilon_-}{2\pi} n_F(\epsilon_+) [1 - n_F(\epsilon_-)] \quad (6.26)$$

$$\times \text{Re} \int \frac{d\omega}{2\pi} \int dt_1 dt_2 \exp \left[-i\omega \left(t + \frac{t_1 + t_2}{2} \right) + i(\epsilon_+ - \epsilon_-) \frac{t_1 - t_2}{2} \right] C_j(t_1, t_2)$$

Some of the integrations can be achieved rather easily, e.g. from the ω -integration we find a delta function $2\delta(2t + t_1 + t_2)$. The integrations over ϵ_+ and ϵ_- can be treated as in the case of persistent currents, see Eq. (2.46). The current fluctuations are the sum over cooperon and diffuson contributions, hence

$$\begin{aligned} \langle I(t)I(0) \rangle = & -\frac{1}{2\pi^2} \int_0^\infty dy y \coth \frac{y}{2T} \\ & \times \left\{ \sum_{q,j} \text{Re} \int dt_1 e^{iyt_1} \left[(\partial_\phi \partial_{\phi'} \Pi^C) 2C_j(t + t_1, t - t_1) + (\partial_\phi \partial_{\phi'} \Pi^D) D_j(t_1, t) \right] \right. \\ & + \sum_{q,j} (\partial_\phi \Pi^C) (\partial_{\phi'} \Pi^C) \text{Re} \int dt_1 dt_2 e^{iy(t_1+t_2)} 2C_j(t + t_1, t - t_1) 2C_j(t + t_2, t - t_2) \\ & \left. + \sum_{q,j} (\partial_\phi \Pi^D) (\partial_{\phi'} \Pi^D) \text{Re} \int dt_1 dt_2 e^{iy(t_1+t_2)} D_j(t_1, t + t_2) D_j(t_2, t - t_1) \right\} \quad (6.27) \end{aligned}$$

The quantities $\Pi^{C,D}$ have been given in Eq. (2.39). The Fourier transformation

$$\text{Re} \int_0^\infty dy y \coth \frac{y}{2T} e^{iyt_1} = \frac{1}{2} \int_{-\infty}^\infty dy y \coth \frac{y}{2T} e^{iyt_1}. \quad (6.28)$$

can be performed by closing the path of integration in the upper half plane ($t_1 > 0$). We find a sum over Matsubara frequencies which can be evaluated analytically, with the result

$$\text{Re} \int_0^\infty dy y \coth \frac{y}{2T} e^{iyt_1} = -\frac{\pi^2 T^2}{[\sinh(\pi T t_1)]^2}. \quad (6.29)$$

In the zero temperature limit, $t_1 T \ll 1$, this expression decays algebraically, while we find in the high temperature limit (or in the long-time limit), $t_1 T \gg 1$ the exponential decay

$$-\frac{\pi^2 T^2}{[\sinh(\pi T t_1)]^2} \approx -4\pi^2 T^2 \exp(-2\pi t_1 T). \quad (6.30)$$

All time integrations in Eq. (6.27) will be cut off at some phase breaking time¹, τ_ϕ , which may assume different values in the different diffuson or cooperon channels. Phase breaking may be due to finite temperatures (see Eq. 6.30), spin-flip scattering, or other processes not considered explicitly. Since we at least have thermal dephasing, i.e. $1/\tau_\phi \geq 2\pi T$, and also have to assume $T \gg 1/\tau_K$ (see Ch. 6.3), the impurity spin dynamics is slow enough for the spin configuration to be considered static during the phase coherence time. Consequently, the diffuson and cooperon can be simplified so that an explicit calculation of (6.27) is straightforward. The solutions to the differential equations (6.20) and (6.22) are

$$\begin{aligned} 2C_j(t + t_1, t - t_1) &= \frac{1}{2\pi\mathcal{N}_0\tau^2} \exp \left\{ -\frac{1}{2} \left[(Dq_+^2 + \frac{1}{\tau_s})2t_1 + \frac{c_j}{\tau_s} \int_{t-t_1}^{t+t_1} dt' e^{-|t'|/\tau_K} \right] \right\} \\ &\approx \frac{1}{2\pi\mathcal{N}_0\tau^2} \exp \left\{ -\left(Dq_+^2 + \frac{1}{\tau_s} + c_j \frac{1}{\tau_s} e^{-|t|/\tau_K} \right) t_1 \right\} \end{aligned} \quad (6.31)$$

and

$$\begin{aligned} D_j(t_1, t - t_2) &= \frac{1}{2\pi\mathcal{N}_0\tau^2} \exp \left\{ -\left(Dq_-^2 + \frac{1}{\tau_s} + d_j \frac{1}{\tau_s} e^{-|t-t_2|/\tau_K} \right) t_1 \right\} \\ &\approx \frac{1}{2\pi\mathcal{N}_0\tau^2} \exp \left\{ -\left(Dq_-^2 + \frac{1}{\tau_s} + d_j \frac{1}{\tau_s} e^{-|t|/\tau_K} \right) t_1 \right\}, \end{aligned} \quad (6.32)$$

where we chose the time arguments as they are needed in Eq. (6.27). On the formal level the approximations are valid since the time integrations in (6.27) have a cutoff at $t_1, t_2 \sim \tau_\phi < \tau_K$, and we can expand in lowest order in the ratios t_1/τ_K and t_2/τ_K .

Considering the current fluctuation for very long time differences t , the decay rate in all diffuson and cooperon channels is equal to $1/\tau_s$. In this limit Eq. (6.27) gives the stochastic fluctuations of the equilibrium current. If we neglect the impurity spin dynamics, $1/\tau_K \rightarrow 0$, the impurity spins are fixed and we recover the results of Ref. [68] and Eq. (6.2).

In the case of strong spin-flip scattering, $1/\tau_s \gg E_c$, the diffuson singlet component is the dominant contribution to the current fluctuations. Within the quasi-static limit discussed above the current fluctuations are given by ($T = 0$)

$$\langle I(t)I(0) \rangle = \sum_{m=1}^{\infty} \frac{12e^2 E_c^2}{\pi^2 m^3} \left(1 + \sqrt{\Gamma_m} + \Gamma_m/3 \right) \exp \left(-\sqrt{\Gamma_m} \right) \quad (6.33)$$

¹Note that this τ_ϕ is different from the phase breaking time known from the theory of weak localization.

with $\Gamma_m = (1/\tau_s T_m)[1 - \exp(-|t|/\tau_K)]$, compare Eq. (4.31). We conclude that in the presence of strong spin-flip scattering there are strong temporal fluctuations of the current. The current follows the actual spin-configuration. The time scale for changes in the spin configuration is the Korringa relaxation time τ_K . Since the current and the spin configuration are coupled nonlinearly, we find a much shorter time scale for the current fluctuations, $t \sim \tau_K(\tau_s E_c)$, from the condition $\Gamma_1(t) \sim 1$.

6.6 Temporal fluctuations in the presence of weak magnetic fields

In this section we extend our calculations in Ch. 6.5 to weak magnetic fields. For $\omega_s \ll T$ the spin configuration can be considered static within the phase coherence time as in Ch. 6.5. In this case the current is found most conveniently using the methods of Ch. 4.1. In a weak magnetic field, the spin correlations are of the form

$$\langle S^z(t)S^z(0) \rangle = \frac{1}{3}S(S+1)e^{-|t|/\tau_K} \quad (6.34)$$

$$\langle S^-(t)S^+(0) \rangle = \frac{2}{3}S(S+1)e^{-i\omega_s t}e^{-|t|/\tau_K}, \quad (6.35)$$

compare Eq. (6.15). The bare diffuson vertex including spin-orbit scattering is

$$D_{\alpha\beta\gamma\delta}^0 = \frac{1}{\tau}\delta_{\alpha\gamma}\delta_{\delta\beta} + \frac{1}{3\tau_{so}}\vec{\sigma}_{\alpha\gamma}\vec{\sigma}_{\delta\beta} + \frac{1}{3\tau_s}e^{-|t|/\tau_K} \left(\sigma_{\alpha\gamma}^z \sigma_{\delta\beta}^z + 2e^{i\omega_s t} \sigma_{\alpha\gamma}^- \sigma_{\delta\beta}^+ + 2e^{-i\omega_s t} \sigma_{\alpha\gamma}^+ \sigma_{\delta\beta}^- \right). \quad (6.36)$$

The diffuson is not diagonal in singlet/triplet representation. For $m = 0$, there are components which mix $j = 0$ and $j = 1$. On the other hand, it is not necessary to diagonalize the matrix $D_{\alpha\beta\gamma\delta}$ or $\langle jm|D|j'm' \rangle$ explicitly, it suffices to calculate the eigenvalues. There are two eigenvalues related to the $m = 0$ components and two related to the $m = 1$ components. Their inverse is proportional to

$$m = 1: -i\omega + Dq_-^2 + \frac{1}{\tau_s} + \frac{1}{3\tau_s}e^{-|t|/\tau_K} + \frac{4}{3\tau_{so}} \quad (6.37)$$

$$m = 0: -i\omega + Dq_-^2 + \frac{1}{\tau_s} - \frac{1}{3\tau_s}e^{-|t|/\tau_K} + \frac{2}{3\tau_{so}} \pm \left| \frac{2}{3\tau_s}e^{i\omega_s t - |t|/\tau_K} + \frac{2}{3\tau_{so}} \right|. \quad (6.38)$$

For the cooperon we find

$$m = 1: -i\omega + Dq_+^2 + \frac{1}{\tau_s} - \frac{1}{3\tau_s}e^{-|t|/\tau_K} + \frac{4}{3\tau_{so}} \quad (6.39)$$

$$m = 0: -i\omega + Dq_+^2 + \frac{1}{\tau_s} + \frac{1}{3\tau_s}e^{-|t|/\tau_K} + \frac{2}{3\tau_{so}} \pm \left| \frac{2}{3\tau_s}e^{i\omega_s t - |t|/\tau_K} - \frac{2}{3\tau_{so}} \right|. \quad (6.40)$$

The explicit expressions for the current fluctuations are found by replacing the $M_0 \dots N_2$ in Eq. (4.27) by the expressions given in Eqs. (6.37)-(6.40) and then taking the derivatives with respect to ϕ and ϕ' .

For vanishing spin-orbit scattering, the eigenvalues are independent of ω_s , since $|e^{i\omega_s t}| = 1$. In the presence of spin-orbit scattering, however, some of the eigenvalues depend on ω_s , and there is a contribution to the current fluctuations, periodic in time due to the rotation of the impurity spins in the magnetic field.

We draw the conclusion, that the dynamic response $\chi(\phi, \omega)$ is strongly frequency dependent. In the absence of a magnetic field, the relevant scale is the spin relaxation rate ($\omega \sim 1/\tau_K$) if spin-flip scattering is weak and $\omega \sim (1/\tau_K) \cdot (1/\tau_s E_c)$ for strong spin-flip scattering. The effects of the magnetic field on the impurity spin dynamics become important for $\omega_s > 1/\tau_K$. There is a contribution to the current fluctuations which is periodic in time. As a consequence, there is a resonance in the response function at the frequency of the periodic oscillations.

Note that Eqs. (6.34) and (6.35), and thus the results of this chapter are only applicable in the limit of weak magnetic fields, $\omega_s < T$.

Chapter 7

Summary

In the presence of a magnetic field, a normal-metal ring carries an equilibrium current, usually called persistent current. In rings where the electron motion is diffusive, several mechanisms which produce a persistent current have been found: A persistent current exists, if the electrons can diffuse around the ring without losing their phase coherence. However, none of the mechanisms known can explain the amplitude of the currents measured in the experiments.

We studied the effect of paramagnetic impurities on the persistent current. Magnetic impurities tend to destroy quantum coherence. In weak magnetic fields the persistent current is strongly reduced due to the impurity spin dynamics. Instead there are temporal current fluctuations following the actual spin configuration. By freezing out the spin dynamics in a magnetic field, the amplitude of the typical current, i.e. the current fluctuations, is of the same order as without magnetic impurities. However the mechanism of restoring the persistent current works rather badly, and the maximum value for the current is only reached for magnetic fields with a Zeeman energy ω_s larger than the spin-flip scattering rate $1/\tau_s$.

We discussed the mean current in a model of non-interacting and for weakly interacting electrons, as well as the stochastic current fluctuations. We found qualitatively different behavior of the current as a function of the Zeeman energy in all these cases. For example, the interaction contribution to the mean current is strongly reduced in the presence of magnetic impurities, regardless of whether the impurity spins are polarized or not.

If the Thouless energy E_c and the temperature T are below the Kondo temperature T_K , the impurity spins are effectively screened, the magnetic impurities scatter like nonmagnetic impurities.

None of these mechanisms ever lead to a persistent current which is larger than in the clean limit, i.e. without magnetic impurities.

Although we cannot explain the large currents observed experimentally, our results for the current as a function of parameters like the impurity concentration,

magnetic field and so on, may serve as a test for the applicability of the theoretical concepts (in comparison with future, systematic experiments).

In Ch. 5 we considered quantum corrections to the free energy of the magnetic impurities; due to these corrections we found a contribution to the persistent current which is – for $1/\tau_s \sim E_c$ and $T \leq E_c$ – larger than in a theory without magnetic impurities. The current as a function of temperature is of the order $I \sim (E_c^2/\phi_0 T) \cdot \exp(-T/3E_c)$. The current depends crucially on spin-orbit scattering: Without spin-orbit scattering, we found diamagnetic currents, and for strong spin-orbit scattering, we found paramagnetic currents. There are also differences in the current as a function of Zeeman energy and spin-flip scattering rate.

These spin induced currents have very interesting dynamical properties, which are determined by the dynamics of the magnetic impurities. In Ch. 6 we studied the dynamic current-current correlation function for frequency $\omega < T$ and Zeeman energy $\omega_s < T$. This correlation function is related to the linear response to a time dependent magnetic flux, $I(\omega) = \chi(\phi, \omega) \delta\phi(\omega)$. Current correlations decay on the time scale of the Korringa relaxation time τ_K or faster, if the spin-flip scattering rate is sufficiently high. In the presence of a magnetic field, there is at $\omega \approx \omega_s$ the well known resonance in the transverse spin susceptibility; in systems without spin-orbit scattering this does not affect the current fluctuations. In systems with spin-orbit scattering, however, there is a component of the current-current correlation function, which is periodic in time, i.e. there is a resonance in the dynamic response function.

The currents are related to an orbital magnetic moment, but in the experiments the total magnetic moment is measured, which is the sum of the orbital magnetism of the electrons plus the spin magnetism of electrons and impurities. One of the problems in an experiment is to extract the small orbital magnetic response from the large total magnetic response.

For low concentrations of magnetic impurities, $\chi(\phi, \omega)$ has a component which is periodic in ϕ and which can therefore be detected even if the total magnetic response is much larger.

For higher concentrations of magnetic impurities, where the persistent current, i.e. $\chi(\phi, \omega = 0)$, is suppressed, there is no such periodic component; in this regime, $\chi(\phi, \omega)$ could be extracted from the total magnetic response due to the resonances mentioned above: the resonances in $\chi(\phi, \omega)$ are in the longitudinal magnetic response, whereas the resonance in the impurity spin-magnetism is in the transverse component only. Further there are resonances in $\chi(\phi, \omega)$ at multiples of ω_s , since impurity spins and currents are coupled nonlinearly.

Appendix A

From real time to imaginary time representation: Some useful relations

The use of real time or imaginary time Green's functions in the calculations of thermodynamic properties is, in most cases, only a matter of taste. But sometimes one representation is more convenient. In Ch. 2 we used mostly the real time representation. In this appendix, we transform the most important formulas of Ch. 2 to imaginary time representation.

The impurity averaged Green's functions are in imaginary time representation given by ($\hbar = k_B = 1$):

$$G(i\omega_n, \mathbf{k}) = \frac{1}{i\omega_n - \epsilon_{\mathbf{k}} + \mu + i/2\tau \cdot \text{sgn}(\omega_n)}. \quad (\text{A.1})$$

The retarded and advanced Green's functions are found easily by analytic continuation:

$$G^{R,A}(\epsilon, \mathbf{k}) = \frac{1}{\epsilon - \epsilon_{\mathbf{k}} + \mu \pm i/2\tau}. \quad (\text{A.2})$$

The imaginary time representation of the polarization bubble Π , defined in Eq. (2.38) for real time Green's functions, is given by ($ql \ll 1$, $|\omega_1 - \omega_2|\tau \ll 1$):

$$\Pi = \int \frac{d^3k}{(2\pi)^3} G(i\omega_1, \mathbf{k}) G(i\omega_2, \pm \mathbf{k} \mp \mathbf{q}) \quad (\text{A.3})$$

$$= 2\pi \mathcal{N}_0 \tau [1 - \tau(|\omega_1 - \omega_2| + Dq^2)] \Theta(-\omega_1 \omega_2). \quad (\text{A.4})$$

The step function Θ assures, that ω_1 and ω_2 have different signs. Remember, that in real time representation, only the product of a retarded and an advanced Green's function contributes to Π .

In Eq. (2.11) we gave the expression for the particle number correlator in real time representation:

$$\langle (\delta N)^2 \rangle = 8 \text{Re} \int \frac{d\epsilon}{2\pi} \frac{d\epsilon_1}{2\pi} n_F(\epsilon) n_F(\epsilon_1) \sum_q \left(\frac{1}{-i(\epsilon - \epsilon_1) + Dq^2} \right)^2 \quad (\text{A.5})$$

The Fermi function has many poles in the complex plane, namely at $\epsilon_n = i\omega_n = i\pi T(2n+1)$ with integer n . Thus ω_n is a fermionic Matsubara frequency. The residue at these poles is T . We close the ϵ integration in the upper half of the complex plane, the ϵ_1 integration in the lower half of the complex plane. We find

$$\langle (\delta N)^2 \rangle = 8T^2 \sum_{\omega_n > 0} \sum_{\omega_{1,m} < 0} \sum_q \left(\frac{1}{\omega_n - \omega_{1,m} + Dq^2} \right)^2 \quad (\text{A.6})$$

$$= 8T \sum_{\nu_n > 0} \frac{\nu_n}{2\pi} \sum_q \left(\frac{1}{\nu_n + Dq^2} \right)^2, \quad (\text{A.7})$$

where $\nu_n = 2n\pi T$ is a Boson frequency.

Some more relations are found using similar arguments:

$$\langle (\delta N)^2 \rangle = -8 \int_{-\infty}^{\infty} \frac{d\epsilon}{2\pi} \frac{d\epsilon_1}{2\pi} [1 - n_F(\epsilon)] n_F(\epsilon_1) \text{Re} \sum_q \left(\frac{1}{-i(\epsilon - \epsilon_1) + Dq^2} \right)^2 \quad (\text{A.8})$$

$$= -8 \int_0^{\infty} \frac{dy}{2\pi} \frac{y}{2\pi} \coth\left(\frac{y}{2T}\right) \text{Re} \sum_q \left(\frac{1}{-iy + Dq^2} \right)^2 \quad (\text{A.9})$$

The flux dependent part of the thermodynamic potential is:

$$\langle \delta \Omega^{EEI} \rangle = -4\pi \lambda_c \int_0^{\infty} \frac{dy}{2\pi} \frac{y}{2\pi} \coth\left(\frac{y}{2T}\right) \text{Re} \sum_q \frac{1}{-iy + Dq^2} \quad (\text{A.10})$$

$$= 4\pi \lambda_c \sum_{\nu_n > 0} \frac{\nu_n}{2\pi} \sum_q \frac{1}{\nu_n + Dq^2} \quad (\text{A.11})$$

$$\langle \Omega(\phi) \Omega(\phi') \rangle_c = 8 \int_0^{\infty} \frac{dy}{2\pi} \frac{y}{2\pi} \coth\left(\frac{y}{2T}\right) \text{Re} \sum_q \ln(-iy + Dq^2) \quad (\text{A.12})$$

$$= -8 \sum_{\nu_n > 0} \frac{\nu_n}{2\pi} \sum_q \ln(\nu_n + Dq^2) \quad (\text{A.13})$$

Appendix B

The electron self energy

In this appendix, we calculate the T -matrix in second order in the coupling constant J . If the number of magnetic impurities is large ($N_s \gg 1$), this is equivalent to the calculation of an electron self-energy: $\Sigma_\sigma^{(2)} = N_s T_{\mathbf{k}\sigma\mathbf{k}\sigma}^{(2)}$, compare Ch. 2 and Ch. 3. For electrons with spin up, we find

$$\Sigma_+^{(2)}(i\epsilon_n) = N_s(-T) \sum_{\omega_l} \sum_{\mathbf{k}\alpha} V_{+\alpha\alpha+} G(i\epsilon_n - i\omega_l, \mathbf{k}). \quad (\text{B.1})$$

The relevant matrix elements of the interaction, which has been defined in Eq. (4.8), are:

$$V_{++++} = -\frac{1}{T} \left(\frac{J}{\mathcal{V}} \right)^2 \frac{1}{4} \delta_{0\omega_l} \quad (\text{B.2})$$

and

$$V_{+--+} = -\left(\frac{J}{\mathcal{V}} \right)^2 \frac{\tanh(\omega_s/2T)}{i\omega_l + \omega_s}. \quad (\text{B.3})$$

The frequency and momentum summation for the first type of interaction is easy, since the interaction does not transfer energy,

$$N_s(-T) \sum_{\omega_l} \sum_{\mathbf{k}} V_{++++} G(i\epsilon_n - i\omega_l, \mathbf{k}) = \frac{1}{4} n_s J^2 \frac{1}{\mathcal{V}} \sum_{\mathbf{k}} G(i\epsilon_n, \mathbf{k}) \quad (\text{B.4})$$

and

$$\frac{1}{\mathcal{V}} \sum_{\mathbf{k}} G(i\epsilon_n, \mathbf{k}) = \int \frac{d^3k}{(2\pi)^3} G(i\epsilon_n, \mathbf{k}) = -i\pi \mathcal{N}_0 \text{sgn}(\epsilon_n). \quad (\text{B.5})$$

With the second type of interaction, Eq. (B.3), the integration over \mathbf{k} can be achieved as in Eq. (B.5). The summation over Matsubara frequencies is more difficult. For $\epsilon_n > 0$ we have

$$\Sigma_+^{(2)}(i\epsilon_n) = -in_s \pi \mathcal{N}_0 J^2 \tanh \frac{\omega_s}{2T} T \sum_{\omega_l} \frac{\text{sgn}(\epsilon_n - \omega_l)}{i\omega_l + \omega_s} - in_s \pi \mathcal{N}_0 J^2 \frac{1}{4}. \quad (\text{B.6})$$

The sum $\sum_{\omega_l}(\dots)$ is cut off at the Fermi energy, and can be expressed using the digamma function Ψ :

$$T \sum_{\omega_l} \frac{\text{sgn}(\epsilon_n - \omega_l)}{i\omega_l + \omega_s} = \frac{i}{2\pi} \left\{ 2\Psi\left(\frac{\epsilon_F}{2\pi T}\right) - \Psi\left(\frac{1}{2} - \frac{\epsilon_n - i\omega_s}{2\pi T}\right) - \Psi\left(\frac{1}{2} + \frac{\epsilon_n - i\omega_s}{2\pi T}\right) \right\}. \quad (\text{B.7})$$

Using the property

$$\Psi(1 - z) = \Psi(z) + \pi \cot(\pi z), \quad (\text{B.8})$$

we find

$$\begin{aligned} \Sigma_+^{(2)}(i\epsilon_n) &= \frac{i}{\pi} \left\{ \Psi\left(\frac{\epsilon_F}{2\pi T}\right) - \Psi\left(\frac{1}{2} + \frac{\epsilon_n - i\omega_s}{2\pi T}\right) - \frac{\pi}{2} \cot\left(\frac{\pi}{2} + \frac{\epsilon_n - i\omega_s}{2T}\right) \right\} \\ &\quad - i n_s \pi \mathcal{N}_0 J^2 \frac{1}{4}. \end{aligned} \quad (\text{B.9})$$

This can be simplified using

$$\cot\left(\frac{\pi}{2} + \frac{\epsilon_n - i\omega_s}{2T}\right) = i \coth \frac{\omega_s}{2T}. \quad (\text{B.10})$$

After analytic continuation, $i\epsilon_n \rightarrow \epsilon + i0$, we use $\text{Im}\Psi(iy + 1/2) = (\pi/2) \tanh(\pi y)$ and arrive at the expressions given in Eqs. (4.11) and (4.12). $\Sigma_-^R(\epsilon)$ can be found in the same way.

Appendix C

Diffuson and cooperon in the presence of magnetic impurities

C.1 Zero magnetic field

As far as we know, the cooperon in the presence of magnetic impurities was first presented in the paper of Hikami, Larkin and Nagaoka [61]. They consider a scattering amplitude of the form

$$f_{\alpha\beta} = a\delta_{\alpha\beta} + ib(\mathbf{k} \times \mathbf{k}') \cdot \vec{\sigma}_{\alpha\beta} + c\vec{S} \cdot \vec{\sigma}_{\alpha\beta}, \quad (\text{C.1})$$

where α and β are spin indices, a , b and c are the amplitudes of non-magnetic, spin-orbit and spin-flip scattering. This means, the scattering Hamiltonian is of the form

$$H = \sum_{\mathbf{R}} \frac{1}{V} \sum_{\mathbf{k}\mathbf{k}'\alpha\beta} e^{-i(\mathbf{k}-\mathbf{k}')\cdot\mathbf{R}} f_{\alpha\beta} c_{\mathbf{k}\alpha}^+ c_{\mathbf{k}'\beta}. \quad (\text{C.2})$$

The (retarded) self energy near the Fermi energy is $\Sigma(\epsilon \sim 0, |\mathbf{k}| \sim k_F) = -i/2\tau - i/2\tau_{so} - i/2\tau_s$,

$$1/\tau = n2\pi\mathcal{N}_0|a|^2 \quad (\text{C.3})$$

$$1/\tau_{so} = n2\pi\mathcal{N}_0|b|^2 \langle (\mathbf{k} \times \mathbf{k}')^2 \rangle_{FS} \quad (\text{C.4})$$

$$1/\tau_s = n2\pi\mathcal{N}_0|c|^2 \langle \vec{S}^2 \rangle, \quad (\text{C.5})$$

with n the density of impurities, $\langle \vec{S}^2 \rangle = S(S+1) = 3/4$, and $\langle (\mathbf{k} \times \mathbf{k}')^2 \rangle_{FS} = 2k_F^4/3$ denotes the average of the expression over the Fermi surface. The bare diffuson vertex can be written as

$$2\pi\mathcal{N}_0 D_{\alpha\beta\gamma\delta}^0 = \frac{1}{\tau} \delta_{\alpha\gamma} \delta_{\delta\beta} + \left(\frac{1}{3\tau_s} + \frac{1}{3\tau_{so}} \right) \vec{\sigma}_{\alpha\gamma} \vec{\sigma}_{\delta\beta}. \quad (\text{C.6})$$

For example the expression for the self-energy can be found very quickly from

$$\Sigma = \sum_{\beta} D_{\alpha\beta\beta\alpha}^0 \int \frac{d^3k}{(2\pi)^3} G_{\beta}^R(\epsilon, \mathbf{k}). \quad (\text{C.7})$$

To find the expression for the bare cooperon, special care is necessary for the spin-orbit term: For the diffuson, we average $(\mathbf{k} \times \mathbf{k}')^2$ over the Fermi surface. For the cooperon, we need the same expression, but with an additional minus sign.

$$2\pi\mathcal{N}_0 C_{\alpha\beta\gamma\delta}^0 = \frac{1}{\tau} \delta_{\alpha\gamma} \delta_{\beta\delta} + \left(\frac{1}{3\tau_s} - \frac{1}{3\tau_{so}} \right) \vec{\sigma}_{\alpha\gamma} \vec{\sigma}_{\beta\delta}. \quad (\text{C.8})$$

Using the Clebsch Gordan coefficients $\langle \sigma\sigma' | jm \rangle$ the components of the cooperon can be written in terms of singlets and triplets:

$$\langle jm | C | j'm' \rangle = \sum_{\sigma\sigma'\nu\nu'} \langle \sigma\sigma' | jm \rangle \langle \nu\nu' | j'm' \rangle C_{\sigma\sigma'\nu\nu'}. \quad (\text{C.9})$$

Explicitly, the vectors $|jm\rangle$ are given by:

$$|00\rangle = (|+-\rangle - |-+\rangle)/\sqrt{2} \quad (\text{C.10})$$

$$|10\rangle = (|+-\rangle + |-+\rangle)/\sqrt{2} \quad (\text{C.11})$$

$$|11\rangle = |++\rangle \quad (\text{C.12})$$

$$|1-1\rangle = |--\rangle. \quad (\text{C.13})$$

Both the bare and the full cooperon are diagonal in the new basis, with the result

$$C_0 = \langle 00 | C | 00 \rangle = \frac{1}{2\pi\mathcal{N}_0\tau^2} \frac{1}{-i\omega + Dq_+^2 + 2/\tau_s} \quad (\text{C.14})$$

$$C_1 = \langle 1m | C | 1m \rangle = \frac{1}{2\pi\mathcal{N}_0\tau^2} \frac{1}{-i\omega + Dq_+^2 + 2/3\tau_s + 4/3\tau_{so}}. \quad (\text{C.15})$$

For the diffuson, we choose another basis set: $|00\rangle = (|++\rangle + |--\rangle)/\sqrt{2}$, $|10\rangle = (|++\rangle - |--\rangle)/\sqrt{2}$, $|11\rangle = |+-\rangle$, and $|1-1\rangle = |-+\rangle$. These vectors can be found from the vectors for the cooperon with the replacements $|\sigma+\rangle \rightarrow -|\sigma-\rangle$ and $|\sigma-\rangle \rightarrow |\sigma+\rangle$. The singlet and triplet components of the diffuson are:

$$D_0 = \langle 00 | D | 00 \rangle = \frac{1}{2\pi\mathcal{N}_0\tau^2} \frac{1}{-i\omega + Dq_-^2} \quad (\text{C.16})$$

$$D_1 = \langle 1m | D | 1m \rangle = \frac{1}{2\pi\mathcal{N}_0\tau^2} \frac{1}{-i\omega + Dq_-^2 + 4/3\tau_s + 2/3\tau_{so}}. \quad (\text{C.17})$$

Note that the diffuson singlet mode, which enters the calculation of the density density response function, does not depend on spin-orbit or spin-flip scattering.

When we consider correlations between two different systems, the impurity spins in the different systems are uncorrelated. As a result, we find in all diffuson and cooperon channels the same spin-flip relaxation rate $1/\tau_s$.

C.2 Magnetic field effects

The expressions we give here for the diffuson and cooperon are valid, when one considers correlations between two different systems, e.g. when calculating the current fluctuations $\langle I(\phi)I(\phi') \rangle_c$. Rather than evaluating $\langle \Omega\Omega \rangle_c$ and subsequently finding the persistent current in terms of the derivative with respect of the flux ϕ , the current can also be found by a direct calculation of the expectation value of the current operator, as described in Ch. 2 without spin effects. In this case we need the expressions for the diffuson and cooperon explicitly; the bare expressions C^0 and D^0 are given in Eqs. (4.17) and (4.18). Using the quantities N and M defined in Eqs. (4.21)-(4.26), we find for the non-zero components of the cooperon

$$2\pi\mathcal{N}_0\tau^2 C_{++++} = \left(N_2 + \frac{\gamma_{++} - \gamma_{--}}{2} - i\frac{\omega_s - \omega'_s}{2} \right)^{-1} \quad (\text{C.18})$$

$$2\pi\mathcal{N}_0\tau^2 C_{----} = \left(N_2 - \frac{\gamma_{++} - \gamma_{--}}{2} + i\frac{\omega_s - \omega'_s}{2} \right)^{-1} \quad (\text{C.19})$$

$$2\pi\mathcal{N}_0\tau^2 C_{+-+-} = \left(\frac{N_0 + N_1}{2} + \frac{\gamma_{-+} - \gamma_{+-}}{2} + i\frac{\omega_s + \omega'_s}{2} \right) / \mathcal{D}_+ \quad (\text{C.20})$$

$$2\pi\mathcal{N}_0\tau^2 C_{-++-} = \left(\frac{N_0 + N_1}{2} - \frac{\gamma_{-+} - \gamma_{+-}}{2} - i\frac{\omega_s + \omega'_s}{2} \right) / \mathcal{D}_+ \quad (\text{C.21})$$

$$2\pi\mathcal{N}_0\tau^2 C_{+---} = \left(\frac{N_0 - N_1}{2} \right) / \mathcal{D}_+ = 2\pi\mathcal{N}_0\tau^2 C_{-++-} \quad (\text{C.22})$$

with

$$\mathcal{D}_+ = N_0 N_1 - \left(\frac{\gamma_{-+} - \gamma_{+-}}{2} + i\frac{\omega_s + \omega'_s}{2} \right)^2. \quad (\text{C.23})$$

The non-zero components of the diffuson are

$$2\pi\mathcal{N}_0\tau^2 D_{+--+} = \left(M_2 - i\frac{\omega_s + \omega'_s}{2} + \frac{\gamma_{+-} - \gamma_{-+}}{2} \right)^{-1} \quad (\text{C.24})$$

$$2\pi\mathcal{N}_0\tau^2 D_{-++-} = \left(M_2 + i\frac{\omega_s + \omega'_s}{2} - \frac{\gamma_{+-} - \gamma_{-+}}{2} \right)^{-1} \quad (\text{C.25})$$

$$2\pi\mathcal{N}_0\tau^2 D_{++++} = \left(\frac{M_0 + M_1}{2} + i\frac{\omega_s - \omega'_s}{2} - \frac{\gamma_{++} - \gamma_{--}}{2} \right) / \mathcal{D}_- \quad (\text{C.26})$$

$$2\pi\mathcal{N}_0\tau^2 D_{----} = \left(\frac{M_0 + M_1}{2} - i\frac{\omega_s - \omega'_s}{2} + \frac{\gamma_{++} - \gamma_{--}}{2} \right) / \mathcal{D}_- \quad (\text{C.27})$$

$$2\pi\mathcal{N}_0\tau^2 D_{+--+} = \left(\frac{M_1 - M_0}{2} \right) / \mathcal{D}_- \quad (\text{C.28})$$

with

$$\mathcal{D}_- = M_0 M_1 - \left(i\frac{\omega_s - \omega'_s}{2} - \frac{\gamma_{++} - \gamma_{--}}{2} \right)^2 \quad (\text{C.29})$$

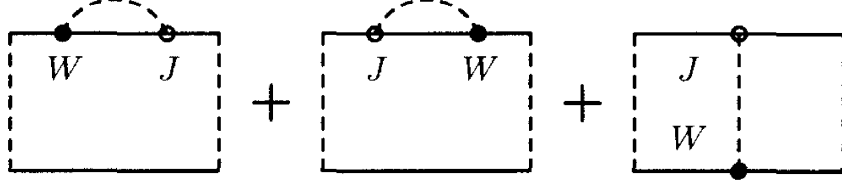


Figure C.1: Diagrams representing mixed potential and spin-flip scattering. The sum of the three diagrams is zero.

C.3 Mixed potential and spin-flip scattering

One may ask why we consider two distinct types of impurities, on the one hand a pure potential scatterer, on the other a pure spin scatterer. A real magnetic impurity will have both, potential and spin-flip scattering, described by a Hamiltonian

$$H_{sd} = -\frac{1}{V} \sum_{\mathbf{R}} \sum_{\mathbf{k}\mathbf{k}'\sigma\sigma'} \exp[-i(\mathbf{k} - \mathbf{k}') \cdot \mathbf{R}] \left(W c_{\mathbf{k}\sigma}^+ c_{\mathbf{k}'\sigma'} \delta_{\sigma\sigma'} + J c_{\mathbf{k}\sigma}^+ c_{\mathbf{k}'\sigma'} \vec{\sigma}_{\sigma\sigma'} \cdot \vec{S}_{\mathbf{R}} \right), \quad (\text{C.30})$$

compare with the Hamiltonian in Ch. 4. In particular, we cannot rule out that $W > J$. In second order in the interaction there are three types of contributions: proportional to W^2 , WJ and $J^2 \sim 1/\tau_s$. The part $\sim W^2$ gives a correction to the non-magnetic scattering rate $1/\tau$. In the absence of magnetic fields, the term $\sim WJ$ is equal to zero. In the presence of magnetic fields, however, this part can be much larger than the terms $\sim J^2$.

Corrections to the diffusion or cooperon from these mixed terms are shown in Fig. (C.1). The sum of these diagrams is exactly zero, which means contributions $\sim JW$ are unimportant for the questions considered.

Appendix D

Persistent currents: Summary of results for single channel systems

Up to now, we always considered quasi-one-dimensional systems, i.e. systems where $L \gg L_\perp$, but $k_F L_\perp \gg 1$. All our results were obtained in perturbation theory. Here we list some results obtained for strictly one-dimensional systems, where a number of exact results are known, even for interacting electrons, and also numerical investigations are easier to perform.

1. Non-interacting electrons (spinless fermions)

(a) Clean limit

odd number of electrons: $I(\phi) = -(ev_F/L)2\phi/\phi_0$; $(-\phi_0/2 < \phi < \phi_0/2)$

even number of electrons: $I(\phi) = -(ev_F/L)(2\phi/\phi_0 - 1)$; $(0 < \phi < \phi_0)$

$I(\phi)$ is periodic with periodicity ϕ_0 , i.e. there are cusps in $I(\phi)$ at $\phi = (n + 1/2)\phi_0$ for odd number of electrons N , and cusps at $\phi = n\phi_0$ for even N .

(b) Single, delta like impurity: $V(x) = a\delta(x - x')$

A weak impurity leads to a round off of the cusps in $I(\phi)$, a strong impurity ($a \gg \hbar v_F$) reduces the current according to ($a^* = \hbar v_F/\pi$) [88, 89]:

$$I(\phi) = \frac{\pi ev_F}{2L} \left[(-)^N \frac{a^*}{|a|} \sin(2\pi\phi/\phi_0) + \left(\frac{a^*}{a}\right)^2 \sin(4\pi\phi/\phi_0) + \dots \right] \quad (\text{D.1})$$

(c) Random impurity potential

The mean current as a function of the system size drops exponentially, due to localization [88, 90]. The current distribution seems to be of the log-normal type [90].

2. Interacting electrons

(a) Clean limit

For a system with translational symmetry, the persistent current is independent of the interaction [91–93]. On a lattice, the current depends on the interaction [94], but the same odd even effects as for non-interacting electrons are found. The amplitude can be determined using the Bethe ansatz solution of the XXZ Heisenberg chain, which is equivalent to spinless fermions with nearest neighbor interaction ($U \sum n_i n_{i+1}$). For the half filled band, the Fermi velocity in the expression for the current has to be replaced by

$$v_F \rightarrow v_F \pi^2 \frac{\sin \mu}{4\mu(\pi - \mu)}, \quad (\text{D.2})$$

where $U = \cos \mu$.

(b) Single impurity (spinless fermions)

A repulsive interaction enhances the effect of the impurity [90]; from a renormalization group analysis [95], it can be expected that the impurity strength scales to infinity for $L \rightarrow \infty$. An attractive interaction has the opposite effect, it makes the barrier transparent, i.e. the persistent current increases as a function of the interaction strength. For very special defects [96], where the model remains integrable, the barrier is transparent for both signs of the interaction.

(c) Random impurity potential (spinless fermions)

For weak disorder, the current is reduced in the presence of a repulsive interaction, the current increases if the interaction is attractive [31, 32, 90].

(d) Random potential (fermions with spin)

Persistent currents are enhanced by repulsive interactions [97, 98].

An interpretation of these results has been formulated by Giamarchi and Shastri [97]: For the attractive Hubbard model, the ground state has strong charge density fluctuations, that pin easily at the impurities. A repulsion favours a ground state with uniform density and makes pinning harder, and thus the persistent currents are enhanced.

In the spinless Fermion model, both the attractive and repulsive ground states have density fluctuations. A second mechanism which is competing with the charge density fluctuations are superconducting fluctuations. Superconducting fluctuations, which exist in the attractive case, increase the persistent current and thus explain why the persistent current increases for an attractive interaction in the spinless Fermion model.

Appendix E

Static and dynamic response in the canonical and grand canonical ensemble

In Ch. 2 we saw that for non-interacting electrons it is essential to calculate the persistent current at a fixed particle number instead at fixed chemical potential. Here we investigate the static and dynamic response functions in the canonical and grand canonical ensemble using very general arguments. Let us consider the linear response to a small magnetic flux, for a given realization of the impurity potential,

$$I(\phi) = \chi\phi. \quad (\text{E.1})$$

The static response function is given by

$$\chi_{static} = - \sum_{m,n} \frac{W(n) - W(m)}{\epsilon_n - \epsilon_m} |\langle n | \hat{I} | m \rangle|^2 - \frac{e^2}{mL^2} \langle \hat{N} \rangle, \quad (\text{E.2})$$

where $\{|n\rangle\}$ are the many particle eigenstates of the unperturbed system, $\{\epsilon_n\}$ are the eigenvalues, $W(n)$ the eigenvalues of the density matrix, $\hat{I} = \sum_{\mathbf{k}\sigma} (-e/mL) k_x c_{\mathbf{k}\sigma}^+ c_{\mathbf{k}\sigma}$ is the current operator and \hat{N} is the particle number operator. The dynamic response is

$$\chi_{dyn}(\omega) = - \sum_{m,n} \frac{W(n) - W(m)}{\epsilon_n - \epsilon_m + \omega + i0} |\langle n | \hat{I} | m \rangle|^2 - \frac{e^2}{mL^2} \langle \hat{N} \rangle. \quad (\text{E.3})$$

This dynamical response function is proportional to the conductivity:

$$\chi_{dyn}(\omega) = \frac{i\omega}{L^2} \mathcal{V}\sigma(\omega). \quad (\text{E.4})$$

For finite temperatures, the susceptibility can be different for the grand canonical and for the canonical ensemble. Even within the same ensemble $\chi_{dyn}(\omega \rightarrow 0) \neq \chi_{static}$, since states with $\epsilon_n = \epsilon_m$ do contribute to the static response, but not to the dynamic response.

In the zero temperature limit, however, all the static susceptibilities for the grand canonical and the canonical ensemble are equal, if the ground state is not degenerate¹: In this case, $W(0) = 1$ for the ground state $|0\rangle$, and $W(n) = 0$ for all other states, whether $W(n)$ is an eigenvalue of the canonical or the grand canonical density matrix. Since the current operator does not change the particle number, it follows immediately that the static response is the same for both ensembles. This means that the differences of the canonical and grand canonical calculations found in Ch. 2 purely appear as a result of the averaging procedures over the impurities, i.e. averaging over impurity configurations at fixed chemical potential or at fixed particle number.

Similarly, we can argue that the static response and the dynamic response for $\omega \rightarrow 0$ are also identical: At zero temperature, the states with $\epsilon_n = \epsilon_m$ do not contribute to the static response, since these states are either not occupied, $W(n) = 0$, or $n = m = 0$; however the ground state does not carry a current, $\langle 0|\hat{I}|0\rangle = 0$.

However, if the ground state is degenerate these arguments do not apply. When averaging over impurity configurations, there will always be configurations, where the difference of the ground state energy of the system with $N + 1$ electrons and N electrons exactly equals the chemical potential, i.e. these states are degenerate! As a consequence, the *averaged* static and dynamic susceptibilities need not be equal, and indeed in calculations of the dynamic response [41] it has been found that $\langle \chi_{dyn}(\omega \rightarrow 0) \rangle \neq \langle \chi_{static} \rangle$ at zero temperature for the grand canonical ensemble.

¹We use the word 'degenerate' in a generalized sense: two states $|n\rangle$ and $|m\rangle$ are degenerate, if $W(n) = W(m)$. Especially, these states can be eigenstates to different particle numbers.

Bibliography

- [1] F. London, J. Phys. (France) **8**, 379 (1937).
- [2] F. Hund, Ann. Phys. (Leipzig) **32**, 102 (1938).
- [3] N. Byers and C. N. Yang, Phys. Rev. Lett. **7**, 46 (1961).
- [4] M. Büttiker, Y. Imry, and R. Landauer, Phys. Lett. **96A**, 365 (1983).
- [5] W. P. Halperin, Rev. Mod. Phys. **58**, 533 (1986).
- [6] P. W. Anderson, E. Abrahams, and T. V. Ramakrishnan, Phys. Rev. Lett. **43**, 718 (1979).
- [7] L. P. Gorkov, A. I. Larkin, and D. E. Khmel'nitskii, JETP Lett. **30**, 248 (1979).
- [8] G. Bergmann, Phys. Rep. **107**, 1 (1984).
- [9] R. A. Lee and T. V. Ramakrishnan, Rev. Mod. Phys. **57**, 287 (1985).
- [10] S. Chakravarty and A. Schmid, Phys. Rep. **140**, 193 (1986).
- [11] B. L. Altshuler, JETP Lett. **41**, 648 (1985).
- [12] P. A. Lee and A. D. Stone, Phys. Rev. Lett. **55**, 1622 (1985).
- [13] P. A. Lee, A. D. Stone, and H. Fukuyama, Phys. Rev. B **35**, 1039 (1987).
- [14] D. Y. Sharvin and Y. V. Sharvin, JETP Lett. **34**, 272 (1981).
- [15] B. L. Altshuler, A. G. Aronov, and B. Z. Spivak, JETP Lett. **33**, 94 (1991).
- [16] R. A. Webb, S. Washburn, C. P. Umbach, and R. B. Laibowitz, Phys. Rev. Lett. **54**, 2696 (1985).
- [17] S. Washburn and R. A. Webb, Adv. Phys. **35**, 375 (1986).
- [18] S. Washburn, in *Mesoscopic Phenomena in Solids*, edited by B. L. Altshuler, P. A. Lee, and R. A. Webb (North Holland, Amsterdam, 1991), p. 1.

- [19] L. P. Lévy, G. Dolan, J. Dunsmuir, and H. Bouchiat, Phys. Rev. Lett. **64**, 2074 (1990).
- [20] L. Lévy, Physica B **169**, 245 (1991).
- [21] V. Chandrasekhar *et al.*, Phys. Rev. Lett. **67**, 3578 (1991).
- [22] D. Mailly, C. Chapelier, and A. Benoit, Phys. Rev. Lett. **70**, 2020 (1993).
- [23] B. Reulet, M. Ramin, H. Bouchiat, and D. Mailly, Phys. Rev. Lett. **75**, 124 (1995).
- [24] A. Schmid, Phys. Rev. Lett. **66**, 80 (1991).
- [25] F. von Oppen and E. Riedel, Phys. Rev. Lett. **66**, 84 (1991).
- [26] B. L. Altshuler, Y. Gefen, and Y. Imry, Phys. Rev. Lett. **66**, 88 (1991).
- [27] V. Ambegaokar and U. Eckern, Phys. Rev. Lett. **65**, 381 (1990).
- [28] U. Eckern and A. Schmid, Europhys. Lett. **18**, 457 (1992).
- [29] U. Eckern and A. Schmid, Ann. Phys. (Leipzig) **2**, 180 (1993).
- [30] R. A. Smith and V. Ambegaokar, Europhys. Lett. **20**, 161 (1992).
- [31] M. Abraham and R. Berkovits, Phys. Rev. Lett. **70**, 1509 (1993).
- [32] H. Kato and D. Yoshioka, Phys. Rev. B **50**, 4943 (1994).
- [33] D. Yoshioka and K. Kato, preprint, cond-mat/9409038, cond-mat/9501105 .
- [34] H.-F. Cheung, E. K. Riedel, and Y. Gefen, Phys. Rev. Lett. **62**, 587 (1989).
- [35] H. Bouchiat and G. Montambaux, J. Phys. (Paris) **50**, 2695 (1989).
- [36] G. Montambaux, H. Bouchiat, D. Sigetti, and R. Friesner, Phys. Rev. B **42**, 7647 (1990).
- [37] B. L. Altshuler and B. I. Shklovskii, Sov. Phys. JETP **64**, 127 (1987).
- [38] B. L. Altshuler and A. G. Aronov, in *Electron-Electron Interactions in Disordered Systems*, edited by A. L. Efros and M. Pollak (North-Holland, Amsterdam, 1985), p. 1.
- [39] D. Vollhardt and P. Wölfle, Phys. Rev. Lett. **48**, 699 (1982).
- [40] K. B. Efetov, Adv. Phys. **35**, 53 (1983).

- [41] K. B. Efetov, Phys. Rev. Lett. **66**, 2794 (1991).
- [42] A. Altland, S. Iida, A. Müller-Groeling, and H. A. Weidenmüller, Europhys. Lett. **20**, 155 (1992).
- [43] J. J. M. Verbaarschot, H. A. Weidenmüller, and M. R. Zirnbauer, Phys. Rep. **129**, 367 (1985).
- [44] G. D. Mahan, *Many-Particle Physics* (Plenum Press, New York, 1990).
- [45] A. A. Abrikosov, L. P. Gorkov, and I. Y. Dzyaloshinskii, *Quantum Field Theoretical Methods in Statistical Physics* (Pergamon Press, Oxford, 1965).
- [46] B. L. Altshuler, in *Nanostructures and Mesoscopic Systems*, edited by W. P. Kirk and M. A. Reed (Academic Press, San Diego, 1992), p. 405.
- [47] P. Kopietz, Phys. Rev. Lett. **70**, 3123 (1993), see also: G. Vignale, *ibid.* **72**, 433 (1994); A. Altland and Y. Gefen, *ibid.* **72**, 2973 (1994).
- [48] B. L. Altshuler and A. G. Aronov, Solid State Commun. **38**, 11 (1981).
- [49] U. Eckern, Z. Phys. B **82**, 393 (1991).
- [50] A. A. Abrikosov, Physics **2**, 21 (1965).
- [51] Y. A. Izyumov and Y. N. Skryabin, *Statistical Mechanics of Magnetically ordered Systems* (Consultants Bureau, New York, 1988).
- [52] M. B. Walker, Phys. Rev. **176**, 432 (1968).
- [53] M. B. Walker, Phys. Rev. B **1**, 3690 (1970).
- [54] P. Nozières, J. Low Temp. Phys. **17**, 13 (1974).
- [55] K. Yosida and K. Yamada, Prog. Theor. Phys. **46**, 244 (1970).
- [56] K. Yosida and K. Yamada, Prog. Theor. Phys. **53**, 1286 (1975).
- [57] K. Yamada, Prog. Theor. Phys. **53**, 970 (1975).
- [58] A. C. Hewson, Phys. Rev. Lett. **70**, 4007 (1993).
- [59] A. C. Hewson, *The Kondo Problem to Heavy Fermions* (Cambridge University Press, Cambridge, 1993).
- [60] A. M. Tsvelick and P. B. Wiegmann, Adv. Phys. **32**, 453 (1983).
- [61] S. Hikami, A. I. Larkin, and Y. Nagaoka, Prog. Theor. Phys. **63**, 707 (1980).

- [62] V. S. Amaral, J. Phys. Condens. Matter **2**, 8201 (1990).
- [63] V. I. Fal'ko, JETP Lett. **53**, 340 (1991).
- [64] B. L. Altshuler and B. Z. Spivak, JETP Lett. **42**, 447 (1985).
- [65] S. Feng, A. J. Bray, P. A. Lee, and M. A. Moore, Phys. Rev. B **36**, 5624 (1987).
- [66] A. A. Bobkov, V. I. Fal'ko, and D. E. Khmel'nitskii, Sov. Phys. JETP **71**, 393 (1990).
- [67] V. I. Fal'ko, J. Phys. Condens. Matter **4**, 3943 (1992).
- [68] U. Eckern, Phys. Scr. T **49**, 338 (1993).
- [69] H. Yoshioka and H. Fukuyama, J. Phys. Soc. Jpn. **62**, 612 (1993).
- [70] A. A. Abrikosov, *Fundamentals of the Theory of Metals* (Noth-Holland, Amsterdam, 1988).
- [71] J. Jaroszynski *et al.*, Phys. Rev. Lett. **75**, 3170 (1995).
- [72] D. R. Haman, Phys. Rev. **158**, 570 (1967).
- [73] G. Bergmann, Phys. Rev. Lett. **67**, 2545 (1991).
- [74] G. Chen and N. Giordano, Phys. Rev. Lett. **66**, 209 (1991).
- [75] M. A. Blachly and N. Giordano, Phys. Rev. B **46**, 2951 (1992).
- [76] M. A. Blachly and N. Giordano, Phys. Rev. B **51**, 12537 (1995).
- [77] J. F. DiTusa *et al.*, Phys. Rev. Lett. **68**, 1156 (1992).
- [78] F. Ohkawa, H. Fukuyama, and K. Yosida, J. Phys. Soc. Jpn. **52**, 1701 (1983).
- [79] F. J. Ohkawa and H. Fukuyama, J. Phys. Soc. Jpn. **53**, 2640 (1984).
- [80] S. Suga, H. Kasai, and A. Okiji, J. Phys. Soc. Jpn. **55**, 2515 (1986).
- [81] S. Suga, H. Kasai, and A. Okiji, J. Phys. Soc. Jpn. **56**, 863 (1987).
- [82] S. Suga, H. Kasai, and A. Okiji, J. Phys. Soc. Jpn. **56**, 4522 (1987).
- [83] O. Ujsaghy, A. Zawadowski, and B. L. Gyorffy, Spin-Orbit Induced Magnetic Anisotropy for Impurities in Metallic Samples of Reduced Dimensions: Finite Size Dependence in the Kondo Effect, 1995, preprint, University of Budapest.
- [84] V. Chandrashekar *et al.*, Phys. Rev. Lett. **72**, 2053 (1994).

- [85] L. Keldysh, Sov. Phys. JETP **20**, 1018 (1965).
- [86] J. Rammer and H. Smith, Rev. Mod. Phys. **58**, 323 (1986).
- [87] B. L. Altshuler, A. G. Aronov, D. E. Khmelnitskii, and A. F. Larkin, in *Quantum Theory of Solids*, edited by I. M. Lifshitz (MIR Publishers, Moscow, 1980), p. 130.
- [88] H.-F. Cheung, Y. Gefen, E. K. Riedel, and W.-H. Shih, Phys. Rev. B **37**, 6050 (1988).
- [89] U. Eckern and P. Schwab, to appear in Adv. Phys. (1996).
- [90] P. Schmitteckert, Dissertation, Universität Augsburg, 1996.
- [91] A. Müller-Groeling, H. A. Weidenmüller, and C. H. Lewenkopf, Europhys. Lett. **22**, 193 (1993).
- [92] H. A. Weidenmüller, Physica A **200**, 104 (1993).
- [93] A. Müller-Groeling and H. A. Weidenmüller, Phys. Rev. B **49**, 4752 (1994).
- [94] D. Loss, Phys. Rev. Lett. **69**, 343 (1992).
- [95] C. L. Kane and M. P. A. Fisher, Phys. Rev. Lett. **68**, 1220 (1992).
- [96] P. Schmitteckert, P. Schwab, and U. Eckern, Europhys. Lett. **30**, 543 (1995).
- [97] T. Giamarchi and B. S. Shastry, Phys. Rev. B **51**, 10915 (1995).
- [98] M. Ramin, B. Reulet, and H. Bouchiat, Phys. Rev. B **51**, 5882 (1995).

Dank

Ich will mich bei all denen bedanken, die zum Gelingen dieser Arbeit beigetragen haben. An erster Stelle sei Prof. U. Eckern genannt, bei dem ich mich für die Themenstellung und die vielen Diskussionen bedanken will, ohne die ich so manches wohl nie verstanden hätte.

Im weiteren gilt mein Dank den Mitarbeitern der theoretischen Physik in Augsburg, besonders aber K.-H. Höck – nicht nur für die Mühe die er sich als zweiter Gutachter der Arbeit gemacht hat – sondern vor allem für die vielen Verbesserungsvorschläge. P. Schmitteckert danke ich für die Einweihung in die Geheimnisse der Bethe-Ansätze und nicht zuletzt C. Wunsch für das Ausmerzen vieler Fehler in meinem Englisch.